

JOURNAL OF THE GEOTECHNICAL ENGINEERING DIVISION

EMPIRICAL STRENGTH CRITERION FOR ROCK MASSES

By Evert Hoek¹ and Edwin T. Brown,² M. ASCE

INTRODUCTION

The design of an excavation in rock requires an assessment of the likely response of the rock mass to a set of induced stresses. In order to predict this response, a knowledge is required of the complete stress-strain behavior and strength characteristics of the rock mass and of the influence of time on these properties. This paper is concerned with only part of this total response, the peak strength developed under a given set of stresses; the influence of time is not considered.

In many cases such as slopes (30) or shallow tunnels (29), instability may be associated with the structural features in the rock mass, and the shear strengths of these discontinuities will be required for use in design calculations. In some deep underground excavations, stability may depend on the relationship between the induced stresses and the strength of the intact rock (27). The processes of drilling and blasting and excavation by tunnelling machinery are also strongly influenced by the strength of the intact rock material (41,47).

There is a further class of rock engineering problem in which the overall stability of a deep surface cut or the components of a system of underground excavations will be determined by the mass behavior of the rock mass surrounding the excavation. In some cases, the rock mass may be heavily jointed so that, on the scale of the problem, it can be regarded as an isotropic assembly of interlocking angular particles. The transition from intact rock to heavily jointed rock mass with increasing sample size in a hypothetical rock mass surrounding an underground excavation is shown in Fig. 1. Which model will apply in a given case will depend on the size of the excavation relative to the discontinuity

Note.—Discussion open until February 1, 1981. To extend the closing date one month, a written request must be filed with the Manager of Technical and Professional Publications, ASCE. This paper is part of the copyrighted Journal of the Geotechnical Engineering Division, Proceedings of the American Society of Civil Engineers, Vol. 106, No. GT9, September, 1980. Manuscript was submitted for review for possible publication on October 25, 1979.

¹Principal, Golder Associates, Vancouver, Canada.

²Prof. of Rock Mechanics, Dept. of Mineral Resources Engrg., Imperial Coll. of Sci. & Tech., London, England.

spacing, the boundary conditions, the imposed stress level, and the orientations and strengths of discontinuities.

A significant proportion of past rock mechanics research effort has been devoted to the search for strength criteria for use in one or more of the classes of design problem previously described. Two general classes of strength criterion have been used—empirical criteria (3,5,25) and criteria based on mechanistic or physical models of the deformation or fracture processes involved (22,26,28,38), or both. Clearly, a fundamental mechanistic approach is to be preferred. However, it must be acknowledged that despite the attention that the subject has received and the volume of the resulting literature, a basic rock mass strength criterion suitable for general practical application, has not been developed as yet.

Because of this, the writers have reexamined the available experimental data in an attempt to develop an empirical strength criterion for rocks and rock

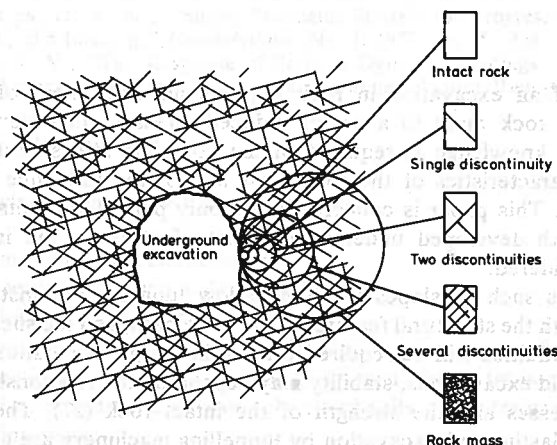


FIG. 1.—Transition from Intact Rock to Heavily Jointed Rock Mass with Increasing Sample Size

masses for use in excavation design. Ideally, such a criterion should:

1. Adequately describe the response of intact rock material to the full range of stress conditions likely to be encountered in practice.
2. Be capable of accounting for anisotropic strength behavior associated with the existence of planes of weakness.
3. Provide some indication, even if approximate, of the likely strength of a full-scale rock mass containing several sets of discontinuities.

GENERAL EMPIRICAL STRENGTH CRITERION

Examination of a wide range of experimental data for intact rock and rock discontinuities, and the very much more limited range of data available for jointed rock masses, shows that the relationships between major and minor principal stresses and between shear and normal stresses at failure (defined here as the attainment of peak stress), are generally nonlinear. By analogy

with the nonlinear failure envelope predicted by classical Griffith crack theory for plane compression (28) and by using a process of trial and error, the writers have developed the following empirical relationship between the principal stresses at failure:

$$\frac{\sigma_1}{\sigma_c} = \frac{\sigma_3}{\sigma_c} + \sqrt{m \frac{\sigma_3}{\sigma_c} + s} \quad (1)$$

in which σ_1 = the major principal stress at failure; σ_3 = the minor principal stress; σ_c = the uniaxial compressive strength of the intact rock material; and m and s = constants that depend on the properties of the rock and on the extent to which it had been broken before being subjected to the failure stresses σ_1 and σ_3 .

For conciseness, Eq. 1 may be rewritten in the form

$$\sigma_{1n} = \sigma_{3n} + \sqrt{m \sigma_{3n} + s} \quad (2)$$

in which σ_{1n} and σ_{3n} are the values of the principal stresses normalized with respect to σ_c ($\sigma_{1n} = \sigma_1/\sigma_c$, $\sigma_{3n} = \sigma_3/\sigma_c$).

By putting $\sigma_3 = 0$ in Eq. 1, the uniaxial compressive strength of the rock is obtained as

$$\sigma_{cs} = \sqrt{s \sigma_c^2} \quad (3)$$

For intact rock material, $s = 1.0$ and $\sigma_{cs} = \sigma_c$ as required. For previously broken rock, $s < 1$ and the compressive strength at zero, confining pressure is given by Eq. 3. It must be emphasized that σ_c is the uniaxial compressive strength of the *intact* rock material making up the specimen. For a completely granulated specimen or a rock aggregate, $s = 0$.

The uniaxial tensile strength of a specimen is found by putting $\sigma_1 = 0$ in Eq. 1 and solving the resulting equation for $\sigma_3 = \sigma_t$ to obtain

$$\sigma_t = \frac{\sigma_c}{2} (m - \sqrt{m^2 + 4s}) \quad (4)$$

When $s = 0$, $\sigma_t = 0$ as would be expected for completely broken material. For intact rock material with $s = 1.0$ and $m \gg 1$, $m \approx \sigma_c/|\sigma_t|$. However, because of the difficulty involved in adopting the uniaxial tensile strength as a fundamental rock property (23), it is preferable to treat m simply as an empirical curve fitting parameter. The value of m will decrease as the degree of prior fracturing of a specimen increases.

Although for many design applications, it will be appropriate to express the rock strength criterion in terms of principal stresses, for cases involving shear failure on a single surface or in a narrow zone, a criterion expressed in terms of the shear and normal stresses on the slip surface may be required. Using the relationship between normal and shear stresses on the critical plane derived by Balmer (2) for a general nonlinear failure criterion, it is found that the normal stress, σ , and the shear strength, τ , defined in Fig. 2, can be written as

$$\sigma = \sigma_3 + \frac{\tau_m^2}{\tau_m + \frac{m \sigma_c}{8}} \quad (5)$$

$$\text{and } \tau = (\sigma - \sigma_3) \sqrt{1 + \frac{m\sigma_c}{4\tau_m}} \dots \dots \dots (6)$$

$$\text{in which } \tau_m = \frac{1}{2} (\sigma_1 - \sigma_3) \dots \dots \dots (7)$$

From Fig. 2 it can be seen that the normalized values of σ and τ , $\sigma_n = \sigma/\sigma_c$ and $\tau_n = \tau/\sigma_c$, may be related by an equation of the form

$$\tau_n = A (\sigma_n - \sigma_{tn})^B \dots \dots \dots (8)$$

in which σ_{tn} = the normalized tensile strength of the rock given by

$$\sigma_{tn} = \frac{1}{2} (m - \sqrt{m^2 + 4s}) \dots \dots \dots (9)$$

and A and B = constants depending upon the value of m .

In developing the criterion, it has been assumed that the intermediate principal stress will have a negligible influence on failure conditions. This may be less

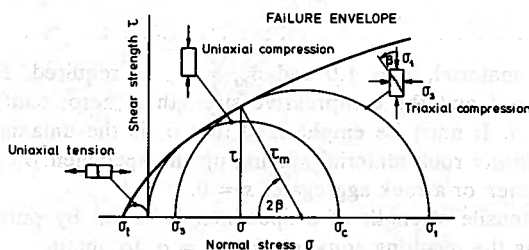


FIG. 2.—Failure Envelope Showing Relationships between Stress Components

acceptable for jointed rock than it is for intact isotropic rock material (49). The criterion has been expressed in terms of total or applied stresses. The effective stress form of the criterion that allows pore—or joint—water pressures to be accounted for can be obtained simply by substituting the effective stresses σ'_1 and σ'_3 for the total stresses σ_1 and σ_3 in the preceding equations. The parameters m and s determined from the effective stress form of the strength criterion will not be necessarily the same as those evaluated in terms of total stresses.

APPLICATION TO ISOTROPIC ROCK MATERIAL

In order to check the applicability of the empirical strength criterion to isotropic rock material, published triaxial test data for a variety of rock types were analyzed. Only those data that were found to be well supported by details of the experimental techniques used were included in the analysis.

It is well recognized that the behavior of most rocks changes from brittle to ductile at some elevated confining pressure, defined by Byerlee (15) as the brittle-ductile transition pressure. Not only does the shape of the stress-strain

curve change at this pressure, but the mechanism of deformation also changes in the transition zone (54). Therefore, it cannot be expected that a strength criterion developed for application in the brittle range should be equally applicable in the ductile range. Mogi (42) found that the brittle-ductile transition for most rocks could be defined approximately by the intersection of the line

$$\sigma_1 = 3.4 \sigma_3 \quad \dots \dots \dots (10)$$

with the principal stress failure envelope. Accordingly, only those data sets containing five or more experimental points well spaced in the stress space defined by $\sigma_1 < \sigma_3 < \sigma_1/3.4$ were accepted for analysis. All data analyzed were for oven- or air-dried samples except where otherwise stated in Table 1.

For intact rock material, $s = 1.0$, and the normalized form of the strength

TABLE 1.—Values of Strength Parameter m for Intact Rock Materials ($s = 1.0$)

Rock type (1)	Data from reference numbers (2)	Number of data points (3)	Range of σ_c , in pounds per square inch (4)	m (5)	Coefficient of determi- nation, r^2 (6)
Limestone	21, 41, 51	84	6,380–29,200	5.4	0.68
Dolomite	9, 43	25	21,500–73,400	6.8	0.90
Mudstone	5, 41	34	— ^a	7.3	0.82
Marble	11, 12, 21, 36, 51, 54	105	7,210–19,300	10.6	0.90
Sandstone	1, 5, 8, 21, 32, 36, 41, 48, 50, 51	375	5,790–57,800	14.3	0.87
Dolerite	9, 21, 27	51	42,600–83,000	15.2	0.97
Quartzite	5, 27, 41	59	32,900–47,500	16.8	0.84
Chert	27	24	84,000	20.3	0.93
Norite	5	17	— ^a	23.2	0.97
Quartz-diorite	12	10	27,300 (saturat- ed)—35,200 (dry)	23.4	0.98
Gabbro	12	10	29,700 (saturat- ed)—50,900 (dry)	23.9	0.97
Gneiss	12	10	26,700 (parallel fo- liation)—25,900 (perpendicular foliation)	24.5	0.91
Amphibolite	36	10	21,300 (parallel fo- liation)—29,200 (perpendicular foliation)	25.1	0.98
Granite	9, 21, 23, 41, 43, 51, 53	109	16,900–50,000	27.9	0.99

^aSource data in Ref. 5 given in normalized form.

Note: 1 psi = 6.9 kPa.

criterion becomes

$$\sigma_{1n} = \sigma_{3n} + \sqrt{m\sigma_{3n} + 1.0} \quad \dots \dots \dots (11)$$

A linear regression analysis was used to determine the values of σ_c and m giving the best fit of Eq. 11 to each individual set of data obtained by a given writer for a particular rock type. These individual sets of data were then grouped according to rock type. Each data set was normalized using its own value of σ_c , and a further linear regression analysis was carried out to determine the value of m giving the best overall fit for each rock type.

Table 1 summarizes the results obtained from this analysis. Typical normalized plots of principal stresses at failure (taken to correspond with the peak value of σ_1) are shown in Figs. 3 and 4 for sandstones and granites, respectively. The grouping and analysis of data according to rock type has obvious disadvan-

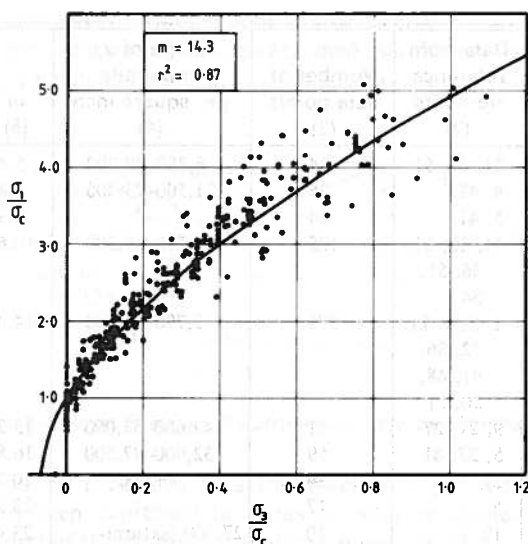


FIG. 3.—Normalized Failure Envelope for Sandstones

tages. Detailed studies of rock strength and fracture indicate that factors such as mineral composition, grain size and angularity, grain packing patterns and the nature of cementing materials between grains, all influence the manner in which fracture initiates and propagates (45). If these factors are relatively uniform within a given rock type, then it might be expected that a single curve would give a good fit to the normalized strength data with a correspondingly high value of the coefficient of determination, r^2 . Such a result is shown for granite in Fig. 4. If, on the other hand, these factors are quite variable from one occurrence of a given rock type to another, then a wider scatter of data points and a poorer fit by a single curve might be anticipated. Table 1 shows that for sandstone (Fig. 3) where grain size, porosity and the nature of the cementing material can vary widely, and for limestone that is a name given to a wide

variety of carbonate rocks, the values of r^2 are, indeed, quite low.

Despite these difficulties and the sometimes arbitrary allocation of a particular name to a given rock, the results shown in Table 1 do serve an important practical purpose. By using the approximate value of m found to apply for a particular rock type, it may be possible to carry out preliminary design calculations on the basis of no testing other than a determination of a suitable value of σ_c made using a simple test such as the point load test (5). A value of σ_c is required as a scaling factor to determine the strength of a particular sample of rock. Thus, although the same value of m may apply to the granites tested by Schwartz (51) and Brace (9), respectively, the strengths of the two rocks at a given confining pressure can differ by a factor of three.

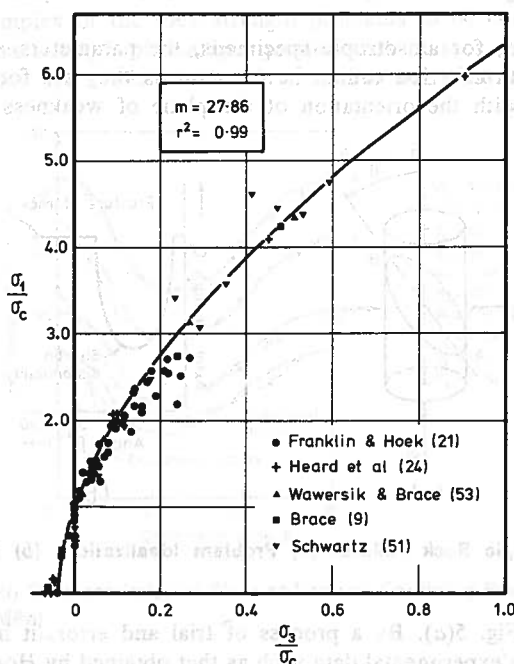


FIG. 4.—Normalized Failure Envelope for Granites

Rock types are listed in Table 1 in increasing order of the value of the parameter m . There is clearly some general pattern to the relationship between intact rock type and m . These and other results not included in the tabulation because of their limited range suggest that m increases with rock type in the following general way: (1) $m \approx 7$ —Carbonate rocks with well developed crystal cleavage (dolomite, limestone, marble); (2) $m \approx 10$ —lithified argillaceous rocks (mudstone, siltstone, shale, slate); (3) $m \approx 15$ —arenaceous rocks with strong crystals and poorly developed crystal cleavage (sandstone, quartzite); (4) $m \approx 17$ —fine-grained polyminerallic igneous crystalline rocks (andesite, dolerite, diabase, rhyolite); and (5) $m \approx 25$ —coarse-grained polyminerallic igneous and metamorphic rocks (amphibolite, gabbro, gneiss, granite, norite, quartz-diorite).

APPLICATION TO ANISOTROPIC ROCK

The influence of single discontinuities or planes of weakness on the strength of otherwise intact rock has been widely investigated. Jaeger's single plane of weakness theory (31), developed for the case shown in Fig. 5(a), postulates two independent failure modes, slip on the discontinuity and shear fracture of the intact rock material, depending on the orientation of the discontinuity to the principal stress directions; see Fig. 5(b). This behavior is reasonably well represented in specimens containing a single open joint or an artificially induced discontinuity (31). The behavior of anisotropic rock such as slate or shale is more complex than that allowed for by this theory, with specimen strengths varying continuously with the orientation of the planes of weakness (18,26,40).

It is clear that, for anisotropic specimens, the parameters m and s in the empirical strength criterion cannot be constant as they are for isotropic rock but must vary with the orientation of the plane of weakness as defined by

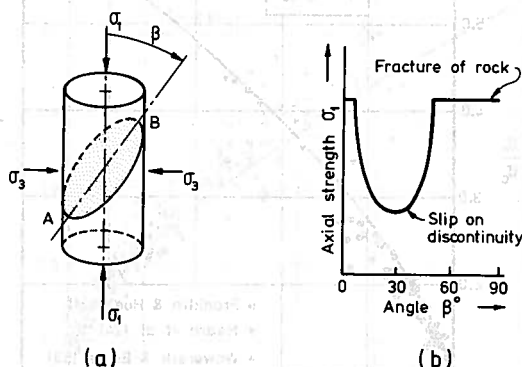


FIG. 5.—Anisotropic Rock Failure: (a) Problem Idealization; (b) $\sigma_1 - \beta$ Failure Characteristic

the angle β in Fig. 5(a). By a process of trial and error, it has been found that a good fit to experimental data such as that obtained by Hoek (26), Donath (18) and McLamore and Gray (40) can be obtained by putting

$$m = m_i [1 - N_1 \exp(-\theta)^4] \quad (12)$$

$$\text{and } s = 1 - P_1 \exp(-\zeta)^4 \quad (13)$$

in which m_i = the value of m for intact rock determined for $\beta = 90^\circ$; and

$$\theta = \frac{\beta - \beta_m}{N_2 + N_3 \beta} \quad (14a)$$

$$\zeta = \frac{\beta - \beta_s}{P_2 + P_3 \beta} \quad (14b)$$

where β_m = the value of β at which m is a minimum; β_s = the value of β at which s is a minimum; and N_1, N_2, N_3, P_1, P_2 , and P_3 = constants.

An example of the application of this approach to the triaxial test data obtained for a slate by McLamore and Gray (40) is shown in Fig. 6. It is hardly surprising that a reasonable fit to the data can be obtained given the large number of parameters and constants involved in the anisotropic formulation of the empirical strength criterion. Indeed, it is unlikely that this approach would be particularly useful in practice given that reasonable fits to experimental data can be obtained with less complicated approaches (26,31,40). However, the results obtained do show that the general criterion can be modified to take account of anisotropic strength behavior.

APPLICATION TO MULTIPLY JOINTED ROCK

The most complex of the rock strength problems to be considered here is that of the mass strength of multiply jointed rock masses. Very little direct experimental data are available for this case, but some understanding of the

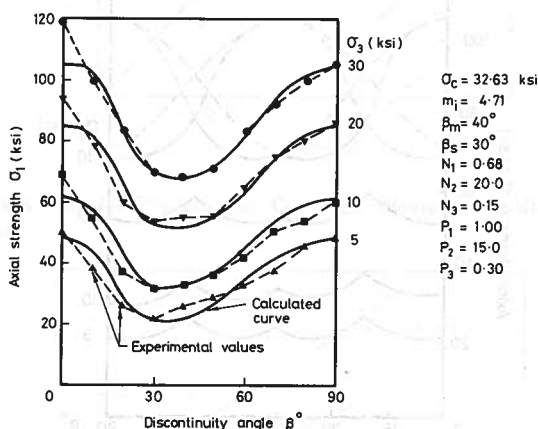


FIG. 6.—Strength Characteristics of Slate at Various Confining Pressures; Note Ref. 40 (1 ksi = 6.9 MPa)

problem can be gained from the results of laboratory model studies (13,14,16,19,35,38). These studies show that a great number of failure modes are possible in jointed rock (13,14), and that the internal distribution of stresses within a jointed rock mass can be highly complex (16). Of particular interest is the finding that, even where failure takes place not along the discontinuities but through the intact rock material, the strength of a jointed mass may be considerably less than that of the unjointed material tested under otherwise identical conditions (13,19). The relative strength reduction measured in triaxial compression tests decreases with increasing confining pressure (13). The quantification of these effects in natural rock masses remains an outstanding problem in rock engineering.

The influence of multiple discontinuities on rock mass strength in a somewhat different case can be illustrated by reconsidering the data for a slate presented in Fig. 6. Assume that, instead of containing one set of planes of weakness, the specimens contain a number of identical sets oriented at equal angles to

each other. It is possible to apply Jaeger's theory in several parts to construct a set of σ_1 versus β characteristics for the composite specimens for the values of σ_3 , represented in Fig. 6. The solution for the case of four identical sets of planes of weakness is shown in Fig. 7. In this case, it is found that failure will always take place by slip on one of the planes of weakness. It will be noted that, to a very good first approximation, the strength of this hypothetical rock mass may be considered to be isotropic. A composite failure envelope for this case, constructed using the minimum strength developed for each value of σ_3 , yields the parameters $m = 1.48$ and $s = 0.007$ with $\sigma_c = 32,630$ psi (225 MPa) measured for $\beta = 90^\circ$; for the intact rock material, $m = 4.71$ and $s = 1.0$.

The result shown in Fig. 7 suggests that if a rock mass contains four or more sets of discontinuities having similar properties, it may be possible to

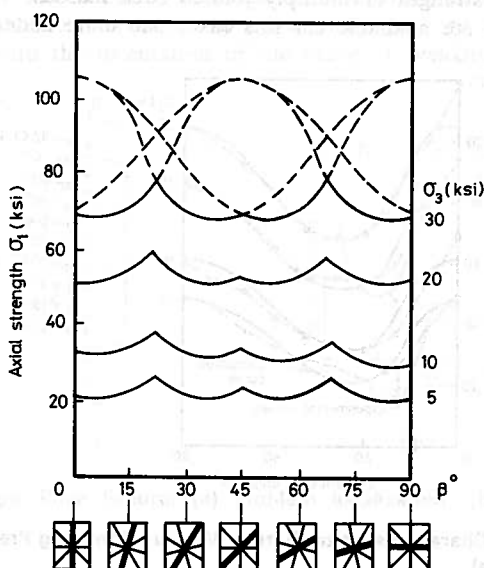


FIG. 7.—Hypothetical Composite Strength Characteristics for Slate Containing Four Identical Sets of Discontinuities (1 ksi = 6.9 MPa)

assume the strength of the rock mass to be isotropic. This will not be the case when one of the discontinuities has a more pronounced influence than the others because of a greater persistence or a lower shear strength due to the presence of gouge, for example.

It is to be expected that the presence of one or more sets of discontinuities in a rock mass will cause a reduction in the values of both m and s . Unfortunately, relatively few sets of reliable triaxial test data for jointed rock are known to exist, and so the choice of m and s for a given rock mass must be based on the very few sets of data available as well as back-analysis of documented cases of rock mass failure and a good measure of judgment. Such data as are available to the writers will be considered in some detail since the lessons

to be learned from them are vital to the development of an understanding of the way in which the parameters m and s vary with rock mass characteristics.

The presence of fractures in a rock mass results in a decrease in both m and s below the intact values because of the greater freedom of movement made available to individual pieces of rock material. This effect can be seen

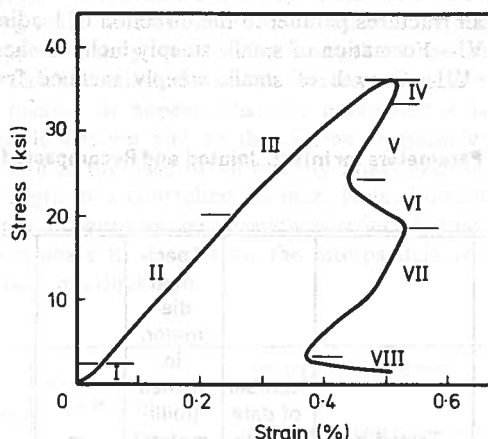


FIG. 8.—Complete Uniaxial Stress-Strain Curve for Westerly Granite; Note Ref. 53 (1 ksi = 6.9 MPa)

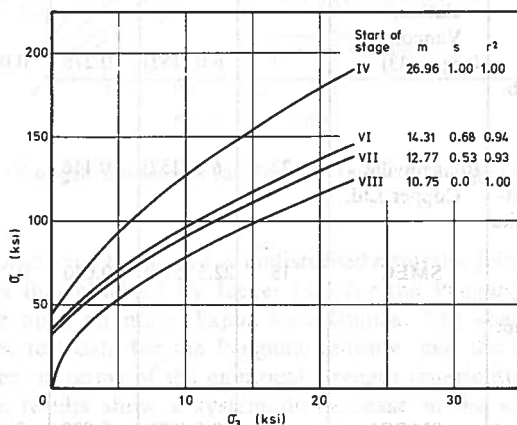


FIG. 9.—Strength Envelopes for Various Stages of Triaxial Tests on Westerly Granite (1 ksi = 6.9 MPa)

in the results of a series of triaxial compression tests carried out on Westerly granite by Wawersik and Brace (53). A stiff testing machine and special testing techniques were used so that the progressive failure of the specimens could be studied. A complete uniaxial stress-strain curve for Westerly granite is shown in Fig. 8. Wawersik and Brace identified a number of well-defined stages in the breakdown process on this and other curves. The same series of stages

could be identified in triaxial compression tests carried out at seven different confining pressures, although the relative importance of the various stages changed with the confining pressure.

For the present analysis, the following stages of each test were used:

1. Start of stage IV—Maximum stress associated with the formation of a large number of small fractures parallel to the direction of loading.
2. Start of stage VI—Formation of small, steeply inclined shear fractures.
3. Start of stage VII—Growth of small, steeply inclined fractures into an open fault.

TABLE 2.—Strength Parameters for Intact, Jointed and Recompacted Panguna Andesite

Specimen description (1)	Tested by (2)	Number of data points (3)	Specimen diameter, in inches (millimeters) (4)	m (5)	s (6)	Coefficient of determination r^2 (7)
Intact fresh rock material	Jaeger (33) Golder Association, Vancouver	5	2.0 (51) 4.0 (102)	18.9	1.00	0.85
Undisturbed closely jointed samples obtained using triple tube core barrel	Jaeger (33)	7	6.0 (152)	0.278	0.0002	0.99
Graded mine bench samples recompacted to close to in situ unit weight	Bougainville Copper Ltd.	72	6.0 (152)	0.116	0	—
Fresh to slightly weathered rock recompacted to a unit weight of 127.5–129.4 pcf (2.04–2.07 t/m ³)	SMEC*	15	22.5 (572)	0.040	0	—
Moderately weathered rock recompacted to a unit weight of 124.3 pcf (1.99 t/m ³)	SMEC*	5	22.5 (572)	0.030	0	—
Highly weathered rock recompacted to a unit weight of 101.5 pcf (1.63 t/m ³)	SMEC*	3	22.5 (572)	0.012	0	—

*Snowy Mountains Engineering Corporation

4. Start of stage VIII—Attainment of the residual strength of loose, broken material held together by friction between the particles.

Each of these points was identified on the stress-strain curve obtained at each confining pressure and the corresponding relationship between the principal stresses plotted (Fig. 9). As shown on Fig. 9, both m and s decrease as the degree of fracturing of the initially intact rock increases. The value of m decreases by a factor of approximately two as the strength of the rock reduces from peak to residual. This is a relatively modest decrease compared with that found for natural rock masses. It appears that the parameter m is sensitive to the angle of interparticle friction and to the degree of particle interlocking that is still relatively high in the case of an initially intact granite specimen loaded to its residual strength in a controlled manner. Note, however, that the value of s decreases from 1.0—zero as the strength is reduced from peak to residual. The parameter s appears to depend on the interparticle tensile strength and the degree of particle interlocking.

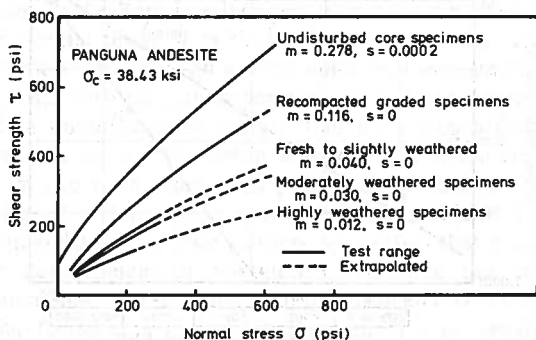


FIG. 10.—Shear Strength Envelopes for Triaxial Tests on Panguna Andesite (1 psi = 6.9 kPa)

The only set of triaxial test data for undisturbed naturally jointed rock known to the writers is that obtained by Jaeger (33) for the Panguna andesite from the Bougainville open pit mine, Papua-New Guinea. The sources and nature of this and other test data for the Panguna andesite, and the results obtained by analyzing them in terms of the empirical strength criterion, are summarized in Table 2. The results show a systematic decrease in the values of m and s with increasing fragmentation and weathering of the samples (Fig. 10).

A decrease in values of m and s with increased jointing intensity was also found by reanalyzing the results of laboratory tests on models of jointed rock (13,19,35) and the case history data presented by Brady (10). Although insufficient data are presented to enable complete analyses to be carried out, John (34), Manev and Avramova-Tacheva (39) and Muller (44) all present information for natural rock masses that indicate similar trends.

It is apparent that, although trends are clearly indicated, the test data available are insufficient to permit the determination of a set of parameters that could be used to quantify the full range of rock mass strength behavior. Indeed,

it is most unlikely that, because of the complexity and expense of obtaining it, such data will ever become available. Accordingly, some other aid must be sought in the development of a means of predicting rock mass strengths. One possible approach is to use the well-known rock mass quality classification schemes developed by Barton, Lien and Lunde (4) of the Norwegian Geotechnical Institute (NGI) and Bieniawski (6), lately of the South African Council for Scientific and Industrial Research (CSIR). Fundamental objections can be raised to the use of these classification schemes in engineering design in that they do not address the mechanics of engineering problems. However they have the advantage of providing reasonably consistent quantification of rock mass quality based on data that can be collected or estimated in the site investigation phase of a construction project.

Fig. 11 shows plots of the parameter s and the ratio m/m_i , in which m_i is the value of the parameter m for intact rock material, against the NGI and

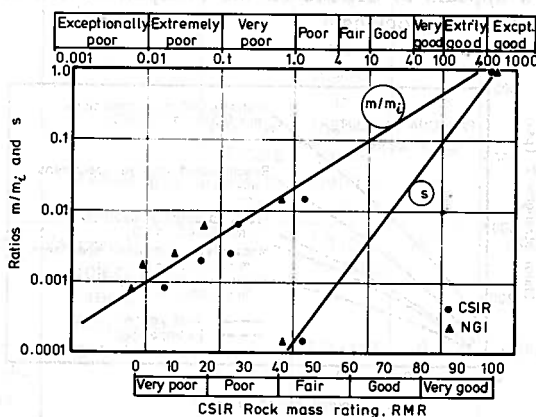


FIG. 11.—Plots of m/m_i and s for Panguna Andesite against Rock Mass Classifications.

CSIR classification ratings estimated for the various categories of Panguna andesite listed in Table 2. Bieniawski (7) proposed the following relationship between the NGI quality index, Q , and the CSIR rock mass rating, RMR:

$$\text{RMR} = 9 \ln Q + 44 \quad (15)$$

This relationship was used in positioning the scales in Fig. 11.

Despite the paucity and approximate nature of the data, straight lines were drawn on Fig. 11 to give approximate relationships between s and m/m_i and the classification ratings. Using these relationships and the limited experimental data available as guides, approximate relationships between rock type, rock quality and normalized strength were developed (Table 3). In any given case the uniaxial compressive strength of approx 2.0 in. (51 mm) diameter samples of fresh intact rock material will be required to apply to the calculated normalized strength as a scaling factor. The rock mass strengths so obtained are intended to include an allowance for the scale effect in rock material strength.

It must be strongly emphasized that the relationships set out in Table 3 are based on very sparse data and are therefore very approximate; they should

be used only as rough guides in preliminary design calculations. Where rock or rock mass failure is likely to be an important consideration in the design of a structure, every attempt should be made to determine the required strength parameters by laboratory and in situ testing and by observations of the full-scale performance of the rock mass around trial excavations (10). The strength relationships given in Table 3 should not be used in cases in which slip is considered likely to take place on one or two dominant planes of weakness.

PRACTICAL APPLICATIONS

The empirical strength criterion has been used successfully in a number of projects involving slopes and underground excavations in rock. Programs for digital computers and programmable calculators have been readily modified to incorporate the nonlinear strength criterion. Generally, the approach has been used for preliminary design calculations in cases in which rock mass strength parameters have had to be estimated from Table 3 using site investigation data to assess rock mass quality. An exception to this general rule was a slope stability analysis for the Bougainville open pit mine in which strength parameters obtained from triaxial test results (Table 2) could be used. The application of the criterion in slope stability and underground excavation analyses will follow.

The criterion has also been incorporated into the ground-support interaction analyses used in tunnel support design. Ladanyi's closed-form solution for a concrete lining to a circular tunnel in a hydrostatic stress field (37) has been modified so that short- and long-term peak and residual strengths of the rock mass are expressed in terms of the new criterion. Ladanyi's approach to the problem is distinguished from many others by the fact that it includes a realistic model of the development of volumetric strains in the failing rock mass surrounding the tunnel. The resulting solution has been coded for a programmable calculator. The formulations used by Daemen (17) in developing numerical solutions to a number of more complex ground-support interaction problems have also been modified to incorporate the empirical rock mass strength criterion.

Slope Stability.—The nonlinear criterion can be incorporated into standard slope stability programs such as those that analyze circular or noncircular slips using Bishop's or Janbu's methods. Since this class of slope stability problem involves shear failure of the rock mass along a continuous slip surface, the shear strength-normal stress form of the criterion (Eq. 8) is used. In modifying existing programs, it is most convenient to define instantaneous values of cohesion, c_i , and friction angle, ϕ_i , from the tangent to the shear strength (τ)—normal stress (σ) curve at the appropriate value of normal stress. These values are given by

$$\tan \phi_i = AB \left(\frac{\sigma}{\sigma_c} - \frac{\sigma_i}{\sigma_c} \right)^{B-1} \dots \dots \dots (16)$$

$$\text{and } c_i = \tau - \sigma \tan \phi_i \dots \dots \dots (17)$$

in which σ_i and τ can be calculated from Eqs. 9 and 8, respectively, for the assumed values of A , B and σ_c . Rather than being constants for the jointed rock mass as assumed by Bieniawski (6) and Stimpson and Ross-Brown (52), c_i and ϕ_i will vary with stress level and so must be calculated individually

TABLE 3.—Approximate Strength Criteria

Rock quality (1)	Carbonate rocks with well devel- oped crystal cleavage (dolo- mite, limestone and marble) (2)	Lithified argill- aceous rocks, (mudstone, siltstone, shale and slate norite and quartz-diorite) (3)
Intact rock samples—laboratory size rock specimens free from structural defects (CSIR rating 100+; NGI rating 500)	$\sigma_{1n} = \sigma_{3n} + \sqrt{7\sigma_{3n} + 1.0}$ $\tau_n = 0.816(\sigma_n + 0.140)^{0.658}$	$\sigma_{1n} = \sigma_{3n} + \sqrt{10\sigma_{3n} + 1.0}$ $\tau_n = 0.918(\sigma_n + 0.099)^{0.677}$
Very good quality rock mass— tightly interlocking undis- turbed rock with unweathered joints spaced at 3 m \pm (CSIR rating 85; NGI rating 100)	$\sigma_{1n} = \sigma_{3n} + \sqrt{3.5\sigma_{3n} + 0.1}$ $\tau_n = 0.651(\sigma_n + 0.028)^{0.679}$	$\sigma_{1n} = \sigma_{3n} + \sqrt{5\sigma_{3n} + 0.1}$ $\tau_n = 0.739(\sigma_n + 0.020)^{0.692}$
Good quality rock mass—fresh to slightly weathered rock, slightly disturbed with joints spaced at 1 m–3 m (CSIR rat- ing 65; NGI rating 10)	$\sigma_{1n} = \sigma_{3n} + \sqrt{0.7\sigma_{3n} + 0.004}$ $\tau_n = 0.369(\sigma_n + 0.006)^{0.669}$	$\sigma_{1n} = \sigma_{3n} + \sqrt{1.0\sigma_{3n} + 0.004}$ $\tau_n = 0.427(\sigma_n + 0.004)^{0.683}$
Fair quality rock mass—several sets of moderately weathered joints spaced at 0.3 m–1 m (CSIR rating 44; NGI rating 1.0)	$\sigma_{1n} = \sigma_{3n} + \sqrt{0.14\sigma_{3n} + 0.0001}$ $\tau_n = 0.198(\sigma_n + 0.0007)^{0.662}$	$\sigma_{1n} = \sigma_{3n} + \sqrt{0.20\sigma_{3n} + 0.0001}$ $\tau_n = 0.234(\sigma_n + 0.0005)^{0.675}$
Poor quality rock mass— numerous weathered joints spaced at 30 mm–500 mm with some gouge filling/clean waste rock (CSIR rating 23; NGI rating 0.1)	$\sigma_{1n} = \sigma_{3n} + \sqrt{0.04\sigma_{3n} + 0.00001}$ $\tau_n = 0.115(\sigma_n + 0.0002)^{0.646}$	$\sigma_{1n} = \sigma_{3n} + \sqrt{0.05\sigma_{3n} + 0.00001}$ $\tau_n = 0.129(\sigma_n + 0.0002)^{0.655}$
Very poor quality rock mass— numerous heavily weathered joints spaced less than 50 mm with gouge filling/waste rock with fines (CSIR rating 3; NGI rating 0.01)	$\sigma_{1n} = \sigma_{3n} + \sqrt{0.007\sigma_{3n} + 0}$ $\tau_n = 0.042(\sigma_n)^{0.534}$	$\sigma_{1n} = \sigma_{3n} + \sqrt{0.010\sigma_{3n} + 0}$ $\tau_n = 0.050(\sigma_n)^{0.539}$

for each slice in slope stability analyses.

As an example, consider a fair quality argillaceous rock mass for which Table 3 gives the normalized shear strength criterion as

$$\tau_n = 0.234(\sigma_n + 0.0005)^{0.675} \quad (18)$$

In this case, $A = 0.234$; $B = 0.675$; and $\sigma_t/\sigma_c = -0.0005$. The resulting normalized shear strength envelope is shown in Fig. 12(a). Note that the unconfined compressive strength of the rock mass is estimated as $0.01 \sigma_c$. Fig. 12(b) shows the variation in instantaneous cohesion and instantaneous angle of friction with normal stress for $\sigma_c = 5,000$ psi (34.5 MPa).

In the stability analyses carried out to date, parameters given in Table 3 have been used for both total and effective stress analyses. As previously noted, it is likely that the total and effective stress values of the parameters m , s , A and B will differ. Because of the lack of adequate field or laboratory data,

for Intact Rock and Jointed Rock Masses

Arenaceous rocks with strong crystals and poorly developed crystal cleavage (sandstone and quartzite) (4)	Fine grained polymineralic igneous crystalline rocks, (andesite, dolerite, diabase and rhyolite) (5)	Coarse grained polymineralic igneous and metamorphic crystalline rocks (amphibolite, gabbro, gneiss, granite, norite and quartz-diorite) (6)
$\sigma_{1n} = \sigma_{3n} + \sqrt{15\sigma_{3n} + 1.0}$ $\tau_n = 1.044(\sigma_n + 0.067)^{0.692}$	$\sigma_{1n} = \sigma_{3n} + \sqrt{17\sigma_{3n} + 1.0}$ $\tau_n = 1.086(\sigma_n + 0.059)^{0.696}$	$\sigma_{1n} = \sigma_{3n} + \sqrt{25\sigma_{3n} + 1.0}$ $\tau_n = 1.220(\sigma_n + 0.040)^{0.705}$
$\sigma_{1n} = \sigma_{3n} + \sqrt{7.5\sigma_{3n} + 0.1}$ $\tau_n = 0.848(\sigma_n + 0.013)^{0.702}$	$\sigma_{1n} = \sigma_{3n} + \sqrt{8.5\sigma_{3n} + 0.1}$ $\tau_n = 0.883(\sigma_n + 0.012)^{0.705}$	$\sigma_{1n} = \sigma_{3n} + \sqrt{12.5\sigma_{3n} + 0.1}$ $\tau_n = 0.998(\sigma_n + 0.008)^{0.712}$
$\sigma_{1n} = \sigma_{3n} + \sqrt{1.5\sigma_{3n} + 0.004}$ $\tau_n = 0.501(\sigma_n + 0.003)^{0.695}$	$\sigma_{1n} = \sigma_{3n} + \sqrt{1.7\sigma_{3n} + 0.004}$ $\tau_n = 0.525(\sigma_n + 0.002)^{0.698}$	$\sigma_{1n} = \sigma_{3n} + \sqrt{2.5\sigma_{3n} + 0.004}$ $\tau_n = 0.603(\sigma_n + 0.002)^{0.707}$
$\sigma_{1n} = \sigma_{3n} + \sqrt{0.30\sigma_{3n} + 0.0001}$ $\tau_n = 0.280(\sigma_n + 0.0003)^{0.688}$	$\sigma_{1n} = \sigma_{3n} + \sqrt{0.34\sigma_{3n} + 0.0001}$ $\tau_n = 0.295(\sigma_n + 0.0003)^{0.691}$	$\sigma_{1n} = \sigma_{3n} + \sqrt{0.50\sigma_{3n} + 0.0001}$ $\tau_n = 0.346(\sigma_n + 0.0002)^{0.700}$
$\sigma_{1n} = \sigma_{3n} + \sqrt{0.8\sigma_{3n} + 0.00001}$ $\tau_n = 0.162(\sigma_n + 0.0001)^{0.672}$	$\sigma_{1n} = \sigma_{3n} + \sqrt{0.09\sigma_{3n} + 0.00001}$ $\tau_n = 0.172(\sigma_n + 0.0001)^{0.676}$	$\sigma_{1n} = \sigma_{3n} + \sqrt{0.13\sigma_{3n} + 0.00001}$ $\tau_n = 0.203(\sigma_n + 0.0001)^{0.686}$
$\sigma_{1n} = \sigma_{3n} + \sqrt{0.015\sigma_{3n} + 0}$ $\tau_n = 0.061(\sigma_n)^{0.546}$	$\sigma_{1n} = \sigma_{3n} + \sqrt{0.017\sigma_{3n} + 0}$ $\tau_n = 0.065(\sigma_n)^{0.548}$	$\sigma_{1n} = \sigma_{3n} + \sqrt{0.025\sigma_{3n} + 0}$ $\tau_n = 0.078(\sigma_n)^{0.556}$

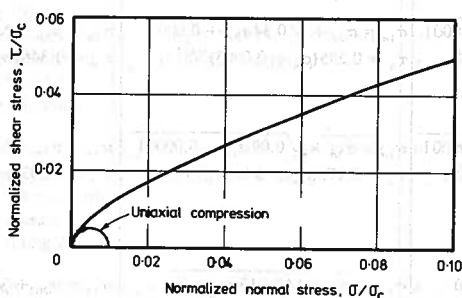
it has not been possible to determine appropriate effective stress parameters. Until this can be done, the values given in Table 3 should be used with σ_c always being measured for field moisture conditions.

Over-Stressed Zones Around Underground Excavations.—The criterion has been used in conjunction with elastic stress analyses to determine the likely extent of overstressed zones around underground excavations. This approach has been particularly useful in the early stages of the design of underground power stations, e.g., when little information about the properties and behavior of the rock mass is available, but design decisions have to be made about excavation shapes and dimensions.

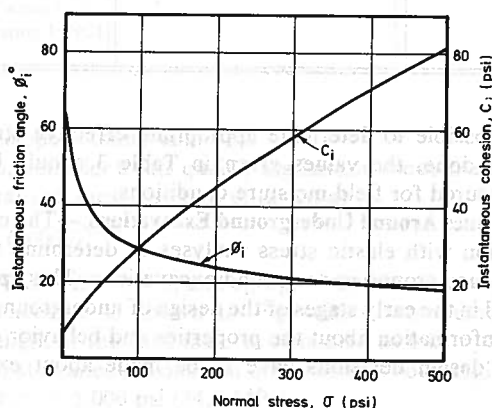
For this purpose, the principal stress form of the criterion has been incorporated into a computer program that uses an indirect formulation of the boundary element method to calculate the plane strain elastic stresses and displacements around underground excavations of any shape (20). The program allows solution

of problems involving deep excavations for which the stress fields may be considered constant with depth, and shallow excavations in which the stress fields are influenced by gravity. Having determined the principal stresses at a series of boundary and internal points, the program calculates the available strength at each point in terms of a major principal stress at failure from Eq. 2 or compressive failure and Eq. 4 or tensile failure, using the computed values of σ_3 and the values of σ_c , m and s chosen as input data. The rock mass strengths that can be developed at each point are then compared with the computed values of σ_1 (compression) or σ_3 (tension) to give a series of strength/stress ratios from which contours can be drawn and potentially over-stressed zones identified.

This approach uses a plane strain elastic stress analysis and does not allow for progressive failure or the post-peak stress-strain behavior of the rock mass. Accordingly, it cannot be expected to provide accurate solutions to all practical problems. Nevertheless, it has been found useful as a quick and inexpensive means of obtaining some indication of the likely behavior of a proposed excavation, particularly in the preliminary stages of design when a series of trial analyses may be required.



(a)



(b)

FIG. 12.—(a) Normalized Shear Strength Envelope for Fair Quality Argillaceous Rock Mass; (b) Variation of c_i and ϕ_i with Normal Stress (1 psi = 6.9 kPa)

As an example of the use of this simple approach, consider a powerhouse cavern to be excavated at a depth of 1210 ft (370 m) in a good quality gneiss. Site investigation data show that the rock material has an unconfined compressive strength of $\sigma_c = 21,750$ psi (150 MPa), the unit weight of rock mass is $\gamma = 170$ pcf (0.027 MN/m³), and the ratio of horizontal to vertical in situ stress at cavern depth is $k = 0.5$. For this rock mass, strength parameters of $m = 2.5$ and $s = 0.004$ are selected from Table 3.

Fig. 13 shows the strength/stress ratio contours calculated for three trial cavern shapes for these conditions. Fig. 13(a) shows a design popular in the 1950's and 1960's in which the cavern roof is supported by a full concrete arch. The arch reaction and the crane beams are supported by notched haunches cut into the cavern walls. The zone of overstressed rock indicated for this

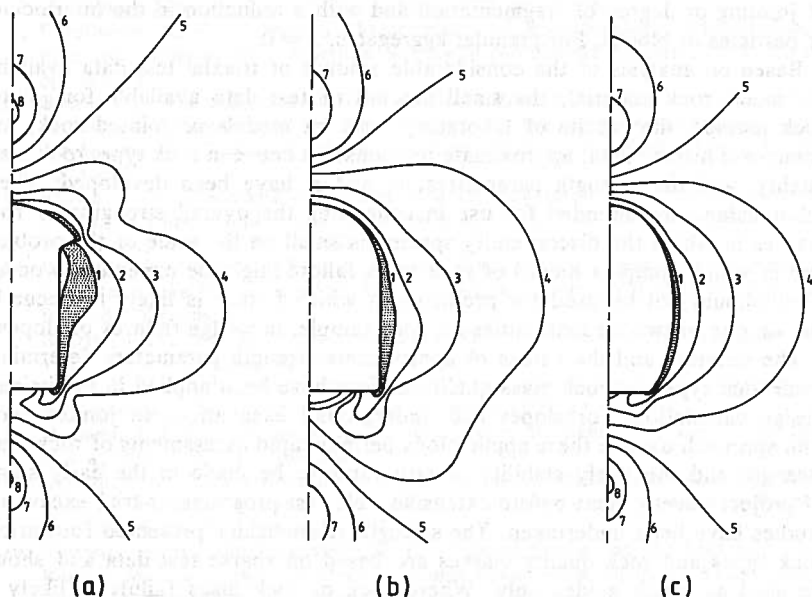


FIG. 13.—Influence of Cavern Shape on Strength/Stress Contours

case is unacceptably large. Long rockbolts could be used to stabilize the walls or, alternatively, the cavern shape could be changed to improve the induced stress distribution. By using rockbolts rather than a concrete arch to support the roof, and by supporting the crane beams on columns, the notch in the wall can be eliminated. As shown in Fig. 13(b), this results in a significant reduction in the volume of overstressed rock adjacent to the cavern wall. Further improvement can be achieved by slightly curving the walls as shown in Fig. 13(c). In this case, the relatively narrow strip of overstressed rock could probably be supported by short rockbolts or shotcrete, or both. If the cavern walls were curved as in Fig. 13(c), it would be necessary that the crane beams be anchored to the cavern walls. This approach offers many constructional advantages and is being increasingly used in cavern design.

SUMMARY AND CONCLUSIONS

A nonlinear empirical peak strength criterion for rocks and rock masses has been developed. The criterion uses the uniaxial compressive strength of the intact rock material as a scaling parameter, and introduces two dimensionless strength parameters, m and s . The parameter m appears to vary with rock type, the angle of interparticle or interblock friction, and the degree of particle interlocking within the rock mass. The parameter s appears to depend on the interparticle tensile strength and the degree of particle interlocking.

For isotropic intact rock material, $s = 1.0$ and m is a constant depending on rock type. For anisotropic rock, both m and s vary with the orientations of the planes of weakness to the principal stress directions. For highly jointed or fragmented rock, both m and s decrease with an increase in the intensity of jointing or degree of fragmentation and with a reduction in the interlocking of particles or blocks. For granular aggregates, $s = 0$.

Based on analysis of the considerable amount of triaxial test data available for intact rock material, the small amount of test data available for jointed rock masses, the results of laboratory tests on models of jointed rock, and some case history data, approximate relationships between rock type, rock mass quality, and the strength parameters, m and s , have been developed. These relationships are intended for use in estimating the overall strengths of rock masses in which the discontinuity spacing is small on the scale of the problem and in which complex modes of rock mass failure might be expected to occur. They should not be used for problems in which failure is likely to occur by slip on one or two discontinuities as, for example, in wedge failures of slopes.

The criterion and the values of approximate strength parameters determined from rock type and rock mass quality indices have been applied in preliminary design calculations for slopes and underground excavations in jointed rock. The approach used in these applications permits rapid assessments of rock mass strength and the likely stability of structures to be made in the early stages of project development before extensive field test programs or trial excavation studies have been undertaken. The strength relationships presented for various rock types and rock quality classes are based on sparse test data and should be used as rough guides only. Where rock or rock mass failure is likely to be an important design consideration, every attempt should be made to determine the required strength parameters by laboratory or in situ testing and by observations of the full-scale performance of the rock mass around trial excavations.

APPENDIX I.—REFERENCES

1. Aldrich, M. J., "Pore Pressure Effects on Berea Sandstone Subjected to Experimental Deformation," *Geological Society of America Bulletin*, Vol. 80, No. 8, Aug., 1969, pp. 1577-1586.
2. Balmer, G., "A General Analytical Solution for Mohr's Envelope," *Proceedings, American Society for Testing Materials*, Vol. 52, 1952, pp. 1260-1271.
3. Barton, N. R., "Review of a New Shear Strength Criterion for Rock Joints," *Engineering Geology*, Vol. 7, No. 4, Amsterdam, Holland, 1973, pp. 287-332.
4. Barton, N., Lien, R., and Lunde, J., "Engineering Classification of Rock Masses for the Design of Tunnel Support," *Rock Mechanics*, Vol. 6, No. 4, Vienna, Austria, Dec., 1974, pp. 189-236.
5. Bieniawski, Z. T., "Estimating the Strength of Rock Materials," *Journal of the South*

- African Institute of Mining and Metallurgy*, Vol. 74, No. 8, Johannesburg, South Africa, Mar., 1974, pp. 312-320.
6. Bieniawski, Z. T., "Rock Mass Classifications in Rock Engineering," *Proceedings of the Symposium on Exploration for Rock Engineering*, Z. T. Bieniawski, ed., Vol. 1, A. A. Balkema, Rotterdam, Holland, 1976, pp. 97-106.
 7. Bieniawski, Z. T., "Determining Rock Mass Deformability. Experience from Case Histories," *International Journal of Rock Mechanics and Mining Sciences*, Vol. 15, No. 5, Oct., 1978, pp. 237-247.
 8. Bodonyi, J., "Laboratory Tests on Certain Rocks under Axial Symmetrical Loading Conditions," *Proceedings of the Second Congress of the International Society for Rock Mechanics*, Vol. 1, Paper 2-17, Belgrade, Yugoslavia, 1970.
 9. Brace, W. F., "Brittle Fracture of Rocks," *State of Stress in the Earth's Crust*, W. R. Judd, ed., American Elsevier Publishing Co., New York, N.Y., 1964, pp. 111-174.
 10. Brady, B. H. G., "An Analysis of Rock Behaviour in an Experimental Stopping Block at the Mount Isa Mine, Queensland, Australia," *International Journal of Rock Mechanics and Mining Sciences*, Vol. 14, No. 2, Mar., 1977, pp. 59-66.
 11. Bredthauer, R. O., "Strength Characteristics of Rock Samples under Hydrostatic Pressure," *Transactions, American Society of Mechanical Engineers*, Vol. 79, 1957, pp. 695-708.
 12. Broch, E., "The Influence of Water on Some Rock Properties," *Advances in Rock Mechanics, Proceedings of the Third Congress of the International Society for Rock Mechanics*, Vol. 2, Part A, National Academy of Sciences, Washington, D.C., 1974, pp. 33-38.
 13. Brown, E. T., "Strength of Models of Rock with Intermittent Joints," *Journal of the Soil Mechanics and Foundations Division, ASCE*, Vol. 96, No. SM6, Proc. Paper 7697, Nov., 1970, pp. 1935-1949.
 14. Brown, E. T., "Modes of Failure in Jointed Rock Masses," *Proceedings of the Second Congress of the International Society for Rock Mechanics*, Vol. 2, 1970, Paper 3-42, Belgrade, Yugoslavia.
 15. Byerlee, J. D., "Brittle-Ductile Transition in Rocks," *Journal of Geophysical Research*, Vol. 73, No. 14, July, 1968, pp. 4741-4750.
 16. Chappell, B. A., "Load Distribution and Deformational Response in Discontinua," *Géotechnique*, Vol. 24, No. 4, London, England, 1974, pp. 641-654.
 17. Daemen, J. J. K., "Problems in Tunnel Support Mechanics," *Underground Space*, Vol. 1, No. 3, 1977, pp. 163-172.
 18. Donath, F. A., "Strength Variations and Deformational Behavior in Anisotropic Rock," *State of Stress in the Earth's Crust*, W. R. Judd, ed., American Elsevier Publishing Co., New York, N.Y., 1964, pp. 281-297.
 19. Einstein, H. H., and Hirschfeld, R. C., "Model Studies on Mechanics of Jointed Rock," *Journal of the Soil Mechanics and Foundations Division, ASCE*, Vol. 99, No. SM3, Proc. Paper 9610, Mar., 1973, pp. 229-248.
 20. Eissa, E. S. A., "Stress Analysis of Underground Excavations in Isotropic and Stratified Rock Using the Boundary Element Method," thesis presented to the University of London, at London, England, in 1979, in partial fulfillment of the requirements for the degree of Doctor of Philosophy.
 21. Franklin, J. A., and Hoek, E., "Developments in Triaxial Testing Equipment," *Rock Mechanics*, Vol. 2, No. 4, Vienna, Austria, Dec., 1970, pp. 223-228.
 22. Gerogiannopoulos, N. G., and Brown, E. T., "The Critical State Concept Applied to Rock," *International Journal of Rock Mechanics and Mining Sciences*, Vol. 15, No. 1, Feb., 1978, pp. 1-10.
 23. Hardy, M. P., Hudson, J. A., and Fairhurst, C., "The Failure of Rock Beams. Part 1—Theoretical Studies," *International Journal of Rock Mechanics and Mining Sciences*, Vol. 10, No. 1, Jan., 1973, pp. 53-67.
 24. Heard, H. C., Abbey, A. E., Bonner, B. P., and Schock, R. N., "Mechanical Behavior of Dry Westerly Granite at High Confining Pressure," *Report UCRL 51642*, University of California Lawrence Livermore Laboratory, Berkeley, Calif., 1974.
 25. Hobbs, D. W., "A Study of the Behavior of Broken Rock under Triaxial Compression and Its Application to Mine Roadways," *International Journal of Rock Mechanics and Mining Sciences*, Vol. 3, No. 1, Mar., 1966, pp. 11-43.

26. Hoek, E., "Fracture of Anisotropic Rock," *Journal of the South African Institute of Mining and Metallurgy*, Vol. 64, No. 10, Johannesburg, South Africa, May, 1964, pp. 501-518.
27. Hoek, E., "Rock Fracture under Static Stress Conditions," *Report MEG 383*, National Mechanical Engineering Research Institute, Council for Scientific and Industrial Research, Pretoria, South Africa, 1965.
28. Hoek, E., "Brittle Fracture of Rock," *Rock Mechanics in Engineering Practice*, K. G. Stagg and O. C. Zienkiewicz, eds., John Wiley and Sons, Inc., London, England, 1968, pp. 99-124.
29. Hoek, E., "Structurally Controlled Instability in Underground Excavations," *Excavation Technology, Proceedings of the Eighteenth U.S. Symposium on Rock Mechanics*, F. D. Wang and G. B. Clark, eds., Colorado School of Mines Press, Colorado, 1977, pp. 5A6.1-5A6.5.
30. Hoek, E., and Bray, J. W., *Rock Slope Engineering*, 2nd ed., The Institution of Mining and Metallurgy, London, England, 1977.
31. Jaeger, J. C., "Shear Fracture of Anisotropic Rocks," *Geological Magazine*, Vol. 97, No. 1, Hertford, England, Jan.-Feb., 1960, pp. 65-72.
32. Jaeger, J. C., "Rock Failures at Low Confining Pressures," *Engineering*, Vol. 89, London, England, Feb., 1960, pp. 283-284.
33. Jaeger, J. C., "Behavior of Closely Jointed Rock," *Rock Mechanics—Theory and Practice, Proceedings of the Eleventh Symposium on Rock Mechanics*, W. H. Somerton, ed., The American Institute of Mining, Metallurgical, and Petroleum Engineers, Inc., New York, N.Y., 1970, pp. 57-68.
34. John, K. W., "An Approach to Rock Mechanics," *Journal of the Soil Mechanics and Foundations Division, ASCE*, Vol. 88, No. SM4, Proc. Paper 3223, Aug., 1962, pp. 1-30.
35. John, K. W., "Civil Engineering Approach to Evaluate Strength and Deformability of Closely Jointed Rock," *Rock Mechanics—Theory and Practice, Proceedings of the Eleventh Symposium on Rock Mechanics*, W. H. Somerton, ed., The American Institute of Mining, Metallurgical and Petroleum Engineers, Inc., New York, N.Y., 1970, pp. 69-80.
36. Kovari, K., and Tisa, A., "Multiple Failure State and Strain Controlled Triaxial Tests," *Rock Mechanics*, Vol. 7, No. 1, Vienna, Austria, Mar., 1975, pp. 17-33.
37. Ladanyi, B., "Use of the Long-Term Strength Concept in the Determination of Ground Pressure on Tunnel Linings," *Advances in Rock Mechanics, Proceedings of the Third Congress of the International Society for Rock Mechanics*, Vol. 2, Part B, National Academy of Sciences, Washington, D.C., 1974, pp. 1150-1156.
38. Ladanyi, B., and Archambault, G., "Simulation of Shear Behavior of a Jointed Rock Mass," *Rock Mechanics—Theory and Practice, Proceedings of the Eleventh Symposium on Rock Mechanics*, W. H. Somerton, ed., The American Institute of Mining, Metallurgical and Petroleum Engineers, Inc., New York, N.Y., 1970, pp. 105-125.
39. Manev, G., and Avramova-Tacheva, E., "On the Valuation of Strength and Resistance Condition of the Rocks in Natural Rock Massif," *Proceedings of the Second Congress of the International Society for Rock Mechanics*, Vol. 1, Paper 1-10, Belgrade, Yugoslavia, 1970.
40. McLamore, R., and Gray, K. E., "The Mechanical Behavior of Anisotropic Sedimentary Rocks," *Journal of Engineering for Industry, Transactions, American Society of Mechanical Engineers*, Vol. 89, Series B, No. 1, Feb., 1967, pp. 62-73.
41. Misra, B., "Correlation of Rock Properties with Machine Performance," Thesis presented to the University of Leeds, at Leeds, England, in 1974, in fulfillment of the requirements for the degree of Doctor of Philosophy.
42. Mogi, K., "Pressure Dependence of Rock Strength and Transition from Brittle Fracture to Ductile Flow," *Bulletin of the Earthquake Research Institute of Tokyo University*, Vol. 44, Tokyo, Japan, 1966, pp. 215-232.
43. Mogi, K., "Effect of Intermediate Principal Stress on Rock Failure," *Journal of Geophysical Research*, Vol. 72, No. 20, Oct. 15, 1967, pp. 5117-5131.
44. Muller, L., "Rock Mass Behaviour—Determination and Application in Engineering Practice," *Advances in Rock Mechanics, Proceedings of the Third Congress of the International Society for Rock Mechanics*, Vol. 1, Part A, National Academy of Sciences, Washington, D.C., 1974, pp. 205-215.

45. Peterson, M. S., *Rock Deformation—The Brittle Field*, Springer-Verlag, Berlin, Germany, 1978.
46. Price, N. J., "The Strength of Coal Measure Rocks in Triaxial Compression," *MRE Report No. 2159*, National Coal Board, England, 1960.
47. Rad, P. F., "Importance of Groove Spacing in Tunnel Boring Machine Operations," *Journal of the Geotechnical Engineering Division*, ASCE, Vol. 101, No. GT9, Proc. Paper 11589, Sept., 1975, pp. 949-962.
48. Ramez, M. R. H., "Fractures and the Strength of a Sandstone under Triaxial Compression," *International Journal of Rock Mechanics and Mining Sciences*, Vol. 4, No. 3, July, 1967, pp. 257-268.
49. Reik, G., and Zacas, M., "Strength and Deformation Characteristics of Jointed Media in True Triaxial Compression," *International Journal of Rock Mechanics and Mining Sciences*, Vol. 15, No. 6, Dec., 1978, pp. 295-303.
50. Schock, R. N., Abbey, A. E., Bonner, B. P., Duba, A., and Heard, H. C., "Mechanical Properties of Nugget Sandstone," *Report UCRL 51447*, University of California Lawrence Livermore Laboratory, Berkeley, Calif., 1973.
51. Schwartz, A. E., "Failure of Rock in the Triaxial Shear Test," *Proceedings of the Sixth Symposium on Rock Mechanics*, Rolla, Mo., Oct., 1964, pp. 109-151.
52. Stimpson, B., and Ross-Brown, D. M., "Estimating the Cohesive Strength of Randomly Jointed Rock Masses," *Mining Engineering*, Vol. 31, No. 2, Feb., 1979, pp. 182-188.
53. Wawersik, W. R., and Brace, W. F., "Post-Failure Behaviour of a Granite and a Diabase," *Rock Mechanics*, Vol. 3, No. 2, Vienna, Austria, June, 1971, pp. 61-85.
54. Wawersik, W. R., and Fairhurst, C., "A Study of Brittle Rock Fracture in Laboratory Compression Experiments," *International Journal of Rock Mechanics and Mining Sciences*, Vol. 7, No. 5, Sept., 1970, pp. 561-575.

Technical Note

Estimating Mohr–Coulomb Friction and Cohesion Values from the Hoek–Brown Failure Criterion

E. HOEK†

INTRODUCTION

Hoek and Brown [1–3] published a rock mass failure criterion and suggested that the values of the material constants m and s could be estimated from Bieniawski's rock mass rating (RMR) [4]. Since this is one of the few techniques available for estimating the rock mass strength from geological data, the criterion has been widely used in rock mechanics analyses.

Most of the analyses which are currently used for the evaluation of the stability of underground excavations or for slope stability calculations are formulated in terms of the Mohr–Coulomb failure criterion. Consequently, a question which frequently arises is how to determine equivalent values for the Mohr–Coulomb friction angle ϕ' and the cohesive strength c' from the tangent to the envelope to the principal stress circles defined by the Hoek–Brown criterion.

This Technical Note sets out the equations required to calculate these values for three conditions:

1. For a specified value of the effective normal stress σ'_n , a condition which generally applies in slope stability analysis.
2. For a specified minor principal effective stress (σ'_3) as would be appropriate in an analysis of stresses around underground openings.
3. For a condition in which the uniaxial compressive strength of the rock mass is the same for both Hoek–Brown and Mohr–Coulomb criteria, i.e. $\sigma_{cmasshb} = \sigma_{cmassmc}$. These conditions can be used when neither the average effective normal stress σ'_n nor the minor principal effective stress σ'_3 are known.

Before giving the solutions for these three conditions, the basic Hoek–Brown criterion and the relation between the constants m and s and Bieniawski's RMR value will be reviewed.

ESTIMATING MATERIAL CONSTANTS FROM ROCK MASS RATING

The Hoek–Brown failure criterion is defined by the following equation [1, 2, 5]:

$$\sigma'_1 = \sigma'_3 + \sqrt{m\sigma'_c\sigma'_3 + s\sigma_c^2}, \quad (1)$$

where:

σ'_1 = the major principal effective stress at failure,
 σ'_3 = the minor principal effective stress or confining pressure,

m, s = material constants,

σ_c = the uniaxial compressive strength of the *intact* rock.

Note that the uniaxial compressive strength of the intact rock refers to the strength which would be determined on a laboratory sized specimen (say a 50 mm dia × 100 mm long core) which is free from discontinuities such as joints or bedding planes. This value is a measure of the contribution of the rock material to the overall strength of the rock mass. The uniaxial compressive strength of the *rock mass* is given by substituting $\sigma'_3 = 0$ into equation (1):

$$\sigma_{cmasshb} = \sqrt{s\sigma_c}. \quad (2)$$

Similarly, substituting $\sigma'_1 = 0$ into equation (1) and solving the resulting quadratic equation gives the uniaxial tensile strength of the rock or rock mass as:

$$\sigma_{tmass} = \frac{\sigma_c}{2} (m - \sqrt{m^2 + 4s}). \quad (3)$$

In order to provide a basis for linking their criterion to measurements or observations which can be carried out in the field, Hoek and Brown [3] suggested a set of relations between the rock mass rating (RMR) from Bieniawski's [4] rock mass classification and the constants m and s . Following Priest and Brown [6], the relations were presented in the form of the following equations:

disturbed rock masses:

$$\frac{m}{m_i} = \exp\left(\frac{\text{RMR} - 100}{14}\right), \quad (4)$$

†Department of Civil Engineering, University of Toronto, Ontario, Canada M5S 1A4.

$$s = \exp\left(\frac{\text{RMR} - 100}{6}\right); \quad (5)$$

undisturbed or interlocking rock masses:

$$\frac{m}{m_i} = \exp\left(\frac{\text{RMR} - 100}{28}\right), \quad (6)$$

$$s = \exp\left(\frac{\text{RMR} - 100}{9}\right); \quad (7)$$

where m_i is the value of m for the *intact* rock, determined from the results of triaxial tests [5]. When no laboratory test data are available, the value of m_i can be estimated from Table 1.

For users who would prefer to use the Tunnelling Quality Index Q from the NGI rock mass classification by Barton *et al.* [7] the RMR value can be calculated from the following relation proposed by Bieniawski [8]:

$$\text{RMR} = 9 \log_e Q + 44 \quad (8)$$

FIND c'_i , ϕ'_i , σ_{cmassmc} AND σ_{tmax} FOR A SPECIFIED VALUE OF THE NORMAL STRESS σ'_i

From Hoek and Brown [3], the calculation sequence is as follows:

$$h = 1 + \frac{16(m\sigma'_n + s\sigma_c)}{3m^2\sigma_c}, \quad (9)$$

$$\theta = \frac{1}{3} \left(90 + \arctan \frac{1}{\sqrt{h^3 - 1}} \right), \quad (10)$$

$$\phi'_i = \arctan \frac{1}{\sqrt{4h \cos^2 \theta - 1}}, \quad (11)$$

$$\tau = (\cot \phi'_i - \cos \phi'_i) \frac{m\sigma_c}{8}, \quad (12)$$

$$c'_i = \tau - \sigma'_n \tan \phi'_i. \quad (13)$$

The uniaxial compressive strength σ_{cmassmc} of rock mass with these ϕ'_i and c'_i values is given by:

$$\sigma_{\text{cmassmc}} = \frac{2c'_i \cos \phi'_i}{(1 - \sin \phi'_i)}. \quad (14)$$

The uniaxial tensile strength of the rock mass is obtained from the Hoek-Brown criterion and is calculated from equation (3). This value can be used as a Mohr-Coulomb "tension cut-off".

FIND c'_i , ϕ'_i , σ_{cmassmc} AND σ_{tmax} FOR A GIVEN VALUE OF σ'_i

Assuming that the value of σ'_i is specified, the corresponding value of σ'_i for failure is calculated from equation (1). The remaining calculation follows:

$$\sigma'_n = \sigma'_i + \frac{(\sigma'_i - \sigma'_j)^2}{2(\sigma'_i - \sigma'_j) + \frac{1}{2}m\sigma_c}, \quad (15)$$

$$\tau = (\sigma'_n - \sigma'_j) \sqrt{1 + \frac{m\sigma_c}{2(\sigma'_i - \sigma'_j)}}, \quad (16)$$

$$\phi'_i = 90 - \arcsin \left(\frac{2\tau}{(\sigma'_i - \sigma'_j)} \right). \quad (17)$$

The cohesive strength c'_i is calculated from equation (13) while the uniaxial compressive and tensile strengths of the rock mass are calculated from equations (14) and (3).

FIND c'_i AND ϕ'_i FOR A CONDITION IN WHICH THE UNIAXIAL COMPRESSIVE STRENGTH OF THE ROCK MASS IS THE SAME FOR BOTH THE MOHR-COULOMB AND HOEK-BROWN FAILURE CRITERION

The uniaxial compressive strength of the rock mass is the same for both criteria, i.e. $\sigma_{\text{cmassmc}} = \sigma_{\text{cmasshb}}$, and is given by equation (2). The rest of the calculation is as follows:

$$\sigma'_n = \frac{2s\sigma_c}{4\sqrt{s} + m}, \quad (18)$$

$$\tau = \sigma'_n \sqrt{1 + \frac{m}{2\sqrt{s}}}, \quad (19)$$

$$\phi'_i = 90 - \arcsin \left(\frac{2\tau}{\sqrt{s}\sigma_c} \right). \quad (20)$$

The cohesive strength c'_i is calculated from equation (13).

EXAMPLE CALCULATIONS

The following examples are given to illustrate the application of the solutions presented earlier and to provide users with a set of values against which to check their own calculations.

Assume a sandstone rock mass in which the uniaxial compressive strength of the intact rock material is

Table 1. Approximate values of m_i for different rock types

Carbonate rocks with well-developed crystal cleavage (dolomite, limestone and marble):	$m_i = 7$
Lithified argillaceous rocks (mudstone, shale and slate (normal to cleavage)):	$m_i = 10$
Arenaceous rocks with strong crystals and poorly-developed crystal cleavage (sandstone and quartzite):	$m_i = 15$
Fine grained polyminerallic igneous crystalline rocks (andesite, dolerite, diabase and rhyolite):	$m_i = 17$
Coarse grained polyminerallic igneous and metamorphic rocks (amphibolite, gabbro, gneiss, granite, norite and granodiorite):	$m_i = 25$

$\sigma_c = 60$ MPa. From Table 1, the value of the material constant $m_i = 15$. A classification of the rock mass using the Tunnelling Quality Index by Barton *et al.* [7] gives a value of $Q = 0.8$. Equation (8) gives an equivalent rock mass rating of $RMR = 42$.

A slope has been excavated into this sandstone rock mass and additional excavations are to be created in the rock mass close to the slope. Under these circumstances it can be assumed that the stress levels in the rock mass have been reduced by excavation of the slope and that some movement along discontinuities in the rock mass will have occurred. Consequently, equations (4) and (5) for a *disturbed* rock mass will be used to calculate the constants m and s .

From equation (4), $m = 0.238$ and, from equation (5), $s = 0.000063$. Substitution of these values into equations (2) and (3) give the uniaxial compressive and uniaxial tensile strengths of the *rock mass* as $\sigma_{cmasshb} = 0.476$ MPa and $\sigma_{tmass} = -0.0159$ MPa.

Solution for a specified normal effective stress σ'_n

Assume an effective normal stress $\sigma'_n = 0.5$ MPa. Substitution of this value into equations (9–13) gives the following values:

$$\begin{aligned} h &= 1.1927, \\ \theta &= 46.7174^\circ, \\ \phi'_i &= 41.896^\circ, \\ \tau &= 0.6610 \text{ MPa}, \\ c'_i &= 0.2124 \text{ MPa}. \end{aligned}$$

The uniaxial compressive strength of the rock mass corresponding to the linear failure envelope defined by $\phi'_i = 41.896^\circ$ and $c'_i = 0.2124$ MPa is given by equation (14) as $\sigma_{cmassmc} = 0.9519$ MPa. The uniaxial tensile strength of the rock mass is given by equation (3) as $\sigma_{tmass} = -0.0159$ MPa.

Solution for a specified minor principal effective stress σ'_3

Assume a minor principal effective stress $\sigma'_3 = 0.25$ MPa. The corresponding value of the major principal effective stress at failure is given by equation (1) as $\sigma_1 = 2.1985$ MPa.

Substitution of these values into equations (15–17) give $\sigma'_n = 0.5940$, $\tau = 0.7429$ MPa, $\phi'_i = 40.31^\circ$ and $c'_i = 0.239$ MPa.

The uniaxial compressive strength of the rock mass corresponding to this linear failure envelope is given by equation (14) as $\sigma_{cmassmc} = 1.0322$ MPa. The uniaxial tensile strength of the rock mass is given by equation (3) as $\sigma_{tmass} = -0.0159$ MPa.

Solution for a the condition in which the uniaxial compressive strength of the rock mass is the same for the Hoek–Brown and Mohr–Coulomb criteria

The uniaxial compressive and uniaxial tensile strengths of the *rock mass* are $\sigma_{cmassmc} = \sigma_{cmasshb} = 0.476$ MPa and $\sigma_{tmass} = -0.0159$ MPa, from equations (2) and (3).

Substitution of the uniaxial compressive strength of the *intact* rock, $\sigma_c = 60$ MPa, and the values of $m = 0.238$ and $s = 0.000063$ into equations (18–20) give $\sigma'_n = 0.028$ MPa, $\tau = 0.112$ MPa and $\phi'_i = 61.94^\circ$. The corresponding value of $c'_i = 0.059$ MPa, from equation (14).

Accepted for publication 13 November 1989.

REFERENCES

1. Hoek E. and Brown E. T., *Underground Excavations in Rock*. London Instn. Min. Metall. (1980).
2. Hoek E. and Brown E. T., Empirical strength criterion for rock masses. *J. Geotech. Engng Div. ASCE* **106**, 1013–1035 (1980).
3. Hoek E. and Brown E. T., The Hoek–Brown failure criterion—a 1988 update. *Proc. 15th Can. Rock Mech. Symp.* University of Toronto, pp. 31–38 (1988).
4. Bieniawski Z. T., Geomechanics classification of rock masses and its application in tunnelling. *Proc. 3rd Congr. Int. Soc. Rock Mech.*, Denver, Vol. 2, Part A, pp. 27–32.
5. Hoek E., 23rd Rankine lecture, strength of jointed rock masses. *Géotechnique* **33**, 187–223 (1983).
6. Priest S. D. and Brown E. T., Probabilistic stability analysis of variable rock slopes. *Trans. Instn Min. Metall.* **92**, A1–A12 (1983).
7. Barton N. R., Lien R. and Lunde J., Engineering classification of rock masses for the design of tunnel support. *Rock Mech.* **6**, 189–239 (1974).
8. Bieniawski Z. T., Rock mass classification in rock engineering. *Exploration for Rock Engineering* (Z. T. Bieniawski, Ed.), Vol. 1, pp. 97–106. Balkema, Rotterdam (1976).

A modified Hoek-Brown failure criterion for jointed rock masses

Evert Hoek, D.Sc., NSERC Industrial Research Professor of Rock Mechanics

David Wood, M.Sc., Research Engineer

Sandip Shah, Ph.D., Graduate Student

Paper submitted for publication in the Proceedings of the International ISRM Symposium on Rock Characterization, Chester, UK, September 1992.

Synopsis

In order to eliminate some of the deficiencies which have been identified in ten years of practical experience with the application of the original Hoek-Brown failure criterion, a simplified rock mass classification and a modified rock mass failure criterion have been developed and are presented in this paper.

Introduction

The original Hoek- Brown failure criterion (Hoek and Brown, 1980) was developed in an attempt to provide a means of estimating the strength of jointed rock masses. The assumptions and limitations involved in the original criterion, derived empirically from the results of laboratory triaxial tests on intact rock samples, were discussed in a 1983 paper by Hoek (1983). Some aspects of the practical applications of the criterion were updated in a 1988 paper by Hoek and Brown (1988) but the criterion itself has remained essentially unchanged since it was first published in 1980.

On the basis of more than ten years of experience in using the Hoek-Brown criterion, a few deficiencies in the original system have become apparent. A modified criterion and an associated rock mass classification, both of which are presented for the first time in this paper, have been developed in an attempt to remedy these deficiencies. The most significant changes are:

- a. A re-formulation of the criterion for jointed rock masses to eliminate the tensile strength predicted by the original criterion.
- b. The introduction of a simplified qualitative rock mass classification for the estimation of the parameters in the modified criterion.
- c. The presentation of a procedure for calculating the parameters defining the Mohr failure envelope or the modified criterion, and for determining the instantaneous friction angle and cohesive strength for a given normal stress value.

Applicability of failure criteria

For the analysis of laboratory test results on intact specimens or for rock engineering problems in which a feature such as a shear zone crosses the tunnel, the Hoek-Brown criterion is only applicable to the intact blocks of rock. This behaviour of the discontinuities should be considered in terms of a shear strength criterion such as the Mohr-Coulomb criterion used in soil mechanics or the criterion proposed by Barton (1971). The stability of the sparsely jointed system can be analyzed by utilizing solutions such as those proposed by Bray (1966) or Amadei (1988).

In cases where the rock mass can be considered to be 'heavily jointed' and where the behaviour is not dominated by one or two individual discontinuities, the modified Hoek-

Brown criterion presented later in this paper can be used. A typical application would be a 5 metre span tunnel in a rock mass with three or four similar discontinuity sets with an average spacing of approximately 100 mm. the overall stability of this tunnel would be controlled by the freedom of the rock pieces to translate and rotate and the rock mass would behave as an isotropic medium. In some cases, a ‘weak’ rock mass such as this may contain a single dominant fault or shear zone. Here the modified Hoek-Brown criterion would be used to define the failure characteristics of the rock mass but the behaviour of the dominant discontinuity would be considered in terms of a shear strength criterion.

In deriving the classification scheme presented later in this paper, it has been assumed that the rock mass is undisturbed and that only its inherent properties are considered. External factors such as in situ or induced stresses, groundwater pressures and blasting damage are assumed to be included in the engineering analysis in which the failure criterion is used.

Failure criterion for intact rock

For intact rock the original Hoek-Brown failure criterion may be written in the following form:

$$\sigma_1' = \sigma_3' + \sigma_c \left(m_i \frac{\sigma_3'}{\sigma_c} + 1 \right)^{1/2} \quad (1)$$

Where

- σ_1' is the major principal effective stress at failure
- σ_3' is the minor principal effective stress at failure
- σ_c is the uniaxial compressive strength of the rock
- m_i is a constant for intact rock .

The derivation of the Mohr failure envelope corresponding to equation (1) is presented in the appendix.

The uniaxial compressive strength (σ_c) of intact rock is an important parameter in the Hoek-Brown failure criterion and should be determined by laboratory testing whenever possible. Where no laboratory test results are available, the value of the uniaxial compressive strength can be estimated from Table 1. When this is done, it is recommended that parametric studies be carried out to determine the sensitivity of the analysis to a range of uniaxial compressive strength values before a final selection is made.

Table 1. Estimates of uniaxial compressive strength σ_c for intact rock

Term	Uniaxial Comp. Strength σ_c MPa	Point Load Index I_p MPa	Field estimate of strength	Examples*
Extremely Strong	>250	>10	Rock material only chipped under repeated hammer blows	Basalt, chert, diabase, gneiss, granite, quartzite
Very Strong	100 - 250	4 - 10	Requires many blows of a geological hammer to break intact rock specimens	Amphibolite, andesite, basalt, dolomite, gabbro, gneiss, granite, granodiorite, limestone, marble, rhyolite, tuff
Strong	50 - 100	2 - 4	Hand held specimens broken by single blow of geological hammer	Limestone, marble, phyllite, sandstone, schist, slate
Medium Strong	25 - 50	1 - 2	Firm blow with geological pick indents rock to 5 mm, knife just scrapes surface	Claystone, coal, concrete, schist, shale, siltstone
Weak	5 - 25	**	Knife cuts material but too hard to shape into triaxial specimens	Chalk, rocksalt, potash
Very Weak	1 - 5	**	Material crumbles under firm blows of geological pick, can be shaped with knife	Highly weathered or altered rock
Extremely Weak	0.25 - 1	**	Indented by thumbnail	Clay gouge

* All rock types exhibit a broad range of uniaxial compressive strengths which reflect heterogeneity in composition and anisotropy in structure. Strong rocks are characterized by well interlocked crystal fabric and few voids.
 ** Rocks with a uniaxial compressive strength below 25 MPa are likely to yield highly ambiguous results under point load testing.

The constant m_i has been found to depend upon the mineralogy, composition and grain size of the intact rock. Table 2 gives values of m_i for rocks described in a standard geological classification based on three major groupings of rock families. Values of m_i included in this table were obtained by a re-assessment of triaxial test data presented in Hoek and Brown (1980) together with more recently published triaxial data, using the Simplex Reflection technique described by Shah and Hoek (1992). This analysis was carried out by Doruk (1991), using a program called ROCKDATA developed by Shah (1992). This program has now been replaced by RocLab which can be downloaded (free) from www.rocscience.com.

Rock names given to test specimens have been taken directly from the literature; no attempt has been made to revise these names. The laboratory results indicate that high values of m_i are attributed to igneous and metamorphic rocks with well interlocked crystal structure, silicate mineralogy and coarse grain size. Lowest values are derived from tests on fine grained sedimentary rocks, and those with carbonate mineralogy.

Table 2. Values of constant m_i for intact rock, by rock group

Grain size	Sedimentary			Metamorphic		Felsic	Igneous	
	Carbonate	Detrital	Chemical	Carbonate	Silicate		Mafic	Mafic
Coarse	Dolomite 10.1	Conglomerate (20)		Marble 9.3	Gneiss 29.2	Granite 32.7	Gabbro 25.8	Norite 21.7
Medium	Chalk 7.2	Sandstone 18.8	Chert 19.3		Amphibolite 31.2		Dolerite 15.2	
Fine	Limestone 8.4	Siltstone 9.6	Gypstone 15.5		Quartzite 23.7	Rhyolite (20)	Andesite 18.9	Basalt (17)
Very fine		Claystone 3.4	Anhydrite 13.2		Slate 11.4			

Values shown were derived from statistical analysis of triaxial test data for each rock type. Values in parenthesis have been estimated.

Failure criterion for jointed rock masses

In applying the original Hoek-Brown failure criterion to jointed rock masses, the predicted strengths are found to be acceptable where the rock mass is subjected to conditions in which the minor principal effective stress (σ_3') has a significant compressive value. For low values of σ_3' , the criterion predicts too high an axial strength and also a finite tensile strength.

Most rock mechanics engineers consider that the type of jointed rock mass to which the Hoek-Brown failure criterion applies should have zero tensile strength. For the past 30 years, finite element numerical models for use in rock mechanics have included a 'no tension' option which allows tensile stresses developed in the model to be transferred onto adjacent elements.

In view of this deficiency in the original Hoek-Brown criterion when applied to jointed rock masses, it was decided that a modified criterion should be developed. This criterion should conform to the strength predictions given by the original criterion, for compressive stress conditions, and should predict a tensile strength of zero for the rock mass. A modified criterion, which satisfies these conditions, was developed by Shah (1992) and can be expressed in the following form:

$$\sigma_1' = \sigma_3' + \sigma_c \left(m_b \frac{\sigma_3'}{\sigma_c} \right)^a \quad (2)$$

where m_b and a are constants for broken rock.

The derivation of the Mohr envelope corresponding to the modified criterion is discussed in the appendix.

For jointed rock masses, the strength characteristics are controlled by the block shape and size and the surface condition of the intersecting discontinuities and should be selected to represent the average condition of the rock mass. Specific features such as faults, dykes or shear zones, should be considered separately.

Block shape and size give a measure of the overall geometry of the rock mass, as well as an indication of the proportion of the volume of rock which is occupied by discontinuities. The amount of geological deformation also has an influence; more highly deformed rock masses usually have a smaller block size.

The surface condition of the joints and other discontinuities also modified the rock mass strength. At best, an unweathered, massive rock with discontinuous, irregular, rough joints would be almost as strong as the intact rock material. At worst, a highly weathered, moderately folded, blocky and seamy rock mass with continuous, slickensided surfaces with soft infilling would be far weaker than the intact rock material pieces in the rock mass.

These consideration have been taken into account in constructing a classification system, presented in Table 3, which can be used to estimate values of the constants m_b and a . Approximate block sizes and discontinuity spacings in jointed rock masses are give in Table 4. These values are based upon recommendations published by the Engineering Group of the Geological Society (1997) and the International Society for Rock mechanics (1978).

The input descriptions of overall geological structure and surface conditions are used to select values of m_b/m_i and a in Table 3. Substitution of the value of m_i from Table 2 into m_b/m_i gives the value of m_b .

Worked example

Detailed engineering geological mapping of an area yields the following rock mass description: moderately weathered, bedded and jointed, pale grey, fine grained, medium strong SANDSTONE, with two sets of widely spaced joints orthogonal to bedding. Discontinuity surfaces are persistent, irregular and smooth with surface iron staining and minor calcite infilling.

In a pre-feasibility study it is unlikely that a comprehensive laboratory testing programme would be carried out so use would be made of Tables 1 and 2 to estimate values uniaxial compressive strength σ_c of 40 MPa, and intact m_i if 18.8. The rock mass has interlocked, medium sized blocks and would have an overall structural condition described as very blocky. The surface condition of the bedding planes and joints would be fair. Table 3 would give values of m_b/m_i of 0.1 and a of 0.5.

Table 3. Estimation of m_b/m_i and a based on rock structure and surface condition.

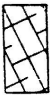



MODIFIED HOEK-BROWN FAILURE CRITERION			SURFACE CONDITION	VERY GOOD Unweathered, discontinuous, very tight aperture, very rough surface, no infilling	GOOD Slightly weathered, continuous, tight aperture, rough surface, iron staining to no infilling	FAIR Moderately weathered, continuous, extremely narrow, smooth surfaces, hard infilling	POOR Highly weathered, continuous, very narrow, polished/slickensided surfaces, hard infilling	VERY POOR Highly weathered, continuous, narrow, polished/slickensided surfaces, soft infilling
STRUCTURE								
$\sigma'_1 = \sigma'_3 + \sigma_c \left(m_b \frac{\sigma'_1}{\sigma_c} \right)^a$ <p>σ'_1 = major principal effective stress at failure σ'_3 = minor principal effective stress at failure σ_c = uniaxial compressive strength of <i>intact</i> pieces in the rock mass m_b and a are constants which depend on the composition, structure and surface conditions of the rock mass</p>								
	BLOCKY - well interlocked, undisturbed rock mass; large to very block size	m_b/m_i a	0.7 0.3	0.5 0.35	0.3 0.4	0.1 0.45		
	VERY BLOCKY - interlocked, partially disturbed rock mass; medium block sizes	m_b/m_i a	0.3 0.4	0.2 0.45	0.1 0.5	0.04 0.5		
	BLOCKY/SEAMY - folded and faulted, many intersecting joints; small blocks	m_b/m_i a		0.08 0.5	0.04 0.5	0.01 0.55	0.004 0.6	
	CRUSHED - poorly interlocked, highly broken rock mass; very small blocks	m_b/m_i a		0.03 0.5	0.015 0.55	0.003 0.6	0.001 0.65	

Table 4. Approximate block sizes and discontinuity spacings for jointed rock masses

Term	Block size	Equivalent discontinuity spacings
Very large	$(>2m)^3$	Extremely wide
Large	$(600mm-2m)^3$	Very wide
Medium	$(200-600mm)^3$	Wide
Small	$(60-200mm)^3$	Moderately wide
Very small	$(<60mm)^3$	<Moderately wide

Preliminary design analyses in this rock mass would be carried out using these strength parameters.

Uniaxial material strength	σ_c	40 MPa
Broken material constant	m_b	1.88
Broken material constant	a	0.5

Figure 1 gives a plot of axial strength σ'_1 versus minor principal stress σ'_3 and also the Mohr failure envelope for these parameters. These curves were generated using the program ROCKDATA.

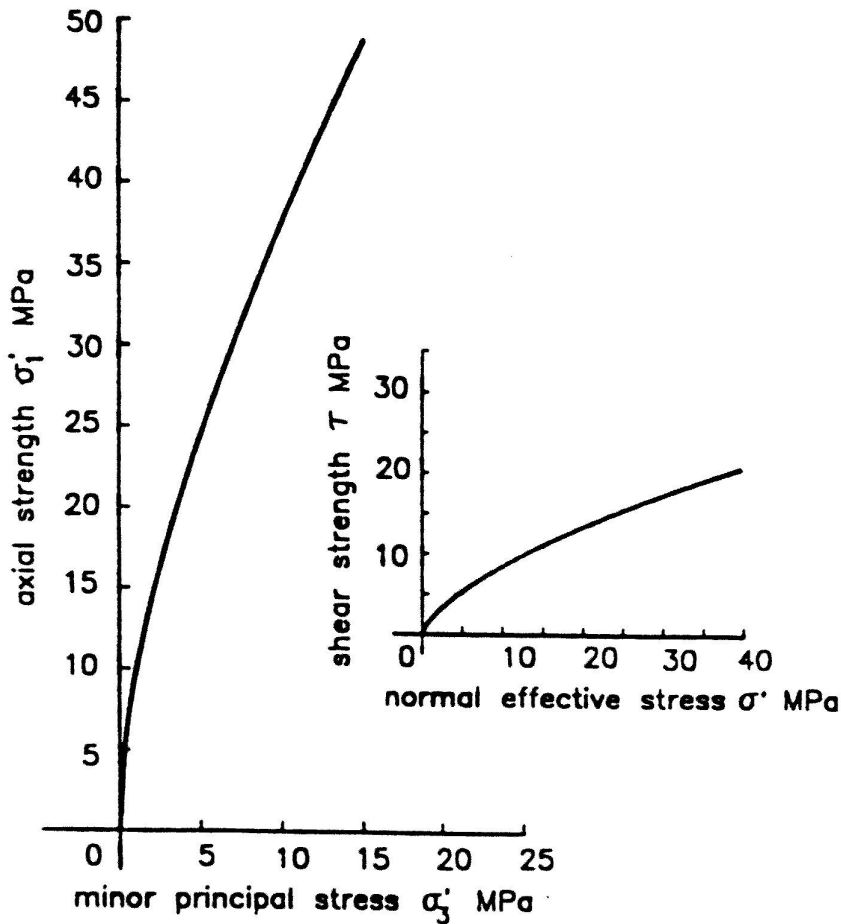


Figure 1. Plot of principal stresses at failure and the Mohr envelope for the example considered

Conclusion

A modified failure criterion for jointed rock masses and a simplified classification scheme, for estimating the parameters for this criterion, have been presented. These tools are intended to provide engineers and geologists with a means of estimating the strength of jointed rock masses during preliminary feasibility studies. It is strongly recommended that more detailed studies, including laboratory or in situ tests, should be carried out for detailed engineering design and that parametric studies should be carried out to check the influence of the rock mass strength before final decisions are made

References

1. Hoek, E and Brown, E.T. (1980). *Underground Excavations in Rock*, Institution of Mining and Metallurgy, London.
2. Hoek, E. (1983). Strength of jointed rock masses. 1983 Rankine Lecture. *Geotechnique*, 1983, vol. 33, no. 186, 187-223.
3. Hoek, E and Brown, E.T. (1988). The Hoek-Brown failure criterion – a 1988 update. *Proceedings of the 15th Canadian Rock Mechanics Symposium*, 1988, 31-38.
4. Barton, N.R. (1971). A relationship between joint roughness and joint shear strength. *Proceedings of the International Symposium on Rock Fracture, Nancy, France*, 1971, paper 1-8.
5. Bray, J.W. (1966). Limiting equilibrium of fractured and jointed rock masses. *Proceedings of the First Congress of the International Society for Rock Mechanics, Lisbon*, 1966, vol. 3, 531-536.
6. Amadei, B. (1988). Strength of a regularly jointed rock mass under biaxial and axisymmetric loading conditions. *International Society for Rock Mechanics and Mining Sciences and Geomechanics Abstracts*, 1988, vol. 25, no. 1, 3-13.
7. Shah, S. and Hoek, E. (1992). Simplex reflection analysis of laboratory rock strength data to obtain Hoek-Brown parameters. *Canadian Geotechnical Journal*, 1992, in press.
8. Doruk, P. (1991). Analysis of the laboratory strength data using the original and modified Hoek-Brown failure criteria. MAsC thesis, 1991. Department of Civil Engineering, University of Toronto, Canada.
9. Shah, S. (1992). A study of the behaviour of jointed rock masses. PhD thesis, 1992. Department of Civil Engineering, University of Toronto, Canada.

10. Anon. (1977). The description of rock masses for engineering purposes. Geological Society Engineering Group Working Party Report. *Quarterly Journal of Engineering Geology*, 1977, vol. 10, 355-388.
11. International Society for Rock Mechanics (1978). Suggested methods for the quantitative description of discontinuities in rock masses. *International Journal of Rock Mechanics and Mining Sciences & Geomechanical Abstracts*, 1978, vol. 15, 319-368.
12. Balmer, G.A. (1952). A general analytical solution for Mohr's envelope. *American Society for Testing Materials*, vol. 52, 1260-1271.

APPENDIX - MOHR ENVELOPES

The Mohr envelope corresponding to the original Hoek-Brown failure criterion is defined by the following relationship, (ref. 2):

$$\tau = \sigma_c \frac{m_i}{8} (\cot \phi'_i - \cos \phi'_i) \quad (3)$$

where

τ is the shear stress at failure

ϕ'_i is the instantaneous friction angle for a given value of the effective normal stress σ'

The value of the instantaneous friction angle ϕ'_i is given by:

$$\phi'_i = \arctan \left(4h \cos^2 \left(30 + \frac{1}{3} \arcsin \frac{1}{\sqrt{h^3}} \right) - 1 \right)^{-1/2} \quad (4)$$

where

$$h = 1 + \frac{16(m_i \sigma' + \sigma_c)}{3m_i^2 \sigma_c} \quad (5)$$

The instantaneous cohesive strength c'_i is given by:

$$c'_i = \tau - \sigma' \tan \phi'_i \quad (6)$$

For the modified Hoek-Brown criterion it is not possible to derive a closed form solution for the Mohr envelope as for the original criterion. Consequently a numerical technique is used to determine the constants α and β in the following empirical equation :

$$\tau = \sigma_c \alpha \left(\frac{\sigma'}{\sigma_c} \right)^\beta \quad (7)$$

A general analytical solution for Mohr envelope published by Balmer (ref. 12) is used in the following calculation of the constants α and β :

The normal and shear stresses for a given value of σ'_3/σ_c are calculated as follows:

$$\sigma' = \sigma'_3 + \frac{\sigma'_1 - \sigma'_3}{1 + \frac{\partial \sigma'_1}{\partial \sigma'_3}} \quad (8)$$

$$\tau = (\sigma' - \sigma'_3) \sqrt{\frac{\partial \sigma'_1}{\partial \sigma'_3}} \quad (9)$$

where, for the modified Hoek-Brown criterion defined by equation (2),

$$\frac{\partial \sigma'_1}{\partial \sigma'_3} = 1 + am_b^a \left(\frac{\sigma'_3}{\sigma_c} \right)^{a-1} \quad (10)$$

Equation (7) can be re-written in the form

$$\log \frac{\tau}{\sigma_c} = \log \alpha + \beta \log \frac{\sigma'}{\sigma_c} \quad (11)$$

Let $x = \log \sigma'/\sigma_c$ and $y = \log \tau/\sigma_c$, then

$$\beta = \frac{\sum x_i y_i - \frac{\sum x_i \sum y_i}{n}}{\sum x_i^2 - \frac{(\sum x_i)^2}{n}} \quad (12)$$

$$\log \alpha = \frac{\sum y_i}{n} - \beta \frac{\sum x_i}{n} \quad (13)$$

Where x_i and y_i are the i th values of x and y and n is the total number of each of the quantities.

The instantaneous friction angle ϕ'_i for a specified value of the normal stress σ'/σ_c is given by:

$$\phi'_i = \arctan \alpha \beta \left(\frac{\sigma'}{\sigma_c} \right)^{\beta-1} \quad (14)$$

The corresponding cohesive strength is given by equation (6).

A convenient method for determining α and β from equations (12) and (13) is to set up this calculation in a spreadsheet as shown in Figure 2. In order to capture the pronounced curvature at low normal stresses it has been found that the values of σ'_3/σ_c which are substituted into equation (10) should follow a geometric progression defined by :

$$\frac{\sigma'_3}{\sigma_c} = \frac{1}{2^k} \quad (15)$$

where k varies from 9 to 1 in increments of -1.

This gives a maximum value of $\sigma'_3/\sigma_c = 0.5$ which has been found to cover the range of stresses encountered in most practical applications of the Hoek-Brown failure criterion.

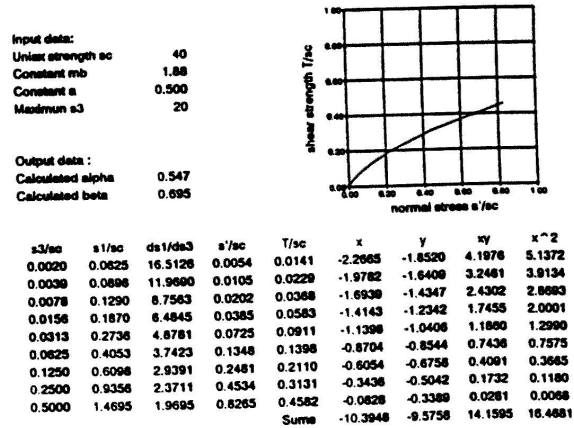


Figure 2. Example of spreadsheet calculation of α and β for the modified Hoek-Brown criterion.

Technical note

Reliability of Hoek-Brown Estimates of Rock Mass Properties and their Impact on Design

EVERT HOEK

INTRODUCTION

Hoek and Brown [1] presented a procedure for estimating the strength and deformation characteristics of isotropic jointed rock masses. When applying this procedure to rock engineering design problems, most users consider only the “average” or mean properties. In fact, all of these properties exhibit a distribution about the mean, even under the most ideal conditions, and these distributions can have a significant impact upon the design calculations.

This technical note examines the reliability of a slope stability calculation and a tunnel support design calculation. In each case, the strength and deformation characteristics of the rock mass are estimated by means of the Hoek-Brown procedure, assuming that the three input parameters are defined by normal distributions.

INPUT PARAMETERS

In the Hoek-Brown criterion, the Geological Strength Index (GSI) is the most important input parameter in terms of the relation between the strength and deformation properties determined in the laboratory and those assigned to the field scale rock mass. In earlier versions of the criterion, Bieniawski's RMR [2] was used for this scaling process.

Figure 1 can be used for estimating the value of GSI from field observations of blockiness and discontinuity surface conditions. Included in this figure is a cross-hatched circle representing the 90% confidence limits of a GSI value of 25 ± 5 (equivalent to a standard deviation of $ca\ 2.5$). This represents the range of values which an experienced geologist would assign to a rock mass described as *blocky/disturbed* or *disintegrated* and *poor*. Typically, rocks such as flysch, schist and some phyllites may fall within this range of rock mass descriptions.

In the author's experience, some geologists go to extraordinary lengths to try to determine an “exact” value of GSI (or RMR). Geology does not lend itself to such precision and it is simply not realistic to assign

a single value. A range of values, such as that illustrated in Fig. 1 is more appropriate. In fact, in some complex geological environments, the range indicated by the cross-hatched circle may be too optimistic.

The two laboratory properties required for the application of the Hoek-Brown criterion are the uniaxial compressive strength of the intact rock (σ_c) and the intact rock material constant m_i . Ideally these two parameters should be determined by triaxial tests on carefully prepared specimens as described by Hoek and Brown [1].

It is assumed that all three input parameters can be represented by normal distributions as illustrated in Fig. 2. The standard deviations assigned to these three distributions are based upon the author's experience of geotechnical programs for major civil and mining projects where adequate funds are available for high quality investigations. For preliminary field investigations or “low budget” projects, it is prudent to assume larger standard deviations for the input parameters.

OUTPUT PARAMETERS

The values of the friction angle ϕ , the cohesive strength c , the uniaxial compressive strength of the rock mass σ_{cm} and the deformation modulus E of the rock mass were calculated by the procedure described by Hoek and Brown [1]. The Excel add-on program @RISK (Palisade Corporation, Newfield, NY, U.S.A.) was used for a Monte Carlo analysis in which 1000 calculations were carried out for randomly selected values of the input parameters. The results of these calculations were analysed using the program BESTFIT (Palisade Corporation) and it was found that all four output parameters could be adequately described by the normal distributions illustrated in Fig. 2.

In several trials it was found that the output parameters ϕ , c and σ_{cm} were always well represented by normal distributions. On the other hand, for GSI values of > 40 , the deformation modulus E was better represented by a lognormal distribution.

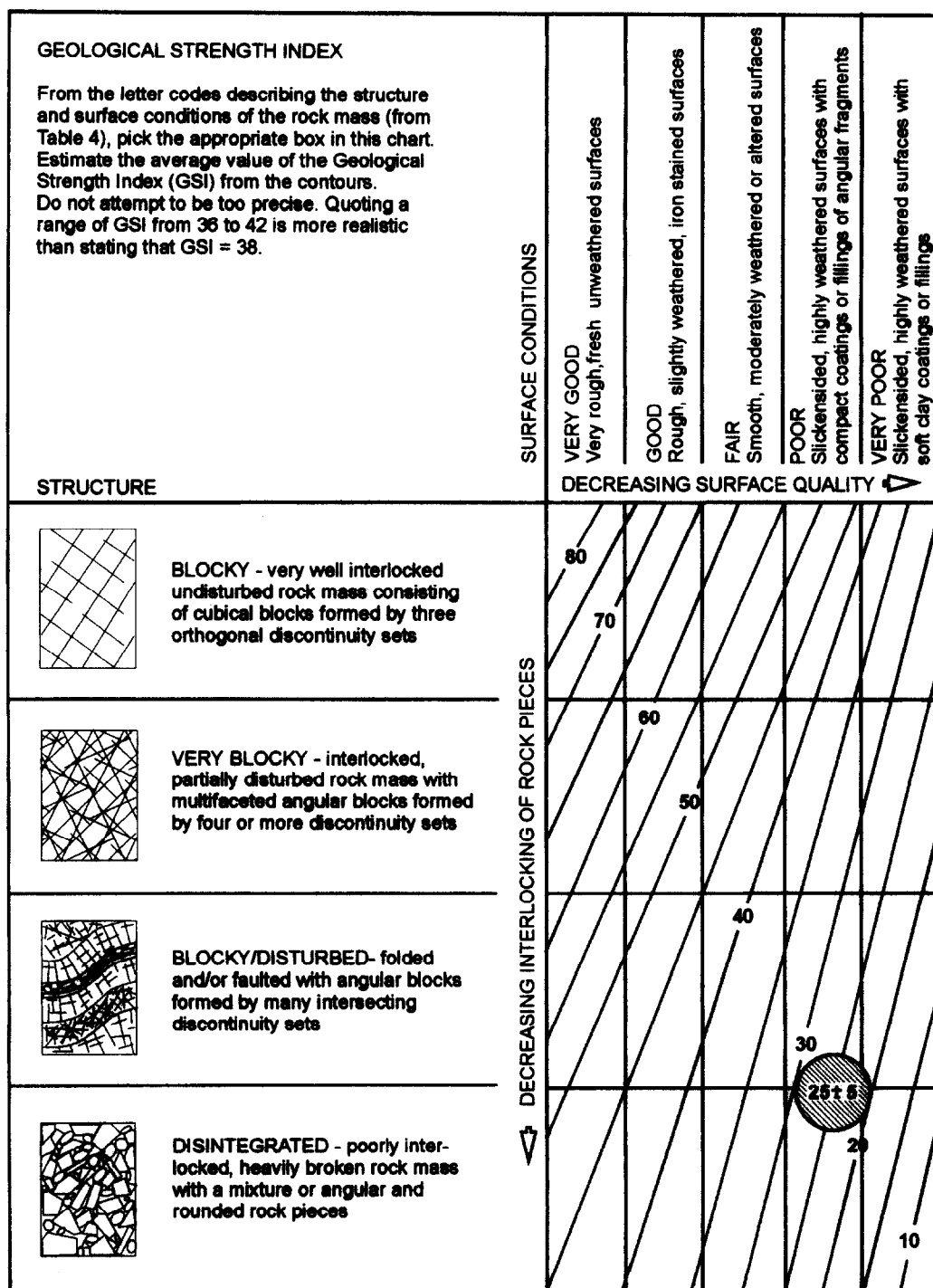


Fig. 1. Estimate of GSI based on geological descriptions.

SLOPE STABILITY CALCULATION

In order to assess the impact of the variation in output parameters, illustrated in Fig. 2, a calculation of the factor of safety for a homogeneous slope was carried out using Bishop's circular failure analysis in the program SLIDE (Rock Engineering Group, University of Toronto, Toronto, Ontario, Canada M4E 3B5). The geometry of the slope and the phreatic surface, the rock mass properties and the critical failure surface for the "average" properties are shown in Fig. 3.

The distribution of the factor of safety was determined by Rosenbleuth's Point Estimate method [3, 4] in which the two values are chosen at one standard deviation on either side of the mean for each variable. The factor of safety is calculated for every possible combination of point estimates, producing 2^m solutions, where m is the number of variables considered. The mean and standard deviation of the factor of safety are then calculated from these 2^m solutions.

This calculation of the mean and standard deviation is given in Table 1. Based upon the fact that the two

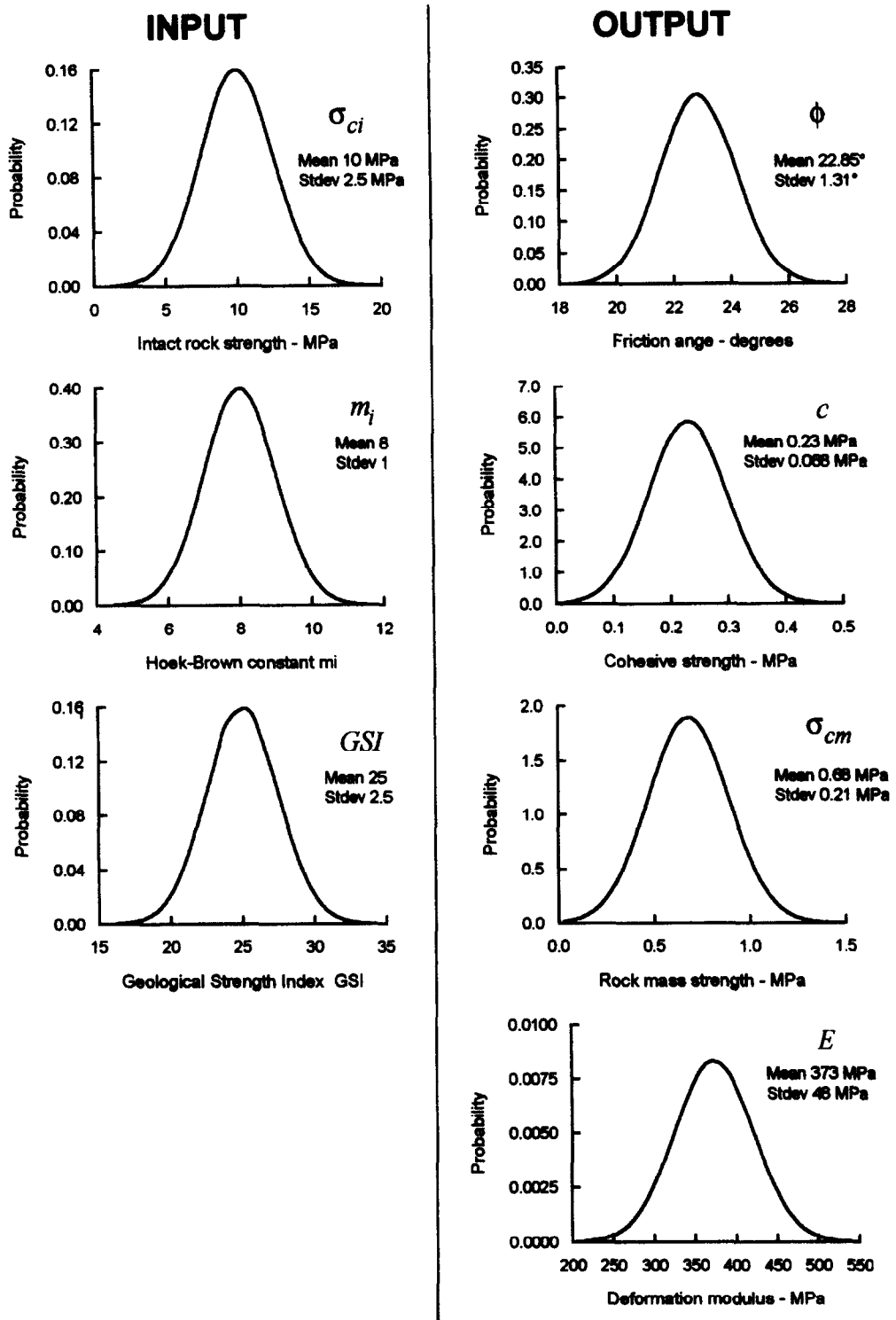


Fig. 2. Assumed normal distributions for input parameters and calculated distributions for output parameters.

Table 1. Calculations for Rosenbleuth's point estimate method using ± 1 SD

Case	Friction angle (°)	Cohesion	Safety factor	$(\bar{SF}-SF_i)^2$
ϕ_-, c_-	21.19	0.162	1.215	0.00922
ϕ_+, c_+	24.16	0.298	1.407	0.00922
ϕ_-, c_+	21.19	0.298	1.217	0.00884
ϕ_+, c_-	24.16	0.162	1.406	0.00912
Sums			5.245	0.0364

Mean safety factor = $\bar{SF} = \frac{1}{n} \sum_{i=1}^n SF_i = 1.31$.
Standard deviation = $S^2 = \frac{1}{n-1} \sum_{i=1}^n (\bar{SF} - SF_i)^2 = 0.11$.

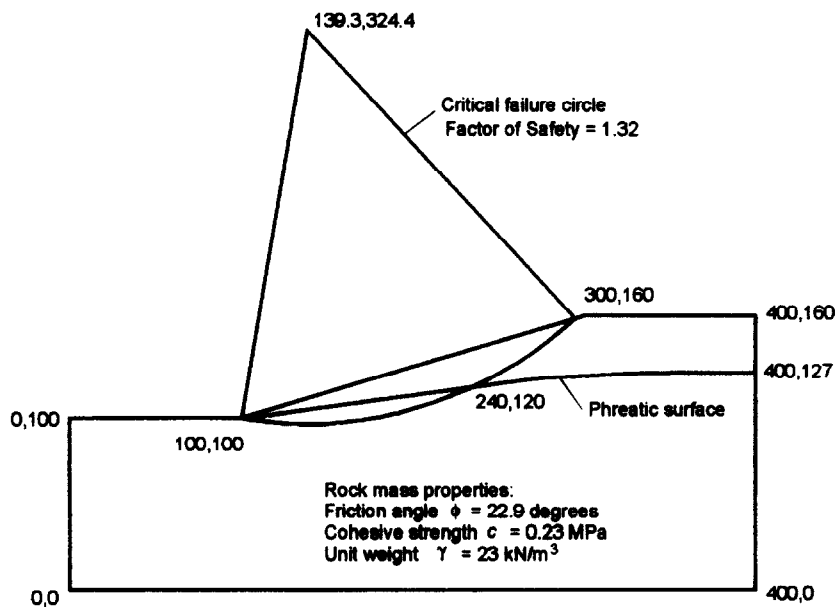


Fig. 3. Slope and phreatic surface geometry, rock mass properties and critical failure surface for a homogeneous slope.

variables included in this analysis are defined by normal distributions and considering the form of the equations used to calculate the factor of safety, it is reasonable to assume that the factor of safety will be adequately represented by a normal distribution. This distribution is illustrated in Fig. 4.

The mean factor of safety for this slope is 1.3 which is a value frequently used in the design of slopes for open pit mines. It is interesting that the probability of failure, given by the portion of the distribution curve for $SF < 1$, is very small. This suggests that, for a high quality geotechnical investigation such as that assumed in this study, a safety factor of 1.3 is adequate to ensure stability under the assumed conditions.

TUNNEL STABILITY CALCULATIONS

Consider a circular tunnel of radius r_o in a stress field in which the horizontal and vertical stresses are both p_o . If the stresses are high enough, a “plastic” zone of damaged rock of radius r_p surrounds the tunnel. A uniform support pressure p_i is provided around

the perimeter of the tunnel. This situation is illustrated in Fig. 5.

Assuming that the rock mass fails with zero plastic volume change, the critical stress level p_{cr} at which failure initiates is given by [5]:

$$p_{cr} = \frac{2p_o - \sigma_{cm}}{1 + k} \tag{1}$$

where

$$k = \frac{1 + \sin \phi}{1 - \sin \phi} \tag{2}$$

Where the support pressure p_i is less than the critical pressure p_{cr} , the radius r_p of the plastic zone and the inward deformation of the tunnel wall u_{ip} are given by:

$$\frac{r_p}{r_o} = \left[\frac{2(p_o(k - 1) + \sigma_{cm})}{(1 + k)((k - 1)p_i + \sigma_{cm})} \right]^{1/(k-1)} \tag{3}$$

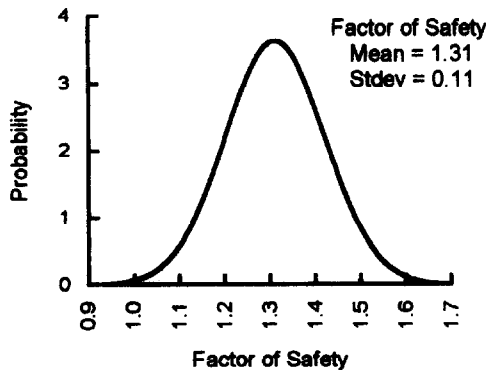


Fig. 4. Normal distribution for factor of safety of slope defined in Fig. 3.

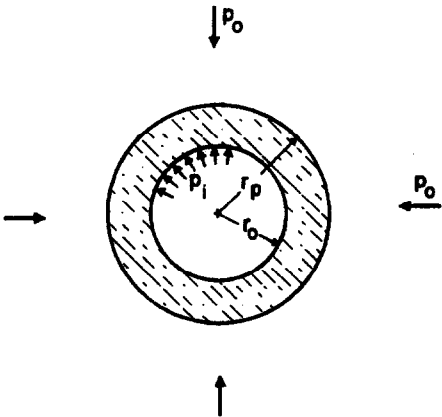


Fig. 5. Development of a plastic zone around a circular tunnel in a hydrostatic stress field.

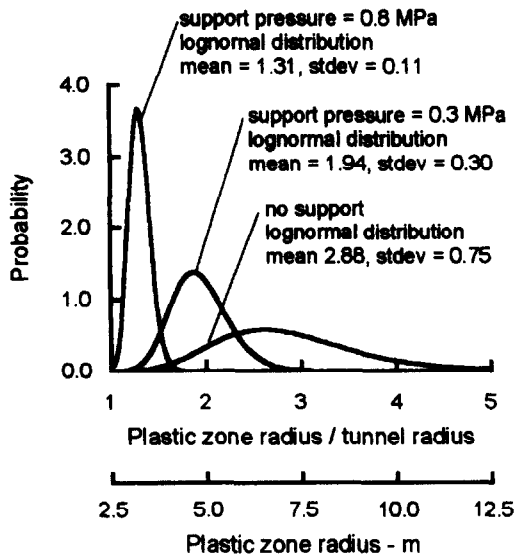


Fig. 6. Lognormal distributions representing the range of plastic zone radii for different support pressures.

$$\frac{u_{ip}}{r_o} = \frac{(1 + \nu)}{E} \left[2(1 - \nu)(p_o - p_{cr} \left(\frac{r_p}{r_o} \right)^2 - (1 - 2\nu)(p_o - p_i) \right] \quad (4)$$

In order to study the influence of the variation in the input parameters, a Monte Carlo analysis was performed using the program @RISK in an Excel spreadsheet which had been programmed to perform the analysis defined above. It was assumed that a 5 m diameter tunnel ($r_o = 2.5$ m) was subjected to uniform *in situ* stress of $p_o = 2.5$ MPa. The rock mass properties were defined by the normal distributions for ϕ , c , σ_{cm} and E defined in Fig. 2.

This analysis was carried out for a tunnel with no support. A second analysis was performed for a tunnel with a support pressure of $p_i = 0.3$ MPa which is approximately that which can be achieved with a closed ring of 50 mm thick shotcrete with a uniaxial compressive strength of 14 MPa (after 1 day of curing). This would represent the early support which would be achieved by the immediate application of shotcrete behind the advancing face. A third analysis was performed for a support pressure $p_i = 0.8$ MPa. This is approximately the support which can be achieved in this size of tunnel by a 75 mm thick shotcrete lining with a uniaxial compressive strength of 35 MPa (cured for 28 days). The results of these analyses are summarized graphically in Figs 6 and 7.

Figures 6 and 7 show that the size of the plastic zone and the tunnel deformation can be represented by lognormal distributions. As would be expected, the mean values for the size of the plastic zone and the magnitude of the sidewall displacements are reduced significantly by the installation of support.

What is surprising is the dramatic reduction in the standard deviations with increasing support pressure.

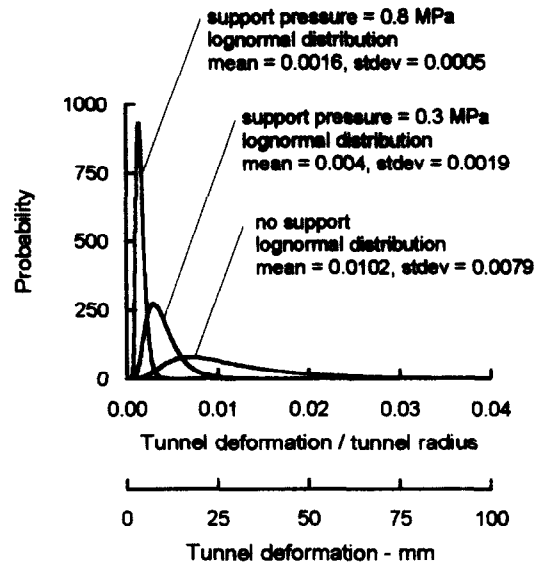


Fig. 7. Lognormal distributions representing the range of tunnel deformations for different support pressures.

This is because of the strong dependence of the size of the plastic zone upon the difference between the critical pressure p_{cr} and the support pressure p_i . A detailed discussion on this dependence is beyond the scope of this technical note and is the subject of ongoing research by the author.

From the results of the analysis described above it is evident that the installation of a relatively simple support system is very effective in controlling the behaviour of this tunnel. Without support there is an *ca* 50% probability of severe instability and possible collapse of the tunnel. A plastic zone diameter of 15 m and a tunnel closure of 50 mm in a 5 m diameter tunnel would certainly cause visible signs of distress. The fact that a relatively thin shotcrete lining can control the size of the plastic zone and the closure of the tunnel provides confirmation of the effectiveness of support.

A word of warning is required at this point. The example described above is for a 5 m diameter tunnel at a depth of *ca* 100 m below the surface. For larger tunnels at greater depths, the plastic zone and the displacements can be significantly larger. The demands on the support system may be such that it may be very difficult to support a large tunnel in poor ground at considerable depth below surface.

CONCLUSIONS

The uncertainty associated with estimating the properties of *in situ* rock masses has a significant impact on the design of slopes and excavations in rock. The examples which have been explored in this technical note show that, even when using the "best" estimates currently available, the range of calculated factors of safety or tunnel behaviour are uncomfortably large. These ranges become alarmingly large when poor site

investigation techniques and inadequate laboratory procedures are used.

Given the inherent difficulty of assigning reliable numerical values to rock mass characteristics, it is unlikely that "accurate" methods for estimating rock mass properties will be developed in the foreseeable future. Consequently, the user of the Hoek–Brown procedure or of any other equivalent procedure for estimating rock mass properties should not assume that the calculations produce unique reliable numbers. The simple techniques described in this note can be used to explore the possible range of values and the impact of these variations on engineering design.

Acknowledgements—Professor E. T. Brown reviewed a draft of this technical note and his comments are gratefully acknowledged.

Accepted for publication 20 August 1997

REFERENCES

1. Hoek, E. and Brown, E. T. Practical estimates of rock mass strength. *Int. J. Rock Mech. Min. Sci.*, in press.
2. Bieniawski, Z. T. Rock mass classification in rock engineering. *Exploration for Rock Engineering, Proc. of the Symp.* (Edited by Bieniawski, Z. T.), Vol. 1, pp. 97–106. Balkema, Cape Town, 1976.
3. Rosenbleuth, E., Two-point estimates in probabilities. *J. Appl. Math. Modelling*, 1981, **5**, 329–335.
4. Harr, M. E. *Reliability-based Design in Civil Engineering*. McGraw-Hill, New York, 1987.
5. Duncan Fama, M. E. Numerical modelling of yield zones in weak rocks. In *Comprehensive Rock Engineering* (Edited by Hudson, J. A.), Vol. 2, pp. 49–75. Pergamon, Oxford, 1993.

Hoek-Brown failure criterion – 2002 Edition

E. Hoek, C. Carranza-Torres and B. Corkum

Proc. NARMS-TAC Conference, Toronto, 2002, **1**, 267-273.

The program RocLab mentioned in this paper will be available for downloading (free) after the meeting from www.rocscience.com.

HOEK-BROWN FAILURE CRITERION – 2002 EDITION

Evert Hoek

Consulting Engineer, Vancouver, Canada

Carlos Carranza-Torres

Itasca Consulting Group Inc., Minneapolis, USA

Brent Corkum

Rocscience Inc., Toronto, Canada

ABSTRACT: The Hoek-Brown failure criterion for rock masses is widely accepted and has been applied in a large number of projects around the world. While, in general, it has been found to be satisfactory, there are some uncertainties and inaccuracies that have made the criterion inconvenient to apply and to incorporate into numerical models and limit equilibrium programs. In particular, the difficulty of finding an acceptable equivalent friction angle and cohesive strength for a given rock mass has been a problem since the publication of the criterion in 1980. This paper resolves all these issues and sets out a recommended sequence of calculations for applying the criterion. An associated Windows program called “RocLab” has been developed to provide a convenient means of solving and plotting the equations presented in this paper.

1. INTRODUCTION

Hoek and Brown [1, 2] introduced their failure criterion in an attempt to provide input data for the analyses required for the design of underground excavations in hard rock. The criterion was derived from the results of research into the brittle failure of intact rock by Hoek [3] and on model studies of jointed rock mass behaviour by Brown [4]. The criterion started from the properties of intact rock and then introduced factors to reduce these properties on the basis of the characteristics of joints in a rock mass. The authors sought to link the empirical criterion to geological observations by means of one of the available rock mass classification schemes and, for this purpose, they chose the Rock Mass Rating proposed by Bieniawski [5].

Because of the lack of suitable alternatives, the criterion was soon adopted by the rock mechanics community and its use quickly spread beyond the original limits used in deriving the strength reduction relationships. Consequently, it became necessary to re-examine these relationships and to introduce new elements from time to time to account for the wide range of practical problems to which the criterion was being applied. Typical of these enhancements were the introduction of the idea of “undisturbed” and “disturbed” rock masses Hoek and Brown [6], and the introduction of a modified criterion to force the rock mass tensile

strength to zero for very poor quality rock masses (Hoek, Wood and Shah, [7]).

One of the early difficulties arose because many geotechnical problems, particularly slope stability issues, are more conveniently dealt with in terms of shear and normal stresses rather than the principal stress relationships of the original Hoek-Brown criterion, defined by the equation:

$$\sigma'_1 = \sigma'_3 + \sigma_{ci} \left(m \frac{\sigma'_3}{\sigma_{ci}} + s \right)^{0.5} \quad (1)$$

where σ'_1 and σ'_3 are the major and minor effective principal stresses at failure

σ_{ci} is the uniaxial compressive strength of the intact rock material and

m and s are material constants, where $s = 1$ for intact rock.

An exact relationship between equation 1 and the normal and shear stresses at failure was derived by J. W. Bray (reported by Hoek [8]) and later by Ucar [9] and Londe¹ [10].

Hoek [12] discussed the derivation of equivalent friction angles and cohesive strengths for various practical situations. These derivations were based upon tangents to the Mohr envelope derived by

¹ Londe's equations were later found to contain errors although the concepts introduced by Londe were extremely important in the application of the Hoek-Brown criterion to tunnelling problems (Carranza-Torres and Fairhurst, [11])

Bray. Hoek [13] suggested that the cohesive strength determined by fitting a tangent to the curvilinear Mohr envelope is an upper bound value and may give optimistic results in stability calculations. Consequently, an average value, determined by fitting a linear Mohr-Coulomb relationship by least squares methods, may be more appropriate. In this paper Hoek also introduced the concept of the Generalized Hoek-Brown criterion in which the shape of the principal stress plot or the Mohr envelope could be adjusted by means of a variable coefficient a in place of the square root term in equation 1.

Hoek and Brown [14] attempted to consolidate all the previous enhancements into a comprehensive presentation of the failure criterion and they gave a number of worked examples to illustrate its practical application.

In addition to the changes in the equations, it was also recognised that the Rock Mass Rating of Bieniawski was no longer adequate as a vehicle for relating the failure criterion to geological observations in the field, particularly for very weak rock masses. This resulted in the introduction of the Geological Strength Index (GSI) by Hoek, Wood and Shah [7], Hoek [13] and Hoek, Kaiser and Bawden [15]. This index was subsequently extended for weak rock masses in a series of papers by Hoek, Marinos and Benissi [16], Hoek and Marinos [17, 18] and Marinos and Hoek [19].

The Geological Strength Index will not be discussed in the following text, which will concentrate on the sequence of calculations now proposed for the application of the Generalized Hoek Brown criterion to jointed rock masses.

2. GENERALIZED HOEK-BROWN CRITERION

This is expressed as

$$\sigma_1' = \sigma_3' + \sigma_{ci} \left(m_b \frac{\sigma_3'}{\sigma_{ci}} + s \right)^a \quad (2)$$

where m_b is a reduced value of the material constant m_i and is given by

$$m_b = m_i \exp \left(\frac{GSI - 100}{28 - 14D} \right) \quad (3)$$

s and a are constants for the rock mass given by the following relationships:

$$s = \exp \left(\frac{GSI - 100}{9 - 3D} \right) \quad (4)$$

$$a = \frac{1}{2} + \frac{1}{6} \left(e^{-GSI/15} - e^{-20/3} \right) \quad (5)$$

D is a factor which depends upon the degree of disturbance to which the rock mass has been subjected by blast damage and stress relaxation. It varies from 0 for undisturbed in situ rock masses to 1 for very disturbed rock masses. Guidelines for the selection of D are discussed in a later section.

The uniaxial compressive strength is obtained by setting $\sigma_3' = 0$ in equation 2, giving:

$$\sigma_c = \sigma_{ci} \cdot s^a \quad (6)$$

and, the tensile strength is:

$$\sigma_t = -\frac{s\sigma_{ci}}{m_b} \quad (7)$$

Equation 7 is obtained by setting $\sigma_1' = \sigma_3' = \sigma_t$ in equation 2. This represents a condition of biaxial tension. Hoek [8] showed that, for brittle materials, the uniaxial tensile strength is equal to the biaxial tensile strength.

Note that the “switch” at $GSI = 25$ for the coefficients s and a (Hoek and Brown, [14]) has been eliminated in equations 4 and 5 which give smooth continuous transitions for the entire range of GSI values. The numerical values of a and s , given by these equations, are very close to those given by the previous equations and it is not necessary for readers to revisit and make corrections to old calculations.

Normal and shear stresses are related to principal stresses by the equations published by Balmer² [20].

$$\sigma_n' = \frac{\sigma_1' + \sigma_3'}{2} - \frac{\sigma_1' - \sigma_3'}{2} \cdot \frac{d\sigma_1'/d\sigma_3' - 1}{d\sigma_1'/d\sigma_3' + 1} \quad (8)$$

$$\tau = (\sigma_1' - \sigma_3') \frac{\sqrt{d\sigma_1'/d\sigma_3'}}{d\sigma_1'/d\sigma_3' + 1} \quad (9)$$

where

$$d\sigma_1'/d\sigma_3' = 1 + am_b \left(m_b \sigma_3' / \sigma_{ci} + s \right)^{a-1} \quad (10)$$

3. MODULUS OF DEFORMATION

The rock mass modulus of deformation is given by:

² The original equations derived by Balmer contained errors that have been corrected in equations 8 and 9.

$$E_m(GPa) = \left(1 - \frac{D}{2}\right) \sqrt{\frac{\sigma_{ci}}{100}} \cdot 10^{((GSI-10)/40)} \quad (11)$$

Note that the original equation proposed by Hoek and Brown [14] has been modified, by the inclusion of the factor D , to allow for the effects of blast damage and stress relaxation.

4. MOHR-COULOMB CRITERION

Since most geotechnical software is still written in terms of the Mohr-Coulomb failure criterion, it is necessary to determine equivalent angles of friction and cohesive strengths for each rock mass and stress range. This is done by fitting an average linear relationship to the curve generated by solving equation 2 for a range of minor principal stress values defined by $\sigma_t < \sigma_3 < \sigma'_{3\max}$, as illustrated in Figure 1. The fitting process involves balancing the areas above and below the Mohr-Coulomb plot. This results in the following equations for the angle of friction ϕ' and cohesive strength c' :

$$\phi' = \sin^{-1} \left[\frac{6am_b(s + m_b\sigma'_{3n})^{a-1}}{2(1+a)(2+a) + 6am_b(s + m_b\sigma'_{3n})^{a-1}} \right] \quad (12)$$

$$c' = \frac{\sigma_{ci} \left[(1+2a)s + (1-a)m_b\sigma'_{3n} \right] (s + m_b\sigma'_{3n})^{a-1}}{(1+a)(2+a) \sqrt{1 + \left(6am_b(s + m_b\sigma'_{3n})^{a-1} \right) / ((1+a)(2+a))}} \quad (13)$$

where $\sigma_{3n} = \sigma'_{3\max} / \sigma_{ci}$

Note that the value of $\sigma'_{3\max}$, the upper limit of confining stress over which the relationship between the Hoek-Brown and the Mohr-Coulomb criteria is considered, has to be determined for each individual case. Guidelines for selecting these values for slopes as well as shallow and deep tunnels are presented later.

The Mohr-Coulomb shear strength τ , for a given normal stress σ , is found by substitution of these values of c' and ϕ' in to the equation:

$$\tau = c' + \sigma \tan \phi' \quad (14)$$

The equivalent plot, in terms of the major and minor principal stresses, is defined by:

$$\sigma'_1 = \frac{2c' \cos \phi'}{1 - \sin \phi'} + \frac{1 + \sin \phi'}{1 - \sin \phi'} \sigma'_3 \quad (15)$$

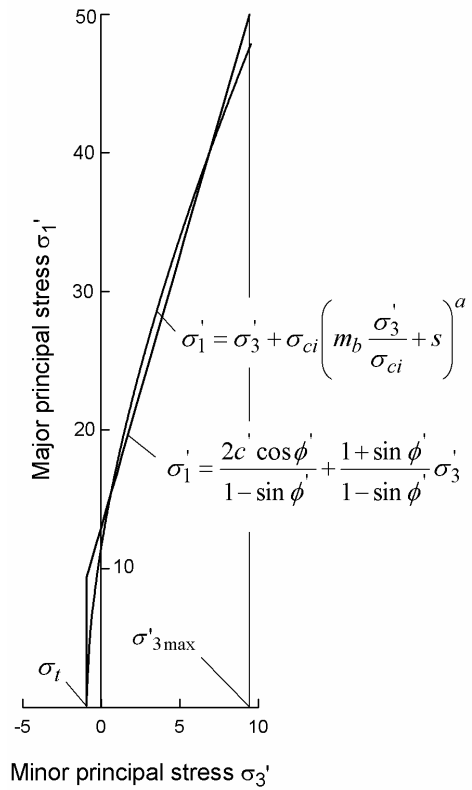


Figure 1: Relationships between major and minor principal stresses for Hoek-Brown and equivalent Mohr-Coulomb criteria.

5. ROCK MASS STRENGTH

The uniaxial compressive strength of the rock mass σ_c is given by equation 6. Failure initiates at the boundary of an excavation when σ_c is exceeded by the stress induced on that boundary. The failure propagates from this initiation point into a biaxial stress field and it eventually stabilizes when the local strength, defined by equation 2, is higher than the induced stresses σ'_1 and σ'_3 . Most numerical models can follow this process of fracture propagation and this level of detailed analysis is very important when considering the stability of excavations in rock and when designing support systems.

However, there are times when it is useful to consider the overall behaviour of a rock mass rather than the detailed failure propagation process described above. For example, when considering the strength of a pillar, it is useful to have an estimate of the overall strength of the pillar rather than a detailed knowledge of the extent of fracture propagation in the pillar. This leads to the concept of a global “rock mass strength” and Hoek and Brown [14] proposed that this could be estimated from the Mohr-Coulomb relationship:

$$\sigma'_{cm} = \frac{2c' \cos \phi'}{1 - \sin \phi'} \quad (16)$$

with c' and ϕ' determined for the stress range $\sigma_t < \sigma'_3 < \sigma_{ci}/4$ giving

$$\sigma'_{cm} = \sigma_{ci} \cdot \frac{(m_b + 4s - a(m_b - 8s))(m_b/4 + s)^{a-1}}{2(1+a)(2+a)} \quad (17)$$

6. DETERMINATION OF σ'_{3MAX}

The issue of determining the appropriate value of σ'_{3max} for use in equations 12 and 13 depends upon the specific application. Two cases will be investigated:

1. Tunnels – where the value of σ'_{3max} is that which gives equivalent characteristic curves for the two failure criteria for deep tunnels or equivalent subsidence profiles for shallow tunnels.
2. Slopes – here the calculated factor of safety and the shape and location of the failure surface have to be equivalent.

For the case of deep tunnels, closed form solutions for both the Generalized Hoek-Brown and the Mohr-Coulomb criteria have been used to generate hundreds of solutions and to find the value of σ'_{3max} that gives equivalent characteristic curves.

For shallow tunnels, where the depth below surface is less than 3 tunnel diameters, comparative numerical studies of the extent of failure and the magnitude of surface subsidence gave an identical relationship to that obtained for deep tunnels, provided that caving to surface is avoided.

The results of the studies for deep tunnels are plotted in Figure 2 and the fitted equation for both cases is:

$$\frac{\sigma'_{3max}}{\sigma'_{cm}} = 0.47 \left(\frac{\sigma'_{cm}}{\gamma H} \right)^{-0.94} \quad (18)$$

where σ'_{cm} is the rock mass strength, defined by equation 17, γ is the unit weight of the rock mass and H is the depth of the tunnel below surface. In cases where the horizontal stress is higher than the vertical stress, the horizontal stress value should be used in place of γH .

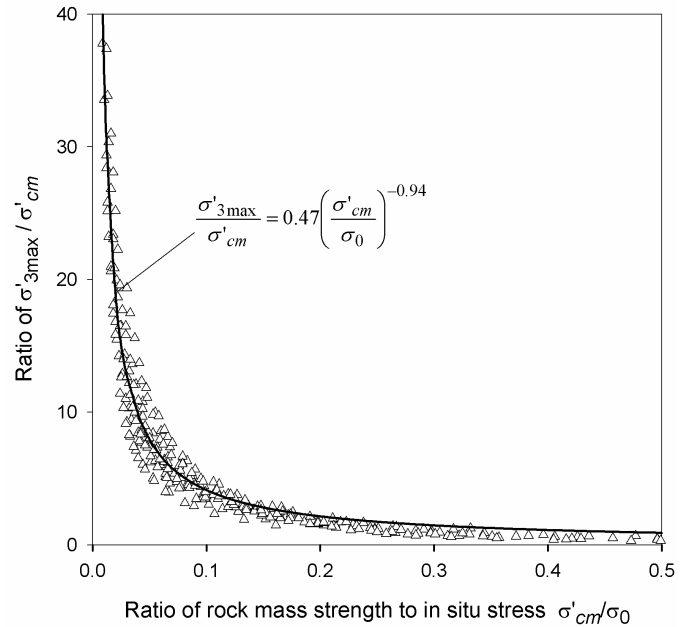


Figure 2: Relationship for the calculation of σ'_{3max} for equivalent Mohr-Coulomb and Hoek-Brown parameters for tunnels.

Equation 18 applies to all underground excavations, which are surrounded by a zone of failure that does not extend to surface. For studies of problems such as block caving in mines it is recommended that no attempt should be made to relate the Hoek-Brown and Mohr-Coulomb parameters and that the determination of material properties and subsequent analysis should be based on only one of these criteria.

Similar studies for slopes, using Bishop's circular failure analysis for a wide range of slope geometries and rock mass properties, gave:

$$\frac{\sigma'_{3max}}{\sigma'_{cm}} = 0.72 \left(\frac{\sigma'_{cm}}{\gamma H} \right)^{-0.91} \quad (19)$$

where H is the height of the slope.

7. ESTIMATION OF DISTURBANCE FACTOR D

Experience in the design of slopes in very large open pit mines has shown that the Hoek-Brown criterion for undisturbed in situ rock masses ($D = 0$) results in rock mass properties that are too optimistic [21, 22]. The effects of heavy blast damage as well as stress relief due to removal of the overburden result in disturbance of the rock mass. It is considered that the “disturbed” rock mass

properties [6], $D = 1$ in equations 3 and 4, are more appropriate for these rock masses.

Lorig and Varona [23] showed that factors such as the lateral confinement produced by different radii of curvature of slopes (in plan) as compared with their height also have an influence on the degree of disturbance.

Sonmez and Ulusay [24] back-analysed five slope failures in open pit coal mines in Turkey and attempted to assign disturbance factors to each rock mass based upon their assessment of the rock mass properties predicted by the Hoek-Brown criterion. Unfortunately, one of the slope failures appears to be structurally controlled while another consists of a transported waste pile. The authors consider that the Hoek-Brown criterion is not applicable to these two cases.

Cheng and Liu [25] report the results of very careful back analysis of deformation measurements, from extensometers placed before the commencement of excavation, in the Mingtan power cavern in Taiwan. It was found that a zone of blast damage extended for a distance of approximately 2 m around all large excavations. The back-calculated strength and deformation properties of the damaged rock mass give an equivalent disturbance factor $D = 0.7$.

From these references it is clear that a large number of factors can influence the degree of disturbance in the rock mass surrounding an excavation and that it may never be possible to quantify these factors precisely. However, based on their experience and on an analysis of all the details contained in these papers, the authors have attempted to draw up a set of guidelines for estimating the factor D and these are summarised in Table 1.

The influence of this disturbance factor can be large. This is illustrated by a typical example in which $\sigma_{ci} = 50$ MPa, $m_i = 10$ and $GSI = 45$. For an undisturbed in situ rock mass surrounding a tunnel at a depth of 100 m, with a disturbance factor $D = 0$, the equivalent friction angle is $\phi' = 47.16^\circ$ while the cohesive strength is $c' = 0.58$ MPa. A rock mass with the same basic parameters but in highly disturbed slope of 100 m height, with a disturbance factor of $D = 1$, has an equivalent friction angle of $\phi' = 27.61^\circ$ and a cohesive strength of $c' = 0.35$ MPa.

Note that these are guidelines only and the reader would be well advised to apply the values given with caution. However, they can be used to provide a realistic starting point for any design and, if the observed or measured performance of the excavation turns out to be better than predicted, the disturbance factors can be adjusted downwards.






8. CONCLUSION

A number of uncertainties and practical problems in using the Hoek-Brown failure criterion have been addressed in this paper. Wherever possible, an attempt has been made to provide a rigorous and unambiguous method for calculating or estimating the input parameters required for the analysis. These methods have all been implemented in a Windows program called “RocLab” that can be downloaded (free) from www.roscience.com. This program includes tables and charts for estimating the uniaxial compressive strength of the intact rock elements (σ_{ci}), the material constant m_i and the Geological Strength Index (GSI).

9. ACKNOWLEDGEMENTS

The authors wish to acknowledge the contributions of Professor E.T. Brown in reviewing a draft of this paper and in participating in the development of the Hoek-Brown criterion for the past 25 years.

Table 1: Guidelines for estimating disturbance factor D

Appearance of rock mass	Description of rock mass	Suggested value of D
	Excellent quality controlled blasting or excavation by Tunnel Boring Machine results in minimal disturbance to the confined rock mass surrounding a tunnel.	$D = 0$
	Mechanical or hand excavation in poor quality rock masses (no blasting) results in minimal disturbance to the surrounding rock mass. Where squeezing problems result in significant floor heave, disturbance can be severe unless a temporary invert, as shown in the photograph, is placed.	$D = 0$ $D = 0.5$ No invert
	Very poor quality blasting in a hard rock tunnel results in severe local damage, extending 2 or 3 m, in the surrounding rock mass.	$D = 0.8$
	Small scale blasting in civil engineering slopes results in modest rock mass damage, particularly if controlled blasting is used as shown on the left hand side of the photograph. However, stress relief results in some disturbance.	$D = 0.7$ Good blasting $D = 1.0$ Poor blasting
	Very large open pit mine slopes suffer significant disturbance due to heavy production blasting and also due to stress relief from overburden removal. In some softer rocks excavation can be carried out by ripping and dozing and the degree of damage to the slopes is less.	$D = 1.0$ Production blasting $D = 0.7$ Mechanical excavation

10. REFERENCES

1. Hoek, E. and Brown, E.T. 1980. Empirical strength criterion for rock masses. *J. Geotech. Engng Div., ASCE* **106** (GT9), 1013-1035.
2. Hoek, E. and Brown, E.T. 1980. *Underground Excavations in Rock*, London, Instn Min. Metall.
3. Hoek, E. 1968. Brittle failure of rock. In *Rock Mechanics in Engineering Practice* . (eds K.G. Stagg and O.C. Zienkiewicz), 99-124. London: Wiley
4. Brown, E.T. 1970. Strength of models of rock with intermittent joints. *J. Soil Mech. Foundn Div., ASCE* **96**, SM6, 1935-1949.
5. Bieniawski Z.T. 1976. Rock mass classification in rock engineering. In *Exploration for Rock Engineering, Proc. of the Symp.*, (ed. Z.T. Bieniawski) **1**, 97-106. Cape Town, Balkema.
6. Hoek, E. and Brown, E.T. 1988. The Hoek-Brown failure criterion - a 1988 update. *Proc. 15th Canadian Rock Mech. Symp.* (ed. J.C. Curran), 31-38. Toronto, Dept. Civil Engineering, University of Toronto.
7. Hoek, E., Wood D. and Shah S. 1992. A modified Hoek-Brown criterion for jointed rock masses. *Proc. Rock Characterization, Symp. Int. Soc. Rock Mech.: Eurock '92*, (ed. J.A. Hudson), 209-214. London, Brit. Geotech. Soc.
8. Hoek, E. 1983. Strength of jointed rock masses, 23rd. Rankine Lecture. *Géotechnique* **33** (3), 187-223.
9. Ucar, R. (1986) Determination of shear failure envelope in rock masses. *J. Geotech. Engg. Div. ASCE*. **112**, (3), 303-315.
10. Londe, P. 1988. Discussion on the determination of the shear stress failure in rock masses. *ASCE J Geotech Eng Div*, **14**, (3), 374-6.
11. Carranza-Torres, C., and Fairhurst, C. 1999. General formulation of the elasto-plastic response of openings in rock using the Hoek-Brown failure criterion. *Int. J. Rock Mech. Min. Sci.*, **36** (6), 777-809.
12. Hoek, E. 1990. Estimating Mohr-Coulomb friction and cohesion values from the Hoek-Brown failure criterion. *Intnl. J. Rock Mech. & Mining Sci. & Geomechanics Abstracts*. **12** (3), 227-229.
13. Hoek, E. 1994. Strength of rock and rock masses, *ISRM News Journal*, **2** (2), 4-16.
14. Hoek, E. and Brown, E.T. 1997. Practical estimates or rock mass strength. *Intnl. J. Rock Mech. & Mining Sci. & Geomechanics Abstracts*. **34** (8), 1165-1186.
15. Hoek, E., Kaiser P.K. and Bawden W.F. 1995. *Support of underground excavations in hard rock*. Rotterdam, Balkema.
16. Hoek, E., Marinos, P. and Benissi, M. 1998. Applicability of the Geological Strength Index (GSI) classification for very weak and sheared rock masses. The case of the Athens Schist Formation. *Bull. Engg. Geol. Env.* **57**(2), 151-160.
17. Marinos, P and Hoek, E. 2000. GSI – A geologically friendly tool for rock mass strength estimation. *Proc. GeoEng2000 Conference, Melbourne*.
18. Hoek, E. and Marinos, P. 2000. Predicting Tunnel Squeezing. *Tunnels and Tunnelling International*. Part 1 – November 2000, Part 2 – December, 2000
19. Marinos. P, and Hoek, E. 2001. – Estimating the geotechnical properties of heterogeneous rock masses such as flysch. Accepted for publication in the *Bulletin of the International Association of Engineering Geologists*
20. Balmer, G. 1952. A general analytical solution for Mohr's envelope. *Am. Soc. Test. Mat.* **52**, 1260-1271.
21. Sjöberg, J., Sharp, J.C., and Malorey, D.J. 2001 Slope stability at Aznalcóllar. In *Slope stability in surface mining*. (eds. W.A. Hustrulid, M.J. McCarter and D.J.A. Van Zyl). Littleton: Society for Mining, Metallurgy and Exploration, Inc., 183-202.
22. Pierce, M., Brandshaug, T., and Ward, M. 2001 Slope stability assessment at the Main Cresson Mine. In *Slope stability in surface mining*. (eds. W.A. Hustrulid, M.J. McCarter and D.J.A. Van Zyl). Littleton: Society for Mining, Metallurgy and Exploration, Inc., 239-250.
23. Lorig, L., and Varona, P. 2001 Practical slope-stability analysis using finite-difference codes. In *Slope stability in surface mining*. (eds. W.A. Hustrulid, M.J. McCarter and D.J.A. Van Zyl). Littleton: Society for Mining, Metallurgy and Exploration, Inc., 115-124.
24. Sonmez,H., and Ulusay, R. 1999. Modifications to the geological strength index (GSI) and their applicability to the stability of slopes. *Int. J. Rock Mech. Min. Sci.*, **36** (6), 743-760.
25. Cheng, Y., and Liu, S. 1990. Power caverns of the Mingtan Pumped Storage Project, Taiwan. In *Comprehensive Rock Engineering*. (ed. J.A. Hudson), Oxford: Pergamon, **5**, 111-132.

A brief history of the development of the Hoek-Brown failure criterion

Evert Hoek and Paul Marinos

Published in
Soils and Rocks, No. 2, November 2007.

A brief history of the development of the Hoek-Brown failure criterion

Evert Hoek¹ and Paul Marinos²

Abstract

The Hoek-Brown failure criterion was developed in the late 1970s to provide input for the design of underground excavations. Bieniawski's RMR was originally used to link the criterion to engineering geology input from the field but a more specific classification system called the Geological Strength Index (GSI) was introduced in 1995. Both the Hoek Brown criterion and the GSI classification have evolved and continue to evolve to meet new applications and to deal with unusual conditions encountered by users.

Introduction

The original Hoek-Brown failure criterion was developed during the preparation of the book *Underground Excavations in Rock* by E. Hoek and E.T. Brown, published in 1980. The criterion was required in order to provide input information for the design of underground excavations. Since no suitable methods for estimating rock mass strength appeared to be available at that time, the efforts were focussed on developing a dimensionless equation that could be scaled in relation to geological information. The original Hoek-Brown equation was neither new nor unique – an identical equation had been used for describing the failure of concrete as early as 1936.

The significant contribution that Hoek and Brown made was to link the equation to geological observations. It was recognised very early in the development of the criterion that it would have no practical value unless the parameters could be estimated from simple geological observations in the field. The idea of developing a 'classification' for this specific purpose was discussed but, since Bieniawski's RMR had been published in 1974 and had gained popularity with the rock mechanics community, it was decided to use this as the basic vehicle for geological input.

By 1995 it had become increasingly obvious that Bieniawski's RMR is difficult to apply to very poor quality rock masses and it was felt that a system based more heavily on fundamental geological observations and less on 'numbers' was needed. This resulted in the development of the Geological Strength Index, GSI, which continues to evolve as the principal vehicle for geological data input for the Hoek-Brown criterion.

Historical development

1980 Hoek E. and Brown E.T. 1980. *Underground Excavations in Rock*. London: Institution of Mining and Metallurgy

Hoek, E. and Brown, E.T. 1980. Empirical strength criterion for rock masses. *J. Geotech. Engng Div., ASCE* **106**(GT9), 1013-1035.

¹ Consulting Engineer, Vancouver, Canada, hoeks.corner@rocscience.com.

² National Technical University of Athens, marinos@central.ntua.gr.

The original criterion was conceived for use under the confined conditions surrounding underground excavations. The data upon which some of the original relationships had been based came from tests on rock mass samples from the Bougainville open pit copper mine in Papua New Guinea. The rock mass here is very strong andesite (uniaxial compressive strength about 270 MPa) with numerous clean, rough, unfilled joints. One of the most important sets of data was from a series of triaxial tests carried out by Professor John Jaeger at the Australian National University in Canberra. These tests were on 150 mm diameter samples of heavily jointed andesite recovered by triple-tube diamond drilling from one of the exploration adits at Bougainville.

The original criterion, with its bias towards hard rock, was based upon the assumption that rock mass failure is controlled by translation and rotation of individual rock pieces, separated by numerous joint surfaces. Failure of the intact rock was assumed to play no significant role in the overall failure process and it was assumed that the joint pattern was 'chaotic' so that there are no preferred failure directions and the rock mass can be treated as isotropic.

1983 Hoek, E. 1983. Strength of jointed rock masses, 23rd. Rankine Lecture. *Géotechnique* **33**(3), 187-223.

One of the issues that had been troublesome throughout the development of the criterion has been the relationship between Hoek-Brown criterion, with the non-linear parameters m and s , and the Mohr-Coulomb criterion, with the parameters c and ϕ . At that time, practically all software for soil and rock mechanics was written in terms of the Mohr-Coulomb criterion and it was necessary to define the relationship between m and s and c and ϕ in order to allow the criterion to be used for to provide input for this software.

An exact theoretical solution to this problem (for the original Hoek-Brown criterion) was developed by Dr John W. Bray at the Imperial College of Science and Technology and this solution was first published in the 1983 Rankine lecture. This publication also expanded on some of the concepts published by Hoek and Brown in 1980 and it represents the most comprehensive discussion on the original Hoek Brown criterion.

1988 Hoek E and Brown E.T. 1988. The Hoek-Brown failure criterion - a 1988 update. *Proc. 15th Canadian Rock Mech. Symp.* (ed. J.H. Curran), pp. 31-38. Toronto: Civil Engineering Dept., University of Toronto

By 1988 the criterion was being widely used for a variety of rock engineering problems, including slope stability analyses. As pointed out earlier, the criterion was originally developed for the confined conditions surrounding underground excavations and it was recognised that it gave optimistic results for shallow failures in slopes. Consequently, in 1998, the idea of *undisturbed* and *disturbed* masses was introduced to provide a method for downgrading the properties for near surface rock masses.

This paper also defined a method of using Bieniawski's 1974 RMR classification for estimating the input parameters. In order to avoid double counting the effects of groundwater (an effective stress parameter in numerical analysis) and joint orientation

(specific input for structural analysis), it was suggested that the rating for groundwater should always be set at 10 (completely dry) and the rating for joint orientation should always be set to zero (very favourable). Note that these ratings need to be adjusted in later versions of Bieniawski's RMR, for example, use 15 for ground water in the 1989 version.

- 1990** Hoek, E. 1990. Estimating Mohr-Coulomb friction and cohesion values from the Hoek-Brown failure criterion. *Intl. J. Rock Mech. & Mining Sci. & Geomechanics Abstracts*. **12**(3), 227-229.

This technical note addressed the on-going debate on the relationship between the Hoek-Brown and the Mohr-Coulomb criterion. Three different practical situations were described and it was demonstrated how Bray's solution could be applied in each case.

- 1992** Hoek, E., Wood, D. and Shah, S. 1992. A modified Hoek-Brown criterion for jointed rock masses. *Proc. rock characterization, symp. Int. Soc. Rock Mech.: Eurock '92*, (J. Hudson ed.). 209-213.

The use of the Hoek Brown criterion had now become widespread and, because of the lack of suitable alternatives, it was now being used on very poor quality rock masses. These rock masses differ significantly from the tightly interlocked hard rock mass model used in the development of the original criterion. In particular it was felt that the finite tensile strength predicted by the original Hoek Brown criterion was too optimistic and that it needed to be revised. Based upon work carried out by Dr Sandip Shah for his Ph.D thesis at the University of Toronto, a modified criterion was proposed. This criterion contains a new parameter a that provides the means for changing the curvature of the failure envelope, particularly in the very low normal stress range. Basically, the modified Hoek Brown criterion forces the failure envelope to produce zero tensile strength.

- 1994** Hoek, E. 1994. Strength of rock and rock masses, *ISRM News Journal*, **2**(2), 4-16.

- 1995** Hoek, E., Kaiser, P.K. and Bawden. W.F. 1995. *Support of underground excavations in hard rock*. Rotterdam: Balkema

It soon became evident that the modified criterion was too conservative when used for better quality rock masses and a 'generalised' failure criterion was proposed in these two publications. This generalised criterion incorporated both the original and the modified criteria with a 'switch' at an RMR value of approximately 25. Hence, for excellent to fair quality rock masses, the original Hoek Brown criterion is used while, for poor and extremely poor rock masses, the modified criterion (published in 1992) with zero tensile strength is used.

These publications (which are practically identical) also introduced the concept of the Geological Strength Index (GSI) as a replacement for Bieniawski's RMR. It had become increasingly obvious that Bieniawski's RMR is difficult to apply to very poor quality rock masses and also that the relationship between RMR and m and s is no longer linear in these very low ranges. It was also felt that a system based more heavily on fundamental geological observations and less on 'numbers' was needed.

The idea of *undisturbed* and *disturbed* rock masses was dropped and it was left to the user to decide which GSI value best described the various rock types exposed on a site. The original *disturbed* parameters were derived by simply reducing the strength by one row in the classification table. It was felt that this was too arbitrary and it was decided that it would be preferable to allow the user to decide what sort of disturbance is involved and to allow users to make their own judgement on how much to reduce the GSI value to account for the strength loss.

1997 Hoek, E. and Brown, E.T. 1997. Practical estimates of rock mass strength. *Intl. J. Rock Mech. & Mining Sci. & Geomechanics Abstracts*. **34**(8), 1165-1186.

This was the most comprehensive paper published to date and it incorporated all of the refinements described above. In addition, a new method for estimating the equivalent Mohr Coulomb cohesion and friction angle was introduced. In this method the Hoek Brown criterion is used to generate a series of values relating axial strength to confining pressure (or shear strength to normal stress) and these are treated as the results of a hypothetical large scale in situ triaxial or shear test. A linear regression method is used to find the average slope and intercept and these are then transformed into a cohesive strength c and a friction angle ϕ .

The most important aspect of this curve fitting process is to decide upon the stress range over which the hypothetical in situ ‘tests’ should be carried out. This was determined experimentally by carrying out a large number of comparative theoretical studies in which the results of both surface and underground excavation stability analyses, using both the Hoek Brown and Mohr Coulomb parameters, were compared.

1998 Hoek, E., Marinos, P. and Benissi, M. 1998. Applicability of the Geological Strength Index (GSI) classification for very weak and sheared rock masses. The case of the Athens Schist Formation. *Bull. Engg. Geol. Env.* **57**(2), 151-160.

This paper extends the range of the Geological Strength Index (GSI) down to 5 to include extremely poor quality schistose rock masses such as the ‘schist’ encountered in the excavations for the Athens Metro and the graphitic phyllites encountered in some of the tunnels in Venezuela. This extension to GSI is based largely on the work of Paul Marinos and Maria Benissi on the Athens Metro. Note that there were now 2 GSI charts. The first of these, for better quality rock masses published in 1994 and the new chart for very poor quality rock masses published in this paper.

2000 Hoek, E. and Marinos, P. 2000. Predicting Tunnel Squeezing. *Tunnels and Tunnelling International*. Part 1, **32/11**, 45-51 – November 2000, Part 2, **32/12**, 33-36 – December, 2000.

This paper introduced an important application of the Hoek-Brown criterion in the prediction of conditions for tunnel squeezing, utilising a critical strain concept proposed by Sakurai in 1983.

2000 Marinos, P. & Hoek, E. 2000. From The Geological to the Rock Mass Model: Driving the Egnatia Highway through difficult geological conditions, Northern

Greece, *Proc. 10th International Conference of Italian National Council of Geologists, Rome*, 325-334

This paper puts more geology into the Hoek-Brown failure criterion than that which has been available previously. In particular, the properties of very weak rocks are addressed in detail for the first time. There is no change in the mathematical interpretation of the criterion in these papers.

2000 Hoek, E. and Karzulovic, A. 2000. Rock-Mass properties for surface mines. In *Slope Stability in Surface Mining* (Edited by W. A. Hustralid, M.K. McCarter and D.J.A. van Zyl), Littleton, CO: Society for Mining, Metallurgical and Exploration (SME), pages 59-70.

This paper repeats most of the material contained in Hoek and Brown, 1997, but adds a discussion on blast damage.

2000 Marinos, P and Hoek, E. 2000. GSI: a geologically friendly tool for rock mass strength estimation. *Proc. International Conference on Geotechnical & Geological Engineering, GeoEng2000*, Technomic publ., 1422-1442, Melbourne.

2001 Marinos, P and Hoek, E. 2001. Estimating the geotechnical properties of heterogeneous rock masses such as flysch. *Bulletin of the Engineering Geology & the Environment (IAEG)*, **60**, 85-92

These papers do not add anything significant to the fundamental concepts of the Hoek-Brown criterion but they demonstrate how to choose appropriate ranges of GSI for different rock mass types. In particular, the 2001 paper on flysch discussed difficult weak and tectonically disturbed materials on the basis of the authors' experience in dealing with these rocks in major projects in northern Greece.

2002 Hoek, E., Carranza-Torres, C. and Corkum, B. 2002. Hoek-Brown criterion – 2002 edition. *Proc. NARMS-TAC Conference*, Toronto, 2002, **1**, 267-273.

This paper represents a major re-examination of the entire Hoek-Brown criterion and includes new derivations of the relationships between m , s , a and GSI . A new parameter D is introduced to deal with blast damage. The relationships between the Mohr Coulomb and the Hoek Brown criteria are examined for slopes and for underground excavations and a set of equations linking the two are presented. The final relationships were derived by comparing hundreds of tunnel and slope stability analyses in which both the Hoek-Brown and the Mohr Coulomb criteria were used and the best match was found by iteration. A Windows based program called *RocLab* was developed to include all of these new derivations and this program can be downloaded (free) from www.rocscience.com. A copy of the paper is included with the download.

2004 Chandler R. J., De Freitas M. H. and P. G. Marinos. 2004. Geotechnical Characterisation of Soils and Rocks: a Geological Perspective. Keynote paper in: *Advances in geotechnical engineering, The Skempton Conference*, **1**, 67-102, Thomas Telford, ICE, London

A brief contribution on the Geological Strength Index within a more general paper on engineering geology of soils and rock.

- 2005** V. Marinos, P. Marinos and E. Hoek 2005. The geological Strength index: applications and limitations, *Bull. Eng. Geol. Environ.*, **64**, 55-65

A discussion on the range of application and the limitations of GSI. General guidelines for the use of GSI are given.

- 2005** E. Hoek, P. Marinos and V. Marinos. 2005. Characterization and engineering properties of tectonically undisturbed but lithologically varied sedimentary rock masses, *International Journal of Rock Mechanics and Mining Sciences*, **42/2**, 277-285

A significant paper in which a new GSI chart for molassic rock masses is introduced. Molasse consists of a series of tectonically undisturbed sediments of sandstones, conglomerates, siltstones and marls, produced by the erosion of mountain ranges after the final phase of an orogeny. They behave as continuous rock masses when they are confined at depth and, even if lithologically heterogeneous, the bedding planes do not appear as clearly defined discontinuity surfaces. The paper discusses the difference between these rock masses and the flysch type rocks which have been severely disturbed by orogenic processes.

- 2006** Marinos, P., Hoek, E., Marinos, V. 2006. Variability of the engineering properties of rock masses quantified by the geological strength index: the case of ophiolites with special emphasis on tunnelling. *Bull. Eng. Geol. Env.*, **65**(2), 129-142.

The paper presents the geological model in which the ophiolitic complexes develop, their various petrographic types and their tectonic deformation, mainly due to overthrusts. The structure of the various rock masses include all types from massive strong to sheared weak, while the conditions of discontinuities are in most cases fair to poor or very poor due to the fact that they are affected by serpentinitisation and shearing. Serpentinisation also reduces the initial intact rock strength. Associated pillow lavas, and tectonic mélanges are also characterised. A GSI chart for ophiolitic rock masses is presented.

- 2006** Hoek, E and Diederichs, M.S. 2006. Empirical estimation of rock mass modulus. *International Journal of Rock Mechanics and Mining Sciences*, **43**, 203–215.

While not directly related to the Hoek-Brown failure criterion, the deformation modulus of a rock mass is an important input parameter in any analysis of rock mass behaviour that includes deformations. Field tests to determine this parameter directly are time consuming, expensive and the reliability of the results of these tests is sometimes questionable. Consequently, several authors have proposed empirical relationships for estimating the value of rock mass deformation modulus on the basis of classification schemes. These relationships are reviewed and their limitations are discussed. Based on data from a large number of in situ measurements from China and Taiwan, a new relationship between the deformation modulus and GSI is proposed. The properties of the intact rock as well as the effects of disturbance due to blast damage and/or stress relaxation are also included in this

new relationship. The program RocLab has been updated (January 2007) to incorporate the method proposed by Hoek and Diederichs for estimating the rock mass deformation modulus.

Conclusions and recommendations

The historical development of the Hoek Brown failure criterion and the associated Geological Strength Index (GSI) has been presented. Evolution of both will continue in order to accommodate processes such as brittle spalling and anisotropy and to include a wider range of rock types. Great care is taken to retain the fundamental components of the system and to avoid changing “ratings” so that users need not go back to question or redo previous applications.

A fundamental assumption of the Hoek-Brown criterion is that the rock mass to which it is being applied is *homogeneous* and *isotropic*. It should *not be applied* to the analysis of structurally controlled failures in cases such as hard rock masses where the discontinuity spacing is similar to the size of the tunnel or slope being analysed and where the failure processes are clearly *anisotropic*.

The criterion also assumes that there is contact between intact rock pieces within the rock masses and it is these contacts that give rise to the highly non-linear characteristics of the criterion at low confining stresses. Where no such contact exists, for example when the components of the rock mass are predominantly soil or clay as in the case of fault gouges, the use of the Mohr-Coulomb criterion, with cohesion and friction parameters determined from laboratory tests, is more appropriate.

One of the greatest sources of error in applying the Hoek-Brown criterion is a misunderstanding of the contribution of the intact rock strength σ_{ci} , the role of which is almost equivalent to GSI in the evaluation of the rock mass properties. It is very common to see geologists confusing the intact strength with the rock mass strength and this results in significant under-estimates of the final rock mass strength. The authors encourage users to pay particular attention to the intact strength of the rock pieces that make up the rock mass. Measurement of the intact strength, using direct compression tests or point load tests where appropriate, should be considered.

Many engineers have requested that the GSI classification should be made more numerical so that input parameters can be “measured” from core or rock exposures rather than estimated from geological observations. The authors and their colleagues have taken note of these request and work on providing quantitative methods for estimating GSI is ongoing, without however neglecting the basic geologic logic expressed by the GSI chart.

Many geotechnical software packages can now accommodate the Hoek-Brown criterion directly and, where this is the case, the exclusive use of the criterion is recommended. All of the necessary parameters can be calculated by means of the free program *RocLab*

(www.roscience.com) and this avoids the approximations and uncertainty associated with trying to determine equivalent Mohr Coulomb parameters.

References

- Hoek E., Brown E.T. (1980) “*Underground Excavations in Rock*”. London: Institution of Mining and Metallurgy
- Hoek E., Brown E.T. (1980) “Empirical strength criterion for rock masses”. *J. Geotech. Engng Div., ASCE* **106**(GT9), 1013-1035.
- Hoek E. (1983) “Strength of jointed rock masses”, 23rd Rankine Lecture. *Géotechnique* **33**(3), 187-223.
- Hoek E., Brown E.T. (1988) “The Hoek-Brown failure criterion - a 1988 update”. *Proc. 15th Canadian Rock Mech. Symp.*, J.H. Curran ed, 31-38, Toronto: Civil Engineering Dept., University of Toronto
- Hoek E. (1990) “Estimating Mohr-Coulomb friction and cohesion values from the Hoek-Brown failure criterion”. *Intl. J. Rock Mech. & Mining Sci. & Geomechanics Abstracts*, **12**(3), 227-229.
- Hoek E., Wood D., Shah S. (1992) “A modified Hoek-Brown criterion for jointed rock masses”. *Proc. rock characterization symp., Int. Soc. Rock Mech.: Eurock '92*, J. Hudson ed, 209-213, London: British Geotechnical Society.
- Hoek E. (1994) “Strength of rock and rock masses”. *ISRM News Journal*, **2**(2), 4-16.
- Hoek E., Kaiser P.K., Bawden. W.F. (1995) “*Support of underground excavations in hard rock*”. Rotterdam: Balkema publ.
- Hoek E., Brown E.T. (1997) “Practical estimates of rock mass strength”. *Intl. J. Rock Mech. & Mining Sci. & Geomechanics, Abstract*, **34**(8), 1165-1186.
- Hoek E., Marinos P., Benissi M. (1998) “Applicability of the Geological Strength Index (GSI) classification for very weak and sheared rock masses. The case of the Athens Schist Formation”. *Bull. Eng. Geol. Env.* **57**(2), 151-160.
- Hoek E., Marinos P. (2000) “Predicting Tunnel Squeezing”. *Tunnels and Tunnelling International*, Part 1, **32/11**, 45-51– November 2000, Part 2, **32/12**, 33-36 – December, 2000.
- Marinos P., Hoek E. (2000) “From The Geological to the Rock Mass Model: Driving the Egnatia Highway through difficult geological conditions, Northern Greece”. *Proc. 10th International Conference of Italian National Council of Geologists, Rome*, 325-334.

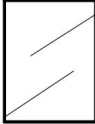
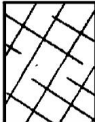




- Hoek E., Karzulovic A. (2000) "Rock-Mass properties for surface mines". In: *Slope Stability in Surface Mining* (Ed: W. A. Hustralid, M.K. McCarter and D.J.A. van Zyl, Littleton, CO: Society for Mining, Metallurgical and Exploration (SME), pages 59-70.
- Marinos P, Hoek E. (2000) "GSI: a geologically friendly tool for rock mass strength estimation". *Proc. International Conference on Geotechnical & Geological Engineering, GeoEng2000*, Technomic publ., 1422-1442, Melbourne.
- Marinos. P, Hoek E. (2001) "Estimating the geotechnical properties of heterogeneous rock masses such as flysch". *Bulletin of the Engineering Geology & the Environment (IAEG)*, **60**, 85-92
- Hoek E., Carranza-Torres C., Corkum B. (2002) "Hoek-Brown criterion – 2002 edition". *Proc. NARMS-TAC Conference*, Toronto, 2002, **1**, 267-273.
- Chandler R. J., De Freitas M. H., P. G. Marinos. (2004) "Geotechnical Characterisation of Soils and Rocks: a Geological Perspective". Keynote paper in: *Advances in geotechnical engineering, The Skempton Conference*, **1**, 67-102, Thomas Telford, ICE, London
- Marinos V., Marinos P., Hoek E. (2005) "The geological Strength index: applications and limitations". *Bull. Eng. Geol. Environ.*, **64**, 55-65
- Hoek E., Marinos P., Marinos V. (2005) "Characterization and engineering properties of tectonically undisturbed but lithologically varied sedimentary rock masses". *International Journal of Rock Mechanics and Mining Sciences*, **42/2**, 277-285
- Marinos P., Hoek E., Marinos V. (2006) "Variability of the engineering properties of rock masses quantified by the geological strength index: the case of ophiolites with special emphasis on tunnelling". *Bull. Eng. Geol. Env.*, **65**(2), 129-142.
- Hoek E, Diederichs M.S. (2006) "Empirical estimation of rock mass modulus". *International Journal of Rock Mechanics and Mining Sciences*, **43**, 203–215.

Appendix - Summary of equations

Publication	Coverage	Equations
Hoek & Brown 1980	Original criterion for jointed hard rock masses tightly interbedded with no fines. Mohr envelope was obtained by statistical curve fitting to a number of (σ'_n, τ) pairs calculated by the method published by Balmer σ'_1, σ'_3 are major and minor effective principal stresses at failure, respectively σ_{ci} is the uniaxial compressive strength of the intact rock σ_t is the tensile strength of the rock mass m and s are material constants ($s=1$ for intact rock) σ'_n, τ are effective normal and shear stresses, respectively.	$\sigma'_1 = \sigma'_3 + \sigma_{ci} \sqrt{m\sigma'_3/\sigma_{ci} + s}$ $\sigma_t = \frac{\sigma_{ci}}{2} \left(m - \sqrt{m^2 + 4s} \right)$ $\tau = A \sigma_{ci} \left((\sigma'_n - \sigma'_t) / \sigma_{ci} \right)^B$ $\sigma'_n = \sigma'_3 + \left((\sigma'_1 - \sigma'_3) / (1 + \partial\sigma'_1 / \partial\sigma'_3) \right)$ $\tau = (\sigma'_n - \sigma'_3) \sqrt{\partial\sigma'_1 / \partial\sigma'_3}$ $\partial\sigma'_1 / \partial\sigma'_3 = m\sigma_{ci} / 2(\sigma'_1 - \sigma'_3)$
Hoek 1983	Original criterion for jointed hard rock masses tightly interlocked with no fines with a discussion on anisotropic failure and an exact solution for the Mohr envelope by Dr J.W. Bray.	$\sigma'_1 = \sigma'_3 + \sigma_{ci} \sqrt{m\sigma'_3/\sigma_{ci} + s}$ $\tau = \left(\cot\phi'_i - \cos\phi'_i \right) m\sigma_{ci} / 8$ $\phi'_i = \arctan \left(1 / \sqrt{4h \cos^2 \theta - 1} \right)$ $\theta = \left(90 + \arctan(1/\sqrt{h^3 - 1}) \right) / 3$ $h = 1 + \left(16(m\sigma'_n + s\sigma_{ci}) / (3m^2\sigma_{ci}) \right)$
Hoek & Brown 1988	As for Hoek 1983 but with the addition of relationships between constants m and s and a modified form of RMR in which the Groundwater rating was assigned a fixed value of 10 and the Adjustment for Joint Orientation was set at 0. Also a distinction between <i>disturbed</i> and <i>undisturbed</i> rock masses was introduced together with means of estimating deformation modulus E (after Serafim and Pereira). Note that the ground water rating assigned a final value of 15 in the RMR 1989 version.	<p><i>Disturbed rock masses:</i></p> $m_b/m_i = \exp((RMR - 100)/14)$ $s = \exp((RMR - 100)/6)$ <p><i>Undisturbed or interlocking rock masses</i></p> $m_b/m_i = \exp((RMR - 100)/28)$ $s = \exp((RMR - 100)/9)$ $E = 10^{((RMR - 10)/40)}$ <p>m_b, m_i are petrographic constants for broken and intact rock, respectively.</p>
Hoek, Wood & Shah 1992	Modified criterion to account for the fact the heavily jointed rock masses have zero tensile strength. Balmer's technique for calculating shear and normal stress pairs was utilised. Material parameter a is introduced.	$\sigma'_1 = \sigma'_3 + \sigma_{ci} \left(m_b \sigma'_3 / \sigma_{ci} \right)^a$ $\sigma'_n = \sigma'_3 + \left((\sigma'_1 - \sigma'_3) / (1 + \partial\sigma'_1 / \partial\sigma'_3) \right)$ $\tau = (\sigma'_n - \sigma'_3) \sqrt{\partial\sigma'_1 / \partial\sigma'_3}$ $\partial\sigma'_1 / \partial\sigma'_3 = 1 + a m_b^a \left(\sigma'_3 / \sigma_{ci} \right)^{a-1}$
Hoek 1994 Hoek, Kaiser & Bawden 1995	Introduction of the Generalised Hoek-Brown criterion, incorporating both the original criterion for excellent to fair quality rock masses and the modified criterion for poor to very poor quality rock masses	$\sigma'_1 = \sigma'_3 + \sigma_{ci} \left(m \sigma'_3 / \sigma_{ci} + s \right)^a$ <p>for $GSI > 25$</p> $m_b/m_i = \exp((GSI - 100) / 28)$

	<p>with increasing fines content. The Geological Strength Index GSI was introduced to overcome the deficiencies in Bieniawski's RMR for very poor quality rock masses. The distinction between disturbed and undisturbed rock masses was dropped on the basis that disturbance is generally induced by engineering activities and should be allowed for by downgrading the value of GSI.</p>	$s = \exp((GSI - 100)/9)$ $a = 0.5$ for $GSI < 25$ $s = 0$ $a = 0.65 - GSI/200$
<p>Hoek, Carranza-Torres and Corkum, 2002</p>	<p>A new set of relationships between GSI, m_b, s and a is introduced to give a smoother transition between very poor quality rock masses ($GSI < 25$) and stronger rocks. A disturbance factor D to account for stress relaxation and blast damage is also introduced. Equations for the calculation of Mohr Coulomb parameters c and ϕ are introduced for specific ranges of the confining stress σ'_{3max} for tunnels and slopes.</p> <p>All of these equations are incorporated into the Windows program RocLab that can be downloaded from the Internet site www.rocscience.com. A copy of the full paper is included with the download.</p>	$\sigma'_1 = \sigma'_3 + \sigma_{ci} \left(m_b \sigma'_3 / \sigma_{ci} + s \right)^a$ $m_b = m_i \exp(GSI - 100 / 28 - 14D)$ $s = \exp(GSI - 100 / 9 - 3D)$ $a = \frac{1}{2} + \frac{1}{6} \left(e^{-GSI/15} - e^{-20/3} \right)$ $E_m (GPa) = \left(1 - \frac{D}{2} \right) \sqrt{\frac{\sigma_{ci}}{100}} \cdot 10^{((GSI - 10) / 40)}$ $\phi' = \sin^{-1} \left[\frac{6am_b(s + m_b\sigma'_{3n})^{a-1}}{2(1+a)(2+a) + 6am_b(s + m_b\sigma'_{3n})^{a-1}} \right]$ $c' = \frac{\sigma_{ci} \left[(1+2a)s + (1-a)m_b\sigma'_{3n} \right] (s + m_b\sigma'_{3n})^{a-1}}{(1+a)(2+a) \sqrt{1 + (6am_b(s + m_b\sigma'_{3n})^{a-1}) / ((1+a)(2+a))}}$ <p>where, for tunnels</p> $\frac{\sigma'_{3max}}{\sigma'_{cm}} = 0.47 \left(\frac{\sigma'_{cm}}{\gamma H} \right)^{-0.94} \quad - H \text{ is the depth below surface}$ <p>for slopes</p> $\frac{\sigma'_{3max}}{\sigma'_{cm}} = 0.72 \left(\frac{\sigma'_{cm}}{\gamma H} \right)^{-0.91} \quad - H \text{ is the slope height}$ <p>γ is the unit weight of the rock mass</p>
<p>Hoek and Diederichs, 2006</p>	<p>Based on an analysis of a data set from China and Taiwan, a new relationship between the rock mass deformation modulus E_{rm} and GSI is proposed. This is based on a sigmoid function and two forms of the relationship are presented. The simplified equation depends on GSI and D only and it should be used with caution, only when no information in the intact rock properties are available. The more comprehensive equation includes the intact rock modulus. When laboratory data for the modulus are not available a means of estimating this modulus from the intact rock strength σ_{ci} is given, based on a modulus reduction factor MR.</p>	<p>Sigmoid function: $y = c + \frac{a}{1 + e^{-((x-x_0)/b)}}$</p> <p>Simplified Hoek and Diederichs equation:</p> $E_{rm} (MPa) = 100000 \left(\frac{1 - D/2}{1 + e^{((75+25D-GSI)/11)}} \right)$ <p>Hoek and Diederichs equation:</p> $E_{rm} = E_i \left(0.02 + \frac{1 - D/2}{1 + e^{((60+15D-GSI)/11)}} \right)$ <p>Estimated intact rock modulus:</p> $E_i = MR \cdot \sigma_{ci}$

Geological Strength Index Chart

<p>GEOLOGICAL STRENGTH INDEX FOR JOINTED ROCKS (Hoek and Marinos, 2000)</p> <p>From the lithology, structure and surface conditions of the discontinuities, estimate the average value of GSI. Do not try to be too precise. Quoting a range from 33 to 37 is more realistic than stating that GSI = 35. Note that the table does not apply to structurally controlled failures. Where weak planar structural planes are present in an unfavourable orientation with respect to the excavation face, these will dominate the rock mass behaviour. The shear strength of surfaces in rocks that are prone to deterioration as a result of changes in moisture content will be reduced if water is present. When working with rocks in the fair to very poor categories, a shift to the right may be made for wet conditions. Water pressure is dealt with by effective stress analysis.</p>		SURFACE CONDITIONS				
STRUCTURE		DECREASING SURFACE QUALITY →				
		VERY GOOD Very rough, fresh unweathered surfaces	GOOD Rough, slightly weathered, iron stained surfaces	FAIR Smooth, moderately weathered and altered surfaces	POOR Slickensided, highly weathered surfaces with compact coatings or fillings or angular fragments	VERY POOR Slickensided, highly weathered surfaces with soft clay coatings or fillings
	INTACT OR MASSIVE - intact rock specimens or massive in situ rock with few widely spaced discontinuities	90	80	70	N/A	N/A
	BLOCKY - well interlocked undisturbed rock mass consisting of cubical blocks formed by three intersecting discontinuity sets	80	70	60	50	40
	VERY BLOCKY- interlocked, partially disturbed mass with multi-faceted angular blocks formed by 4 or more joint sets	70	60	50	40	30
	BLOCKY/DISTURBED/SEAMY - folded with angular blocks formed by many intersecting discontinuity sets. Persistence of bedding planes or schistosity	60	50	40	30	20
	DISINTEGRATED - poorly interlocked, heavily broken rock mass with mixture of angular and rounded rock pieces	50	40	30	20	10
	LAMINATED/SHEARED - Lack of blockiness due to close spacing of weak schistosity or shear planes	N/A	N/A			



Contents lists available at ScienceDirect

Journal of Rock Mechanics and Geotechnical Engineering

journal homepage: www.rockgeotech.org

Full Length Article

The Hoek–Brown failure criterion and GSI – 2018 edition

E. Hoek^{a,*}, E.T. Brown^b^a North Vancouver, British Columbia, V7R 4H7, Canada^b Brisbane, Queensland 4169, Australia

ARTICLE INFO

Article history:

Received 22 July 2018

Received in revised form

2 August 2018

Accepted 3 August 2018

Available online xxx

Keywords:

Hoek–Brown criterion

Geological strength index (GSI)

Rock mass strength

Uniaxial compressive strength (UCS)

Tension cut-off

Rock mass deformation modulus

ABSTRACT

The Hoek–Brown criterion was introduced in 1980 to provide input for the design of underground excavations in rock. The criterion now incorporates both intact rock and discontinuities, such as joints, characterized by the geological strength index (GSI), into a system designed to estimate the mechanical behaviour of typical rock masses encountered in tunnels, slopes and foundations. The strength and deformation properties of intact rock, derived from laboratory tests, are reduced based on the properties of discontinuities in the rock mass. The nonlinear Hoek–Brown criterion for rock masses is widely accepted and has been applied in many projects around the world. While, in general, it has been found to provide satisfactory estimates, there are several questions on the limits of its applicability and on the inaccuracies related to the quality of the input data. This paper introduces relatively few fundamental changes, but it does discuss many of the issues of utilization and presents case histories to demonstrate practical applications of the criterion and the GSI system.

© 2018 Institute of Rock and Soil Mechanics, Chinese Academy of Sciences. Production and hosting by Elsevier B.V. This is an open access article under the CC BY-NC-ND license (<http://creativecommons.org/licenses/by-nc-nd/4.0/>).

1. Introduction

The Hoek–Brown criterion was derived from the results of research into the brittle failure of intact rock by Hoek (1965) and on model studies of jointed rock mass behaviour by Brown (1970).

The brittle fracture theory published by Griffith (1924), modified by McClintock and Walsh (1962) to account for friction on sliding surfaces, formed the basis for the nonlinear failure criterion for intact rock published by Hoek and Brown (1980a, b). This 2018 edition of the criterion incorporates all the modifications that have been implemented in the past 38 years, based on experiences gained in applying this criterion to practical problems.

The geological strength index (GSI) is a system of rock mass characterization that was developed, by Hoek (1994) and Hoek et al. (1995), to link the failure criterion to engineering geology observations in the field. The most complete description of the current use of the GSI and the Hoek–Brown criterion is given in a chapter entitled “Rock mass properties” in an eBook by Hoek, called *Practical Rock Engineering*, which can be downloaded from <http://www.rocscience.com>.

The Hoek–Brown failure criterion and the associated GSI have gained wide acceptance as tools for estimating the strength and deformation characteristics of heavily jointed rock masses. Because of the lack of suitable alternatives, the criterion was adopted by the rock mechanics community and its use quickly spread beyond the original assumptions based on interlocking joint-defined blocks in hard rocks. Consequently, it became necessary to re-examine these assumptions and to introduce new elements from time to time to account for the wide range of practical problems to which the criterion was being applied.

One of the early difficulties arose because many geotechnical problems, particularly slope stability issues, are more conveniently dealt with in terms of shear and normal stresses rather than the principal stresses used in the definition of the original Hoek–Brown criterion. At that time, geotechnical software did not allow the incorporation of the constitutive relationships, including flow rules that describe the behaviour of the rock after reaching the peak strength predicted by the Hoek–Brown criterion. Hence, it was necessary to find equivalent Mohr–Coulomb parameters for use with existing software. In 2018, most geotechnical software for stress and slope stability analysis allows the Hoek–Brown criterion to be used directly. Consequently, in this context, only the Hoek–Brown criterion is discussed in detail.

For readers who require equivalent Mohr–Coulomb friction angles and cohesive strengths, a detailed discussion on how these can be obtained is given in Hoek et al. (2002). It is recommended

* Corresponding author.

E-mail addresses: ehoek@mailas.com (E. Hoek), et_brown@bigpond.com (E.T. Brown).

Peer review under responsibility of Institute of Rock and Soil Mechanics, Chinese Academy of Sciences.

<https://doi.org/10.1016/j.jrmge.2018.08.001>

1674-7755 © 2018 Institute of Rock and Soil Mechanics, Chinese Academy of Sciences. Production and hosting by Elsevier B.V. This is an open access article under the CC BY-NC-ND license (<http://creativecommons.org/licenses/by-nc-nd/4.0/>).

that these friction angles and cohesive strengths, derived from the Hoek–Brown criterion, should not be used without a tension cut-off.

The GSI was extended to cover folded and tectonically sheared rock masses in a series of papers by Hoek et al. (1998, 2005), Hoek and Marinos (2000), Marinos and Hoek (2000, 2001), Marinos (2017), Marinos et al. (2005), and Marinos and Carter (2018). The GSI is discussed in detail in Sections 6 and 11.

For clarity, the equations provided and discussed here are expressed in total stress terms. However, as discussed by Hoek and Brown (1997), the solution to some rock engineering problems requires an effective stress approach. In this case, effective stress equivalents of the equations given here may be used.

2. The origin of the Hoek–Brown criterion

There is abundant evidence to show that the failure in brittle materials such as rock, concrete, ceramic and glass originates from micro-cracks or flaws in the intact material. In rock, these flaws are typically grain boundaries or inter-granular cracks and tensile cracks that propagate from their tips when frictional sliding occurs along the flaw.

Griffith (1921) proposed that tensile failure in brittle materials such as glass initiates at the tips of defects which he represented by flat elliptical cracks. His original work dealt with fracture in material subjected to tensile stress, but later he extended this concept to include biaxial compression loading (Griffith, 1924), thereby obtaining a nonlinear compressive failure envelope for brittle materials.

Murrell (1958) proposed the application of the Griffith theory to rock. This suggestion was immediately implemented by researchers such as McClintock and Walsh (1962), Brace (1964), Hoek (1964), Cook (1965) and many others. The early findings of this research were summarized by Jaeger and Cook (1969). More recent research has been summarized by Andriev (1995).

Based on this research on the nonlinear Griffith failure criterion, Hoek and Brown (1980a, b) proposed the following empirical equation to fit the results of a wide range of triaxial tests on intact rock samples:

$$\sigma_1 = \sigma_3 + \sigma_{ci} \sqrt{m_i \frac{\sigma_3}{\sigma_{ci}} + 1} \quad (1)$$

where σ_1 and σ_3 are the major and minor principal stresses, respectively; σ_{ci} is the unconfined compressive strength; and m_i is a material constant for the intact rock.

Zuo et al. (2008, 2015) showed that a very similar equation could be derived from an analysis of failure propagation from a penny-shaped crack in a triaxial stress field. Their equation can be written:

$$\sigma_1 = \sigma_3 + \sigma_{ci} \sqrt{\left(\frac{\mu}{\kappa} \frac{\sigma_{ci}}{|\sigma_t|} \right) \frac{\sigma_3}{\sigma_{ci}} + 1} \quad (2)$$

where $\mu = \tan \phi$ (ϕ is the crack surface friction angle); κ is a coefficient used for mixed mode fracture which can be derived from various approximations, such as $\kappa = \sqrt{3/2}$ for a maximum stress criterion, with $\kappa = 1$ for a maximum energy release criterion; and $|\sigma_t|$ is the absolute value of the uniaxial tensile strength.

Substitution of $m_i = \mu \sigma_{ci} / (\kappa |\sigma_t|)$ in Eq. (2) results in the Hoek–Brown Eq. (1) for intact rock. Hence, the constant m_i has a physical meaning. As will be shown later in this paper, the relationship between m_i and $\sigma_{ci}/|\sigma_t|$ is important in the application of the Hoek–Brown criterion to rock and rock mass failure.

3. Generalized Hoek–Brown criterion

The generalized Hoek–Brown criterion for the estimation of rock mass strength, introduced by Hoek (1994) and Hoek et al. (1995), is expressed as

$$\sigma_1 = \sigma_3 + \sigma_{ci} \left(m_b \frac{\sigma_3}{\sigma_{ci}} + s \right)^a \quad (3)$$

where m_b , s , and a are the rock mass material constants, given by

$$m_b = m_i \exp[(GSI - 100)/(28 - 14D)] \quad (4)$$

$$s = \exp[(GSI - 100)/(9 - 3D)] \quad (5)$$

$$a = 1/2 + 1/6 \left(e^{-GSI/15} - e^{-20/3} \right) \quad (6)$$

where, for intact rock, the material constants are denoted by m_i , $s = 1$ and $a = 0.5$; D is a factor which depends upon the degree of disturbance to which the rock mass has been subjected to blast damage and stress relaxation. Guidelines for the selection of D are discussed in Section 8.

Eqs. (4)–(6) were developed to deal with rock masses, such as that illustrated in Fig. 1, comprised of interlocking angular blocks in which the failure process is dominated by block sliding and rotation without a great deal of intact rock failure, under low to moderate confining stresses.

In dealing with the application of Eqs. (4)–(6) to rock masses which fall outside the range of conditions as described above, several authors have proposed modifications to the values of the constants or even the form of these equations. This is a completely

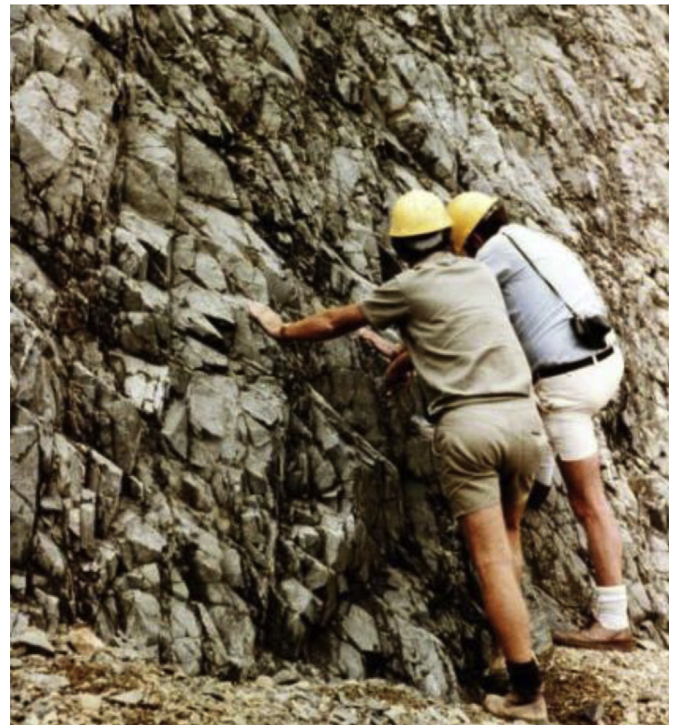


Fig. 1. Interlocking blocks of very strong Panguna andesite and granodiorite in the Bougainville open pit mine in Papua New Guinea for which the original Hoek–Brown criterion for rock mass strength estimation was developed (Hoek and Brown, 1980a, b).

understandable and acceptable approach. However, readers intending to apply these modifications should ensure that they have done sufficient reading and research to enable them to define the range of applicability of these modifications and whether they apply to the problem under consideration. In other words, do not apply equations, other than Eqs. (4)–(6), simply because they appear to be new or interesting.

Originally, the GSI term in these equations was estimated directly from Bieniawski's rock mass rating (RMR) classification (Brown and Hoek, 1988). The GSI was introduced by Hoek (1994) as a direct replacement for RMR.

4. Strength of intact rock

In Eq. (3), the unconfined compressive strength, σ_{ci} , is the dominant parameter which sets the scale of the rock mass strength failure curve on a σ_1 vs σ_3 plot. The constants m_b , s , and a define the shape of the curvilinear failure plot. At this point, it is important to explain the difference between the unconfined compressive strength, σ_{ci} , and the uniaxial compressive strength (UCS) of intact rock. The UCS is generally determined by testing several specimens without applying a confining stress. Fig. 2 shows the distribution curves obtained from high quality laboratory UCS tests on a range of rock types encountered on a typical construction project.

In developing the Hoek–Brown criterion, it was recognized that including a collection of UCS test results in a series of triaxial test data would result in a significant bias in the curve fitting process required to determine the constants of the equation. Consequently, it was decided to use only the average value for a UCS data set to represent the value of the principal stress at zero confining stress. The triaxial data set, including this average value, was then used in a regression analysis to determine the unconfined compressive strength, σ_{ci} , and the constant, m_i .

The Hoek–Brown criterion was developed to deal with shear failure in rock. Fig. 3 plotting the results of triaxial compression tests on Indiana limestone by Schwartz (1964) shows that the range of applicability of the criterion is determined by the transition from shear to ductile failure at approximately $\sigma_1 = 4.0\sigma_3$. Mogi (1966) investigated the transition from shear to ductile failure in a wide range of rock types and found that the average transition is defined by $\sigma_1 = 3.4\sigma_3$. This is a useful guide for the maximum confining pressure for triaxial testing of intact

rock specimens. In some laboratories, triaxial tests are carried out by applying a constant confining stress and increasing the axial load until the onset of shear failure is detected in the stress–strain plot. The confining stress is then increased, and the axial load is again increased until the onset of the next failure is detected. This stage testing process is repeated several times to arrive at a complete failure plot from a single specimen. Since the specimen has been damaged in the first loading cycle and all subsequent test stages involve the damaged rock, this method does not produce an acceptable peak strength plot for intact rock. Therefore, it is recommended that this type of triaxial test should not be used for determining the Hoek–Brown parameters σ_{ci} and m_i .

Tensile failure ($\sigma_3 < 0$) is not dealt with by the Hoek–Brown criterion. However, tensile failure is an important factor in some rock engineering problems. In the context of this discussion, the most effective solution to this problem is the Griffith theory which, as proposed by Fairhurst (1964), can be generalized in terms of the ratio of compressive to tensile strength, $\sigma_{ci}/|\sigma_t|$, as follows:

- (1) If $w(w-2)\sigma_3 + \sigma_1 \leq 0$, failure occurs when $\sigma_3 = \sigma_t$
- (2) If $w(w-2)\sigma_3 + \sigma_1 > 0$, failure occurs when

$$\sigma_1 = \frac{(2\sigma_3 - A\sigma_t) + \sqrt{(A\sigma_t - 2\sigma_3)^2 - 4(\sigma_3^2 + A\sigma_t\sigma_3 + 2AB\sigma_t^2)}}{2} \quad (7)$$

where

$$A = 2(w-1)^2, B = \left(\frac{w-1}{2}\right)^2 - 1, w = \sqrt{\frac{\sigma_{ci}}{|\sigma_t|} + 1}$$

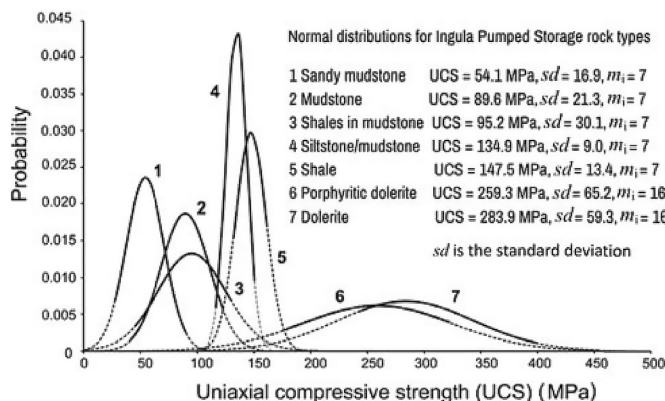


Fig. 2. Normal distributions and UCS values determined from tests on cores from seven rock types recovered during the site investigation and design phase for the Ingula Pumped Storage Project in South Africa (Keyter et al., 2008).

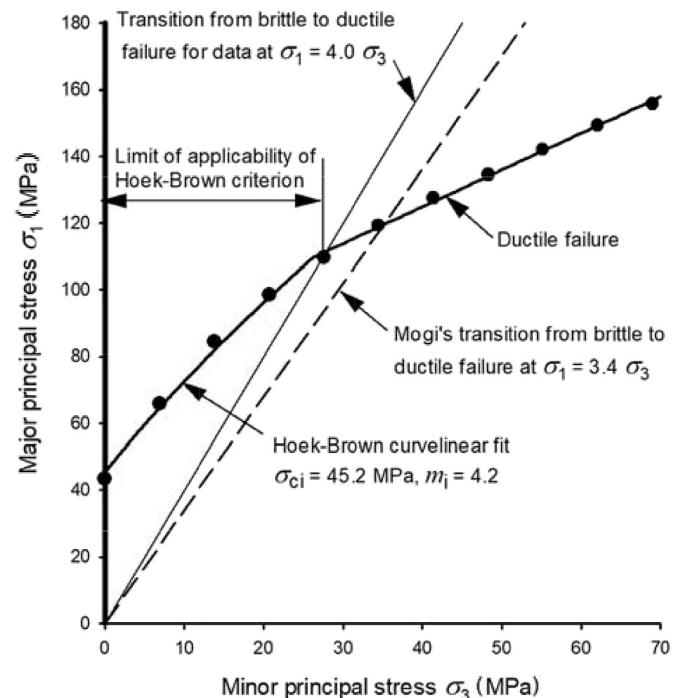


Fig. 3. Limit of applicability of the Hoek–Brown criterion and for the maximum confining pressure for triaxial tests on Indiana limestone.

The combination of two failure criteria on one plot can result in significant complications in programming for numerical analyses. Therefore, it is preferable to simplify the resulting combination as far as possible. Hoek and Martin (2014) proposed that, for practical rock engineering purposes, a Hoek–Brown failure envelope with a tensile cut-off, based on the generalized Griffith failure criterion theory proposed by Fairhurst (1964), can provide an effective solution. This is illustrated in the plot presented in Fig. 4.

The tests conducted by Ramsey and Chester (2004) and Bobich (2005) are among the very few reliable triaxial data sets which include direct tensile tests. Some suggestions on testing procedures required to provide reliable data are given in the Appendix. As an interim measure, the following approximate relationship between the compressive to tensile strength ratio, $\sigma_{ci}/|\sigma_t|$, and the Hoek–Brown parameter m_i is proposed:

$$\sigma_{ci}/|\sigma_t| = 0.81m_i + 7 \quad (8)$$

Eq. (8) is based on triaxial test data and curve fitting estimates, as listed in Table 1 and plotted in Fig. 5.

An example of plotting the Hoek–Brown failure curve with a tension cut-off is presented in Fig. 6. The data for this plot were obtained from triaxial tests on specimens of Granite Aplite, a uniformly fine grained intrusive igneous rock from South Africa. These tests were carried out by Dr. W. Brace at Massachusetts Institute of Technology in the USA and Dr. E. Hoek at the Council for Scientific and Industrial Research in South Africa. The average unconfined compressive strength of 588 MPa was used, with the triaxial test results, to fit the peak strength curve. The tension cut-off was calculated using Eq. (8).

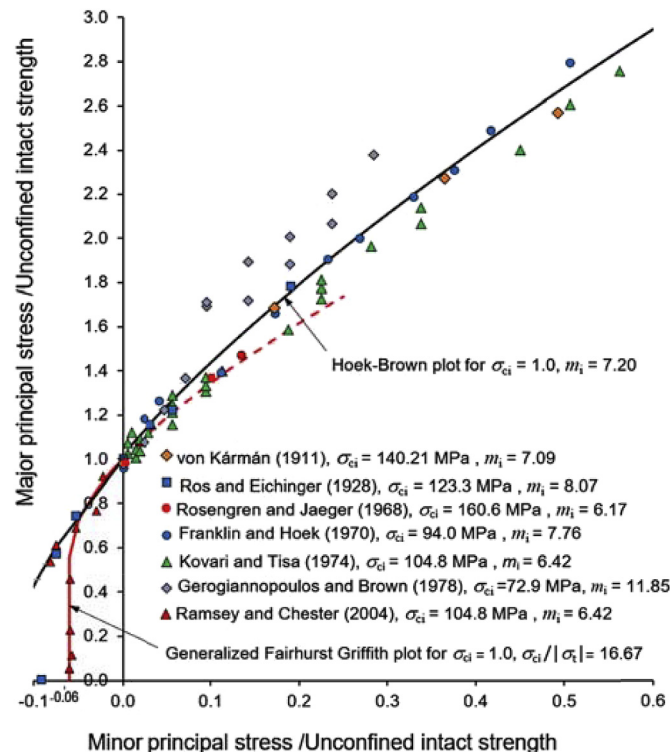


Fig. 4. Dimensionless plot of triaxial test data for Carrara marble showing the use of the generalized Griffith theory for tensile failure and the Hoek–Brown criterion for shear failure. (Von Kármán, 1911, Ros et al., 1928, Rosengren and Jaeger, 1968, Franklin and Hoek, 1970, Kovari and Tisa, 1974, Gerogiannopoulos and Brown, 1978, Ramamurthy, 1993, Kalamaris and Bieniawski, 1995, Sheorey, 1997, Aydan and Dalgic, 1998).

Table 1
Analysis of data containing tensile values.

σ_{ci} (MPa)	m_i	$\sigma_{ci}/ \sigma_t $	Data set
224	32.4	32	Granite (Lau and Gorski, 1992)
600.4	18.8	22.2	Granite Aplite (Hoek, 1965)
95.5	9.65	14.9	Berea sandstone (Bobich, 2005)
125.5	10.6	14.4	Webtuck dolomite (Brace, 1964)
516.5	8.45	13.9	Blair dolomite (Brace, 1964)
128.5	8.25	16.6	Marble (Ramsey and Chester, 2004)
228	14.1	18.6	Quartzite (Hoek, 1965)
1	5	10	Estimated by matching Hoek–
1	7.2	12	Brown and Fairhurst generalized
1	10	14	Griffith curves as illustrated in Fig. 4.
1	15	20	
1	20	24	
1	30	32	

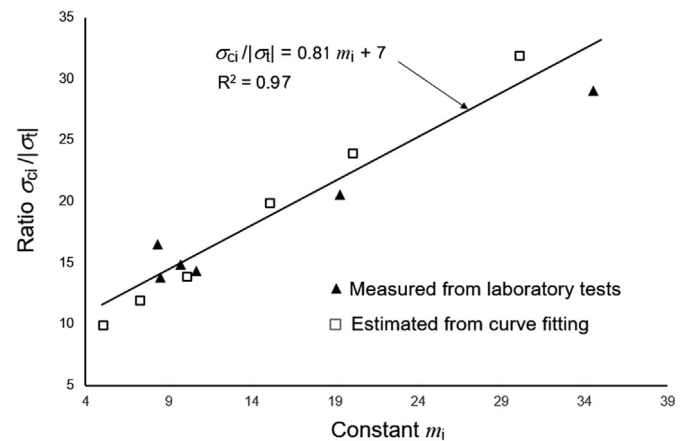


Fig. 5. Relationship between $\sigma_{ci}/|\sigma_t|$ and m_i .

It will be noted that, for intact rock, only two variables are needed to define the Hoek–Brown failure envelope with a tension cut-off. These are the unconfined compressive strength of the intact rock, σ_{ci} , and the material parameter, m_i . For hard intact rock, the parameter s is always equal to 1 and the constant $a \approx 0.5$.

Note that the Brazilian test, in which the tensile failure is induced as a centre of a diametrically loaded disc specimen, is not an acceptable direct tensile test for inclusion in the analysis as described above. Due to the complex stress distribution and the influence of the stress concentrations at the loading points, the calculation of the tensile strength requires significant correction (Perras and Diederichs, 2014). At best, the Brazilian test can be regarded as an index test which must be calibrated against direct tensile tests for each rock type.

5. Limits of applicability of the Hoek–Brown criterion

Fig. 3 shows that the Hoek–Brown criterion is only applicable for confining stresses within the range defined by $\sigma_3 = 0$ and the transition from shear to ductile failure.

A case in which the Hoek–Brown criterion does not apply may arise when massive rock is in a state of relatively high confinement. Kaiser et al. (2010) discuss this case in the context of highly stressed pillars in hard, brittle rock at depth. In this case, it was found that the amount of rock mass strength degradation given by Eqs. (4) and (5) for m_b and s was reduced by replacing the constants 28, in Eq (4), and 9, in Eq (5) with higher values that Kaiser et al. (2010) related to the GSI and confining pressure. Importantly, in this case, higher

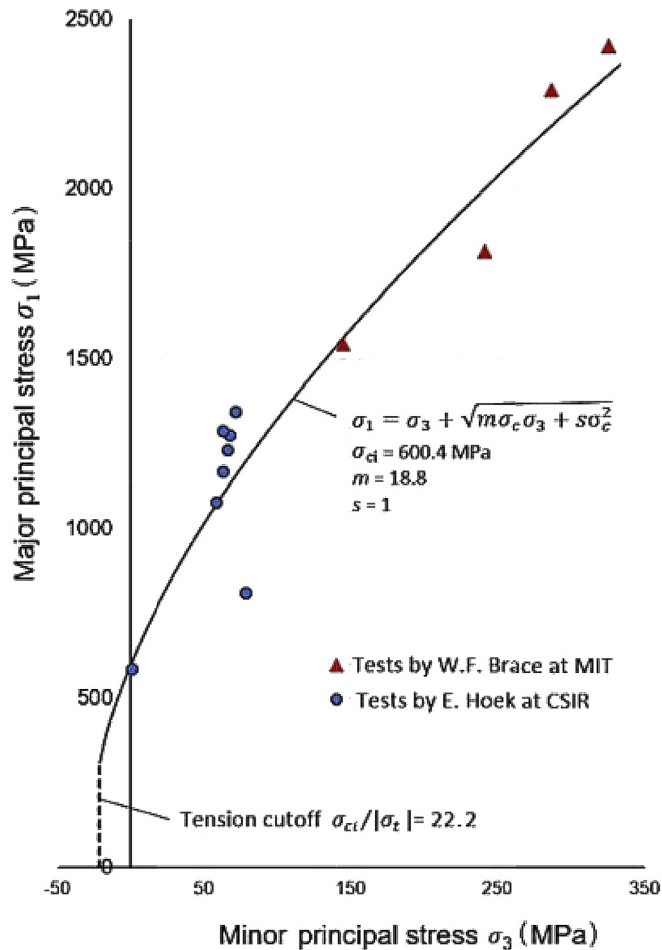


Fig. 6. Hoek–Brown failure plot for triaxial tests on Granite Aplite carried out by Hoek (1965) and Brace (1964).

confinement produced rock mass strengths that were greater than those given by the conventional application of Eqs. (3)–(6).

A more general case in which Eqs. (3)–(6) may not apply is in massive to moderately jointed hard rock having high values of GSI. For example, for $GSI \geq 65$, Bewick et al. (2019) show how carefully distinguishing the failure modes of heterogeneous hard rock specimens in laboratory uniaxial and triaxial compression strength tests can allow the conventional Hoek–Brown criterion and GSI approach to be used for strength estimation. The parameters should be adjusted to provide good fits to test data for massive to moderately jointed rock.

6. The geological strength index (GSI)

Hoek (1994) and Hoek et al. (1995) introduced the GSI as a tool for collecting field information for incorporation in Eqs. (4)–(6). This is used to estimate the constants m_i , s and a in the Hoek–Brown criterion defined by Eq. (3). The GSI classification was set up to address the two principal factors considered to have important influences on the mechanical properties of a rock mass, i.e. the structure (or blockiness) and the condition of the joints. The latest major revision of the GSI and its use in Eqs. (4)–(6) was made by Hoek et al. (2002). The basic version of the GSI chart, for use with jointed rocks, is reproduced in Fig. 7, from Hoek and Marinos (2000).

The Hoek–Brown failure criterion was originally developed based on the assumption that intact rock is free from defects other than microcracks and flaws. The GSI system was developed to deal with rock masses comprised of interlocking angular blocks in which the failure process is dominated by block sliding and rotation without a great deal of intact rock failure.

Figs. 8–12 show the typical applications of the GSI chart to exposed faces in a range of rock formations. The original purpose of the GSI chart was to provide a guide for the initial estimation of rock mass properties. It was always assumed that the user would improve the initial estimates with more detailed site investigations, numerical analyses, and back analyses of the tunnel or slope performance to validate or modify these estimates.

In dealing with the tectonically disturbed rock masses, as illustrated in Figs. 10 and 11, the original GSI chart is adequate for estimates during the site investigation stage. However, during the later design stages, it becomes more difficult to apply this chart effectively unless observations and measurements of the rock mass behaviours in response to excavation are available to provide a basis for calibration.

To simplify this problem, Marinos and Hoek (2001) published a GSI chart for heterogeneous and tectonically deformed sedimentary rocks. An extended version of this chart was published by Marinos (2017) and Marinos and Carter (2018). Additional charts for ophiolites (Marinos et al., 2005) and tectonically undisturbed molassic rocks (Hoek et al., 2005) were also developed to cover tunnelling projects in northern Greece.

7. Estimating rock mass deformation modulus

In addition to the estimate of the strength of intact rock and rock masses, the analysis of the behaviour of a slope, foundation or tunnel also requires an estimate of the deformation modulus of the rock mass in which these structures are excavated. This is a significant challenge and numerous authors have presented various suggestions on how these estimates can be made.

Hoek and Diederichs (2006), using a database of rock mass deformation modulus measurements from projects in China (including Taiwan), proposed the following equation for estimating rock mass modulus (Fig. 13):

$$E_{rm} = E_i \left\{ 0.02 + \frac{1 - D/2}{1 + \exp[(60 + 15D - GSI)/11]} \right\} \quad (9)$$

where E_i is the intact rock deformation modulus (MPa).

Hoek and Diederichs (2006) recommended that, when the laboratory measured values for E_i are not available, the rock mass reduction values (MR) proposed by Deere (1968) can be used for estimating the intact rock modulus. When no information on the intact rock deformation modulus is available, the following alternative equation for estimating the rock mass modulus E_{rm} (MPa) was proposed by Hoek and Diederichs (2006):

$$E_{rm} = 10^5 \frac{1 - D/2}{1 + \exp[(75 + 25D - GSI)/11]} \quad (10)$$

Fig. 14 gives a comparison between the deformation modulus estimated from Eq. (10) and a number of field measurements and predictions by Bieniawski (1978), Serafim and Pereira (1983), Stephens and Banks (1989), Read et al. (1999), and Barton (2002). The general agreement between these results suggests that all these predictions, including those of Hoek and Diederichs (2006), can be used with confidence for estimating field values.

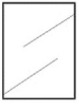
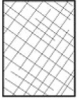




<p>GEOLOGICAL STRENGTH INDEX FOR JOINTED ROCKS (Hoek and Marinos, 2000)</p> <p>From the lithology, structure and surface conditions of the discontinuities, estimate the average value of GSI. Do not try to be too precise. Quoting a range from 33 to 37 is more realistic than stating that $GSI = 35$. Note that the table does not apply to structurally controlled failures. Where weak planar structural planes are present in an unfavourable orientation with respect to the excavation face, these will dominate the rock mass behaviour. The shear strength of surfaces in rocks that are prone to deterioration as a result of changes in moisture content will be reduced if water is present. When working with rocks in the fair to very poor categories, a shift to the right may be made for wet conditions. Water pressure is dealt with by effective stress analysis.</p>		<p>SURFACE CONDITIONS</p> <p>VERY GOOD Very rough, fresh unweathered surfaces</p> <p>GOOD Rough, slightly weathered, iron stained surfaces</p> <p>FAIR Smooth, moderately weathered and altered surfaces</p> <p>POOR Stickensided, highly weathered surfaces with compact coatings or fillings or angular fragments</p> <p>VERY POOR Stickensided, highly weathered surfaces with soft clay coatings or fillings</p>				
<p>STRUCTURE</p>		<p>DECREASING SURFACE QUALITY →</p>				
<p>DECREASING INTERLOCKING OF ROCK PIECES</p> <p>↓</p>	 <p>INTACT OR MASSIVE - intact rock specimens or massive in situ rock with few widely spaced discontinuities</p>	90			N/A	N/A
	 <p>BLOCKY - well interlocked undisturbed rock mass consisting of cubical blocks formed by three intersecting discontinuity sets</p>	80	70			
	 <p>VERY BLOCKY - interlocked, partially disturbed mass with multi-faceted angular blocks formed by 4 or more joint sets</p>		60			
	 <p>BLOCKY/DISTURBED/SEAMY - folded with angular blocks formed by many intersecting discontinuity sets. Persistence of bedding planes or schistosity</p>			50		
	 <p>DISINTEGRATED - poorly interlocked, heavily broken rock mass with mixture of angular and rounded rock pieces</p>			40		
	 <p>LAMINATED/SHEARED - Lack of blockiness due to close spacing of weak schistosity or shear planes</p>				30	
					20	
						10
		N/A	N/A			

Fig. 7. Basic GSI chart (Hoek and Marinos, 2000).

Cai et al. (2004) carried out a detailed review of the application of the GSI system for the estimation of rock mass strength and deformation properties in two underground powerhouse projects in Japan. In their conclusion they state:

"The GSI system was applied to characterize the jointed rock masses at Kannagawa and Kazunogawa underground powerhouses in Japan. Based on the estimated GSI values and intact rock strength properties, equivalent Mohr–Coulomb strength parameters and elastic modulus of the jointed rock mass were calculated and compared to in situ test results. The Point Estimate Method was applied to approximate variance of the mechanical properties of the jointed rock masses. It is found that both the means and variances of c , ϕ and E predicted from the quantified GSI approach are generally in good agreement with field data. Hence, the quantitative approach added to the GSI system provides a means

for consistent rock mass characterization and thus improves the utility of the GSI system."

8. Disturbance factor D

When tunnels, slopes or foundations are excavated in rock masses, removal of the rock results in stress relief which allows the surrounding rock mass to relax and dilate. The aim of any good design is to control this dilation, and the consequent displacements, in order to minimize rock failure. This can be achieved by a careful selection of excavation shape, method of excavation and, if necessary, the installation of reinforcement and support. In many cases, drainage of the rock mass is also an important factor in maintaining the stability of the excavation.

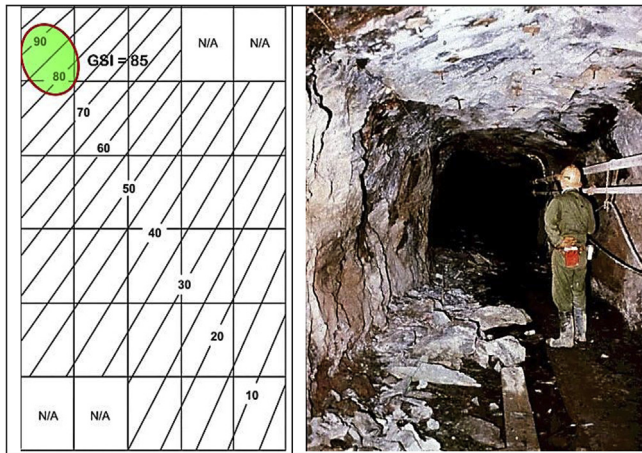


Fig. 8. Spalling in the sidewalls of a mine tunnel in intact hard rock subjected to anisotropic horizontal stresses. GSI is not applicable in the analysis of these stress-induced spalls but it can be used for other applications.

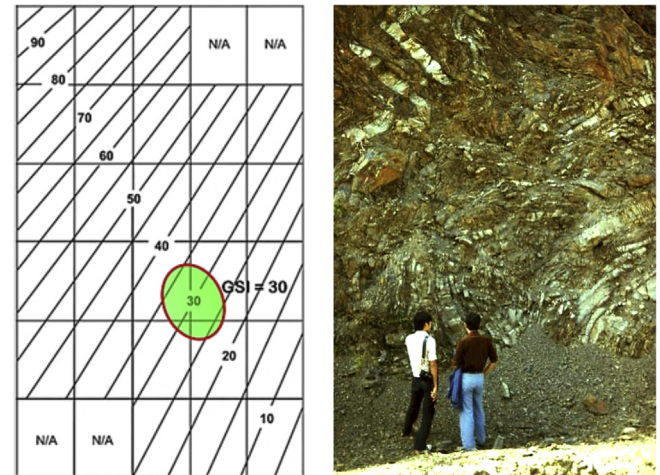


Fig. 11. Complex folding in a bedded sedimentary deposit. GSI is applicable with care since averaging of the intact properties is required to calculate rock mass properties.

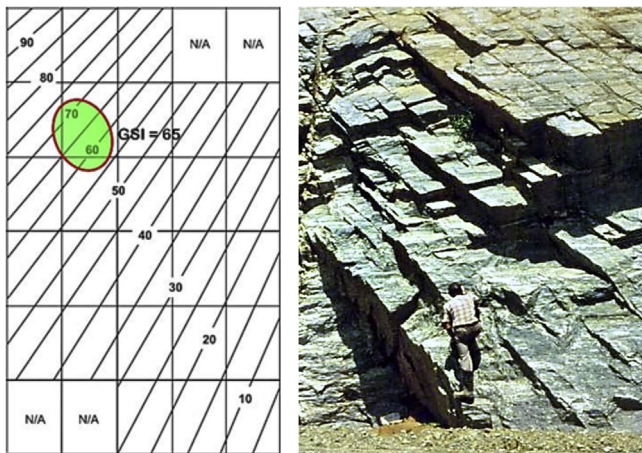


Fig. 9. Orthogonal jointing in granitic rock on a dam site. GSI is not applicable on this scale since the stability of the exposed face is controlled by the geometry of intersecting joints. It can be applied to larger scale excavations.

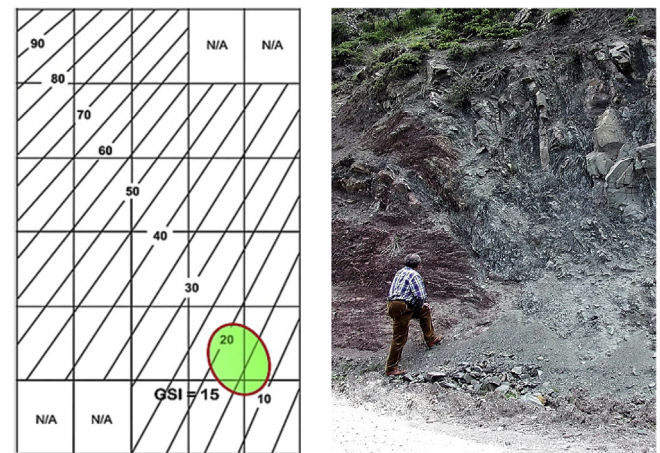


Fig. 12. Tectonically deformed sediments with almost complete loss of structural patterns. Care is required in using GSI in this type of rock mass. Use the GSI charts by [Marinos et al. \(2005\)](#) and [Marinos \(2017\)](#).

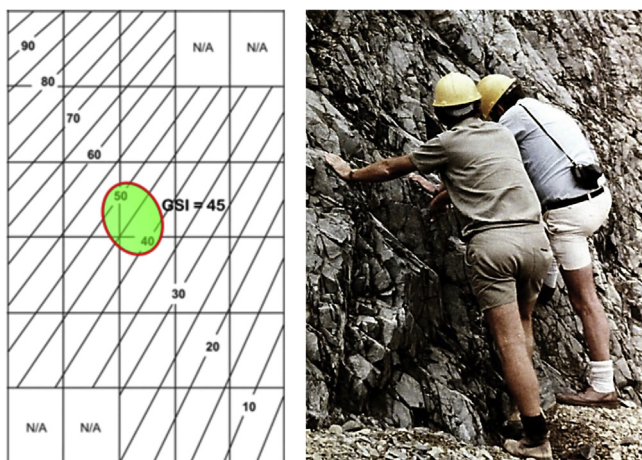


Fig. 10. Interlocking angular Andesite blocks defined by several joint sets, exposed in an open pit mine bench. GSI is fully applicable in this situation and on this scale.

Table 2 sets out several examples in which the method of excavation and the control of blasting are of great importance. In the case of tunnels, this is particularly important since the limited

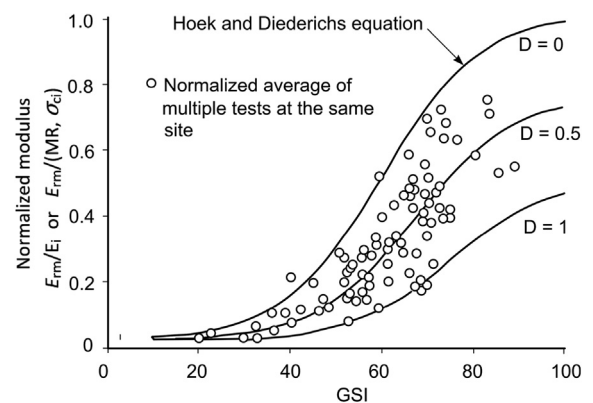


Fig. 13. Plot of normalized in situ rock mass deformation modulus from China (including Taiwan) against Hoek and Diederichs (see Eq. (9)). Each data point represents the average of multiple tests at the same site in the same rock mass.

amount of space available in a tunnel means that any failure can have a serious impact on the excavation schedule and cost and even on the performance of the final tunnel. Careful excavation by a well-

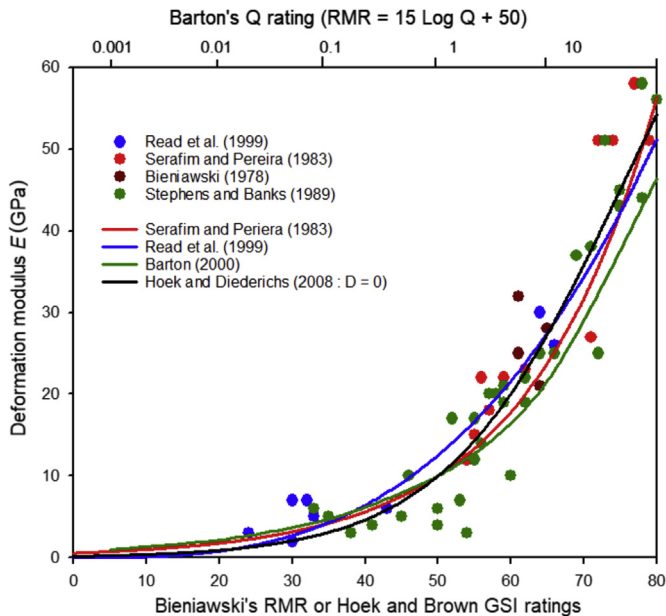


Fig. 14. Comparison between field measurements and deformation modulus values predicted by several authors.

chosen tunnel boring machine (TBM) or road-header can reduce many of these problems. However, in a drill-and-blast tunnel, the blasting design and execution is of critical importance.

A common error is to assume that the disturbance factor D should be applied to the entire rock mass in which the excavation is conducted. This will result in an extremely conservative and inappropriate design.

The first illustration in Table 2 shows a tunnel in which the blast-hole pattern, explosive charges, and detonation sequence have all been carefully designed and executed. Of importance is the careful control of the drillhole alignment for the ultimate smooth blast used to create the tunnel walls. In this case, the disturbance factor $D = 0$ can be used with confidence since there is minimal damage to the surrounding rock mass.

A more complex situation is illustrated in the second photograph in Table 2, showing a tunnel excavated by the top heading and bench method. Unless the displacements induced by the excavation of the lower bench are controlled by the placement of an invert strut, excessive displacements in the lower part of the tunnel can result in significant rock mass failure. In this case, a disturbance factor of $D = 0.5$ is considered appropriate for the rock mass in which the lower half of the tunnel is excavated. Note that this damage factor should only be applied to a zone of about 2 m width around the bottom half of this 12 m span tunnel.

An example of a very poorly designed and executed tunnel blast is shown in the third illustration in Table 2. Poor drillhole alignment control and lack of attention to the blast design and detonation sequence have resulted in damage to the rock walls. A disturbance factor of $D = 1.0$, with a linear decrease to zero, has been assigned to the first 3 m of the rock mass surrounding this 8 m span tunnel.

The fourth illustration in Table 2 shows a 15 m high slope in a dam spillway in which pre-split blasting has been used to create the face on the left. Relaxation of the face can still occur and a blast disturbance factor of $D = 0.5$ has been assigned to 1–2 m of rock behind this face. The rock mass on the right has been mass blasted with little control of the drillhole spacing and alignment of the charges and detonation sequence. The most severe disturbance

factor of $D = 1.0$ has been assigned to 2–3 m of the rock mass behind this slope.

The final illustration in Table 2 shows a very large open pit with slopes approaching 1000 m in total height. Several different disturbance factors must be considered in this example. It is important to differentiate between slopes created during active mining and the final design slopes which are required to remain stable for many years. During active mining, the blasting is required to produce large volumes of uniformly fragmented ore to meet the requirements of ore processing for mineral extraction. On the other hand, the final slopes are required to remain stable to ensure access to the ore and safe and efficient disposal of the waste.

Individual 18 m high benches will generally have suffered significant damage because of their proximity to the production blasts required for removal and fragmentation of the ore. A disturbance factor of $D = 1.0$ is assigned to the rock immediately behind these benches. This disturbance factor can be graded downward, to a final value of $D = 0$, as the distance behind the face increases to about 30% of the slope height.

The inter-ramp and final slopes will also have suffered stress relaxation damage which can exceed the effects of blasting in large excavations. Rose et al. (2018) state that: "Selection of an appropriate range of depth or stress defining the disturbance transition requires consideration of whether slope stability conditions are dominated by geologic structure, rock mass conditions, groundwater, in situ stresses, slope geometry, poor blasting, or a combination of these factors." They have developed a disturbance rating for open pit mine slopes which can provide guidelines for the selection of the depth of the fully disturbed conditions behind the slope and the decrease in the damage factor D over a range of slope heights.

While much smaller blasts are used for slopes for roadcuts, dam spillways and foundation excavations, the application of the damage factor should be like that applied in open pit mining. However, the overall factor of safety of the design may be higher than that for open pit mine slopes to accommodate the longer life expectancy.

9. The overall design process






Having set out all the input data required for a full analysis using the Hoek–Brown failure criterion and GSI system, it is useful to consider the full sequence of data acquisition, interpretation, utilization, and back analysis. Fig. 15 is a flow chart in which the sequence of data acquisition from laboratory tests and field observations are combined to calculate the principal stress relationship for a rock mass. This is followed using analytical or numerical models to produce an excavation design which is then implemented, and its performance monitored by convergence measurements.

A final step is the back analysis of the monitoring results and the feed-back of the results of this analysis into the early stages of the flow chart. This step is critical since it is the only means whereby the design method and the input parameters used in the calculations can be validated. Back analysis should be an ongoing process throughout and even after the construction process so that adjustments and corrections can be made at all stages. This provides not only confidence in the design but also information which can be used to improve on the determination of input parameters and the design methodology.

10. Determination of intact rock strength properties

The starting point for the procedure outlined in the flow chart in Fig. 15 is the determination of the intact rock properties. This involves laboratory uniaxial and triaxial tests on carefully collected and prepared rock core samples. Generally, care is taken to ensure

Table 2Guidelines for estimating disturbance factor D due to stress relaxation and blasting damage.

The disturbance factor D should never be applied to the entire rock mass surrounding an excavation		
Appearance of rock mass	Description of rock mass	Suggested value of D
	Excellent quality-controlled blasting or excavation by a road-header or tunnel boring machine results in minimal disturbance to the confined rock mass surrounding a tunnel. The blasting design for this tunnel is discussed in http://www.rocksience.com/assets/resources/learning/hoek/Practical-Rock-Engineering-Chapter-16-Blasting-Damage-in-Rock.pdf	$D = 0$
	Mechanical or manual excavation in poor quality rock masses gives minimal disturbance to the surrounding rock mass. Where squeezing problems result in significant floor heave, disturbance can be severe unless a temporary invert, as shown in the photograph, is placed.	$D = 0$ $D = 0.5$ with no invert
	Poor control of drilling alignment, charge design and detonation sequencing results in very poor blasting in a hard rock tunnel with severe damage, extending 2 or 3 m, in the surrounding rock mass.	$D = 1.0$ at surface with a linear decrease to $D = 0$ at ± 2 m into the surrounding rock mass
	Small-scale blasting in civil engineering slopes results in modest rock mass damage when controlled blasting is used, as shown on the left-hand side of the photograph. Uncontrolled production blasting can result in significant damage to the rock face.	$D = 0.5$ for controlled presplit or smooth wall blasting with $D = 1.0$ for production blasting
	In some weak rock masses, excavation can be carried out by ripping and dozing. Damage to the slopes is due primarily to stress relief. Very large open pit mine slopes suffer significant disturbance due to heavy production blasting and stress relief from overburden removal.	$D = 0.7$ for mechanical excavation effects of stress reduction damage $D = 1.0$ for production blasting A transitional D relationship incorporating the effects of stress relaxation can be derived from the disturbance rating*

Note: *A disturbance rating for open pit slopes has been published by Rose et al. (2018).

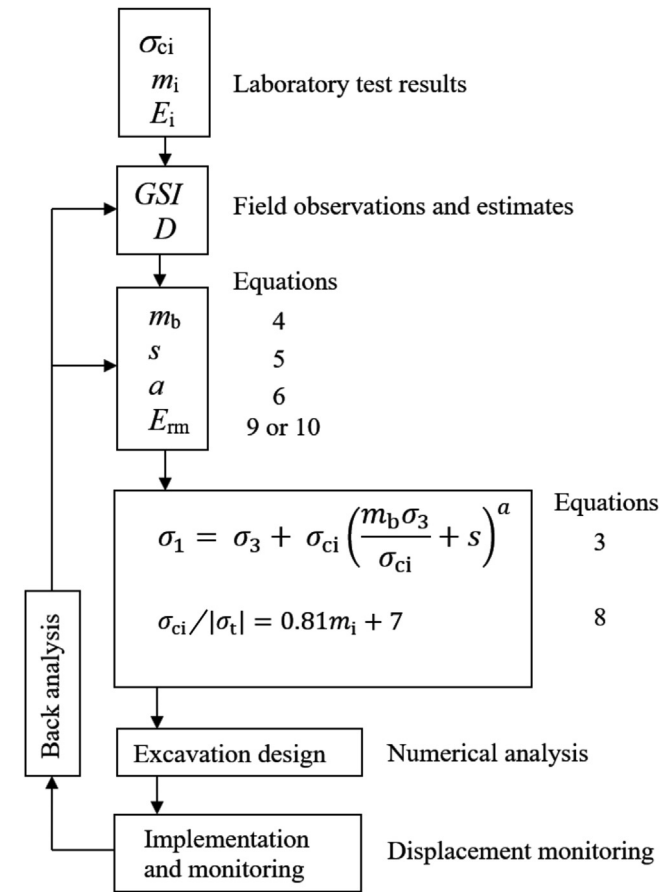


Fig. 15. Flow chart for the application of the Hoek–Brown criterion and GSI system to an excavation design.

that the core is recovered from homogeneous rock in which failure will occur through intact rock material. These samples are tested using current standard and suggested methods outlined in the ISRM suggested methods (Ulusay and Hudson, 2007).

When the Hoek–Brown criterion was introduced, it was recommended that triaxial test results should be analysed by linear regression of the following version of Eq. (1) (Hoek, 1983):

$$(\sigma_1 - \sigma_3)^2 = m_i \sigma_{ci} \sigma_3 + \sigma_{ci}^2 \quad (11)$$

This approach was used for several years until it was realized that the method was inadequate for the analysis of data other than closely spaced points with very little scatter about a general trend line. A variety of methods are available for fitting curves through non-uniform distribution of triaxial test data. One of these, known as the modified Cuckoo search (Walton et al., 2011), is included in the Rocscience program RocData which can be used for the interpretation of laboratory test data.

Bozorgzadeh et al. (2018) and Contreras et al. (2018) used Bayesian statistics to quantify the uncertainty of intact rock strength. This approach provides an alternative to conventional probabilistic or frequentist methods such as those described above. To deal with the problem of outliers in sets of test data for rock, Contreras et al. (2018) use Student's *t* distribution in place of the commonly assumed normal distribution as a starting point in the analysis. The difference between these two distributions, for a hypothetical but not unrealistic data set, is illustrated in Fig. 16 in which the impact of a single outlier is evident.

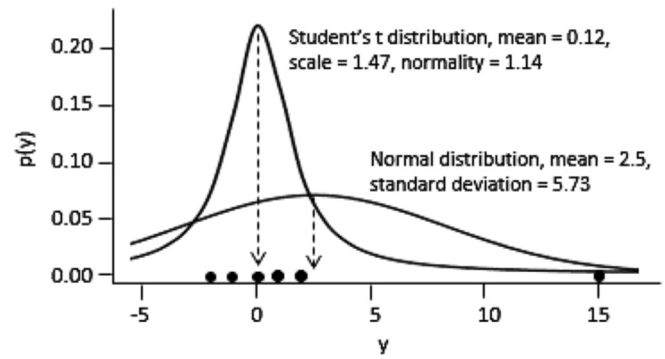


Fig. 16. Comparison between a normal distribution and Student's *t* distribution for the analysis of a small data set with an outlier (after Kruschke, 2015).

Fig. 17 is a plot of the results obtained from a Bayesian analysis of a triaxial data set, giving an unconfined compressive strength of $\sigma_{ci} = 114.5$ MPa and $m_i = 11.5$. For comparison, the result given by the RocScience RocData modified Cuckoo nonlinear regression analysis with absolute residuals is $\sigma_{ci} = 116.2$ MPa and $m_i = 10.6$, which has also been plotted in Fig. 17. In this case, the differences between the Bayesian analysis and the nonlinear regression analysis are not large. As Bozorgzadeh et al. (2018) demonstrated, the advantages of their novel Bayesian regression analysis technique become more apparent for sparser and more widely scattered data sets.

In estimating the σ_{ci} of intact rock, an important issue is the size of the rock block under consideration, as compared to the strength determined from laboratory tests on 50 mm core samples. Fig. 18, published by Hoek and Brown (1980a), includes the results of laboratory tests on a wide range of rock types and specimen sizes. The trend shown in this plot is typical of that suggested by the reasoning that the greater the volume of rock, the greater the probability that a larger number of defects are available for the formation of through-going failures. This trend should be kept in mind when estimating the σ_{ci} of in situ rock blocks.

In the preceding discussion, it has been assumed that the intact rock specimens are homogeneous and isotropic and that the values of the unconfined compressive strength σ_{ci} and the constant m_i are representative of the intact rock in the blocks of the rock mass. In fact, this assumption is not always valid since in many rock masses, defects such as veins, micro-fractures and weathered or altered components can reduce the intact rock strength. Ideally, tests should be carried out on specimens large enough to include representative sections containing these defects, but collection and preparation of such specimens can be challenging.

In discussing rock mass classifications, such as GSI, Day et al. (2012) described the blocks, defined by intersecting joints, as interblock structures. They defined the veins, stockwork and other defects as intrablock structures and pointed out that these should also be considered in the rock mass characterization since they have a significant influence on intact rock strength. They suggested that the defects in both the interblock and intrablock structures can be incorporated into the GSI classification.

Day et al. (2012)'s suggestion is illustrated in Fig. 19 in which the influence of size is considered in determining the use of GSI. The starting point for this chart is a typical intact rock core, but there is no reason why this starting point should not be the intrablock structure within the core as suggested by Day et al. (2012). They emphasized that the reduction of the intact rock strength by this method must be carried out with care to avoid over-penalization of the rock mass strength.

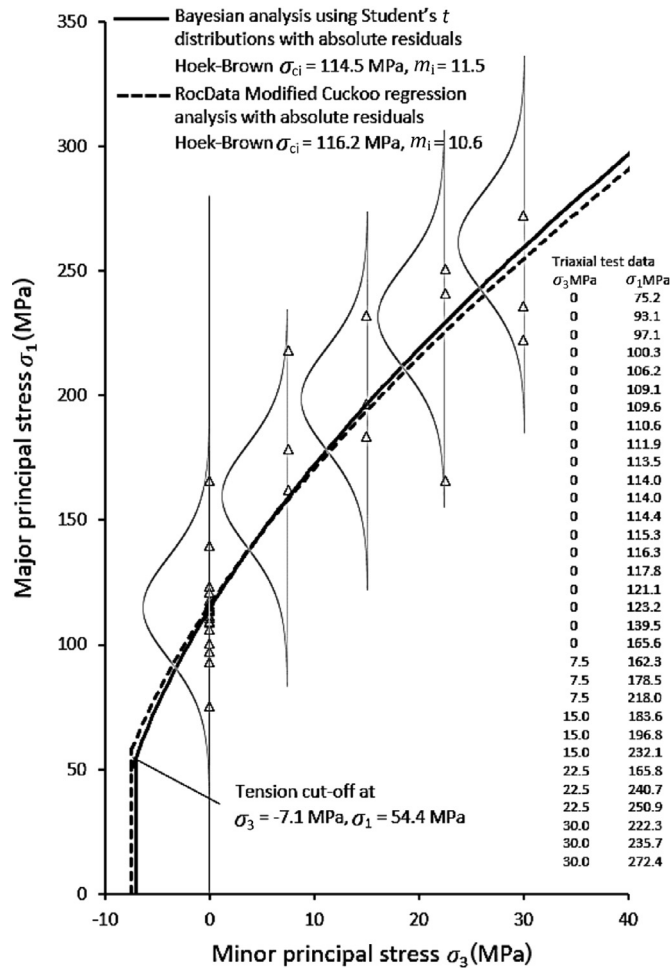


Fig. 17. Analysis of triaxial tests on Coburg limestone using a Bayesian analysis incorporating Student's t distribution, compared with an analysis using the RocData modified Cuckoo method.

Bewick et al. (2015, 2019) and Kaiser et al. (2015) have examined the issue of veins and microfractures in intact rock core or blocks. Their emphasis is on the effects of these veins and micro-fractures on rock mass classification and rock block strength. As noted in Section 5, these authors have proposed that, for sparsely jointed hard rock with a GSI rating of greater than 65, Eqs. (4)–(6) may require modification to reduce the strength of rock masses under high in situ stress conditions.

Weathering, alteration and deterioration of the core in storage are factors that need to be considered during collection and preparation of rock specimens. An example of the deterioration of mudstones and siltstones due to changes in moisture content during storage is illustrated in Fig. 20. In such cases, care needs to be taken to seal the core during transportation and storage or, in extreme cases, to carry out the strength tests on site as soon as possible after core recovery. In the example illustrated, immediate sealing of excavated surfaces with shotcrete was necessary to preserve the rock mass strength.

The triaxial cell, illustrated in Fig. A1 in the Appendix, was originally designed to permit triaxial testing of rock specimens, such as those illustrated in Fig. 20, on drilling sites.

11. Practical application of the GSI characterization

The starting point for any site investigation program is a good geological model of the site. Ideally, this model should be

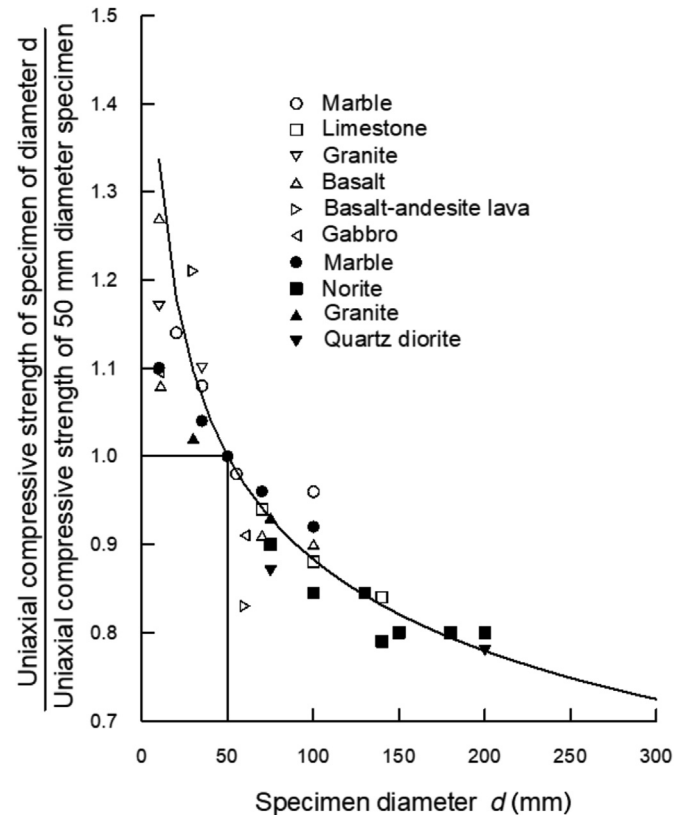


Fig. 18. Influence of specimen size on the UCS of intact rock, compared to that of a 50 mm diameter core sample (after Hoek and Brown, 1980a).

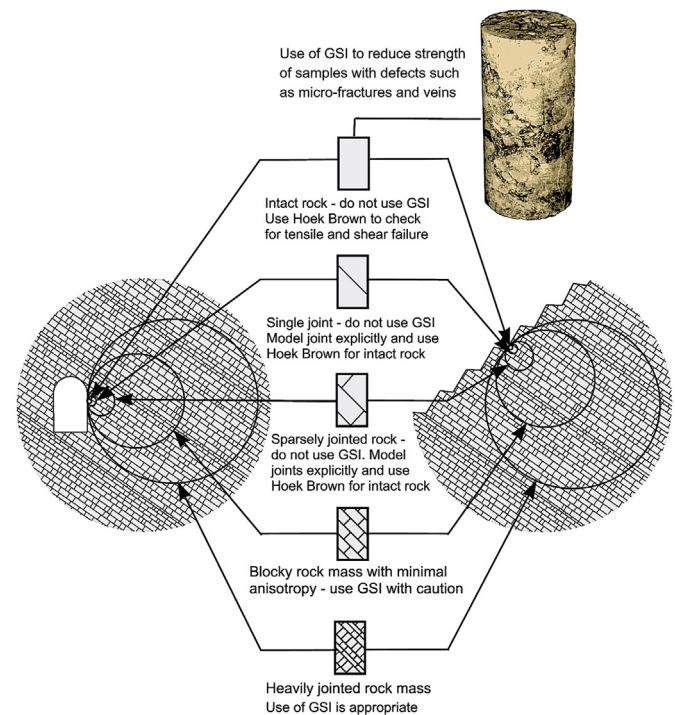


Fig. 19. Size effects in rock mass characterization. Modified after Hoek and Brown (1980a).

constructed by local geologists who have familiarity with the regional geology and experience in working with the rock types encountered on the site. Without such a model, the application of



Fig. 20. Core of sandstone, siltstone and mudstone immediately after recovery (left) and after several months of storage in a core shed (right).

GSI can become a confusing array of numbers being manipulated by engineers anxious to obtain input for analytical or numerical models.

The GSI characterization scheme was devised for engineering geologists and geologists who can utilize all the information contained in the chart presented in Fig. 7 to arrive at a range of probable GSI numbers for each rock unit. As for the case of triaxial test data obtained from laboratory testing, discussed in Section 10, the range of GSI values should also be treated as a distribution. Langford and Diederichs (2015) and Contreras and Brown (2018) advocated that the same statistical processes should be applied to both the intact rock properties and the GSI estimates to provide the ranges of the final rock mass properties chosen for design.

Many projects have been completed successfully using a deterministic approach in which the mean values for intact rock properties and GSI are chosen and applied to the design process outlined in Fig. 15. This approach is acceptable when it is associated with a well-planned rigorous back analysis program and where the contract can accommodate the changes which are necessary to utilize the information from this back analysis. Examples of this type of approach are presented in the next sections.

The GSI system assumes that, because the rock mass is made up of a sufficiently large number of joint sets and randomly oriented discontinuities, it can be treated as a homogeneous and isotropic mass of interlocking blocks. Failure of this rock mass is the result of sliding along discontinuities or rotation of blocks, with relatively little failure of the intact rock blocks. The ideal rock mass for which GSI was originally developed is a heavily jointed rock mass with high intact rock strength, such as that illustrated in Fig. 1.

Fig. 19 shows that the ratio of the size of the blocks to the size of the structure in which they exist is an important factor to be considered when deciding whether GSI should be used. For example, in the face of a 10 m span tunnel, an average joint spacing of 0.5 m would result in about 400 blocks being exposed in a square mine tunnel or about 315 blocks in a circular tunnel. This would be considered a reasonable scale for the application of GSI. The same GSI rating would be applied to smaller blocks with similar geometry. It is the shape of the blocks and the characteristics of the discontinuities which separate them, rather than their size, that controls their

interlocking behaviour. In this example, joint spacings of 2 m or more would result in fewer than 25 blocks which, as shown in Fig. 9, would result in the failure of individual blocks rather than the overall failure of a jointed rock mass. GSI should not be used in this case.

In a 100 m high rock slope, a blocky rock mass with an average joint spacing of 3 m would expose about 1000 blocks in a 100 m length of the slope. This would qualify for a condition in which GSI could be applied. On the other hand, 15 m high benches in the same rock mass would not qualify since only about 25 blocks would occur in a 15 m length of the slope.

In cases where GSI is not applicable, the failures will be controlled by the three-dimensional geometry of the intersecting features in the rock mass. Stability analyses in these cases should be carried out using tools that are available for calculating the factors of safety of sliding blocks or wedges.

Many of the applications and limitations of the GSI were discussed by Marinou and Hoek (2000) and Marinou et al. (2005). Users who are not already familiar with the GSI system are advised to read these papers before embarking on applications in the field. The following three case histories have been chosen to illustrate the practical application of the Hoek–Brown criterion and the GSI system in a variety of geological environments and project settings.

12. The Driskos tunnel on the Egnatia Highway

The 670 km long Egnatia Highway across northern Greece has 77 twin tunnels of almost 100 km in total length. These 12 m span tunnels pass through complex geological conditions in a converging rim between the European and African plates. Many unfavourable geotechnical environments occur along the highway route leading to difficult tunnelling conditions. One of the tunnels on this route is the Driskos tunnel, which will be discussed in this example.

Between 1998 and 2006, Dr. Evert Hoek and Professor Paul Marinou formed a Panel of Experts to advise Egnatia Odos S.A. the company set up to manage the construction of the project, on geotechnical issues related to tunnel design and construction. In 2000, they reviewed the design of the 4.6 km long Driskos tunnel. A longitudinal profile along the tunnel, depicting the geological formations, is presented in the upper half of Fig. 21.

Based on their knowledge of the regional geology of the area and the site investigations that had been carried out, they estimated the GSI values along the tunnel route and calculated the percentage strain which could be anticipated. These percentage strains are plotted along the tunnel in the lower graph in Fig. 21.

The largest strains were anticipated in a section of very poor-quality flysch at the deepest central section of the tunnel. A typical outcrop of this flysch, a tectonically deformed sequence of sandstones, siltstones and mudstones, is illustrated in Fig. 12.

Hoek and Marinou (2000) developed a method for estimating the strain, defined as the ratio of tunnel closure to tunnel diameter $\times 100$, for a tunnel subjected to in situ stresses sufficiently high to cause squeezing.

To carry out the calculations of strain, an estimate of the rock mass strength is required, and this can be made using the approximation given for line 6 in Fig. 22. A comparison between this estimate and estimates made by other authors and in situ test results shows acceptable agreement for values of GSI up to 65.

In the case of the Driskos tunnel, the in situ stress p_0 is assumed to equal the product of the depth of the tunnel and the unit weight of the rock mass. The calculated percentage strains, for the lowest and highest GSI estimates, are plotted along the tunnel alignment

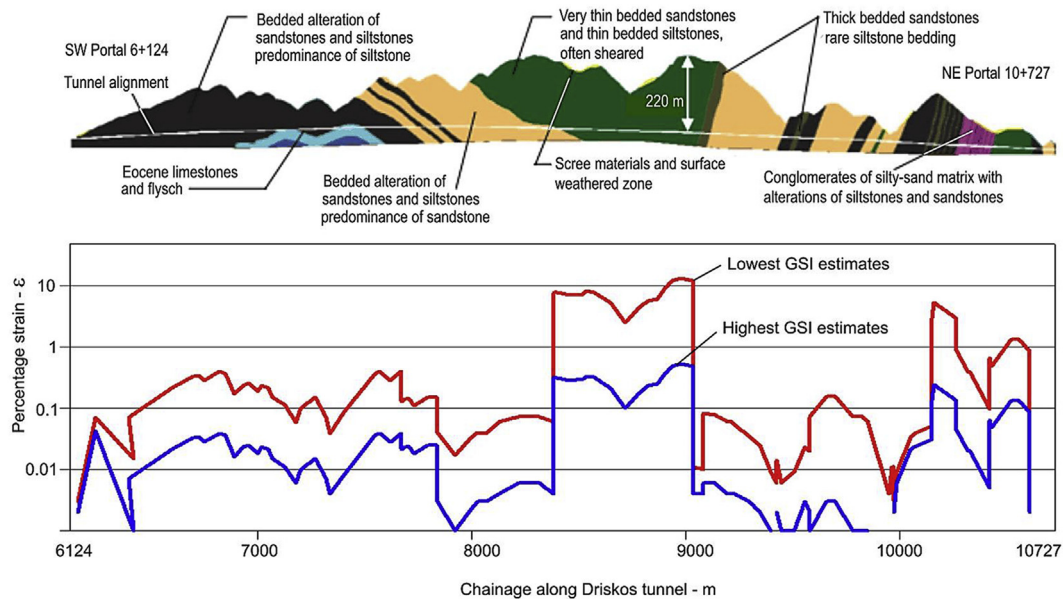


Fig. 21. Longitudinal profile along the Driskos tunnel depicting the geological formations encountered and the predicted percentage closure strain in these sections. Adapted from Vlachopoulos et al. (2012).

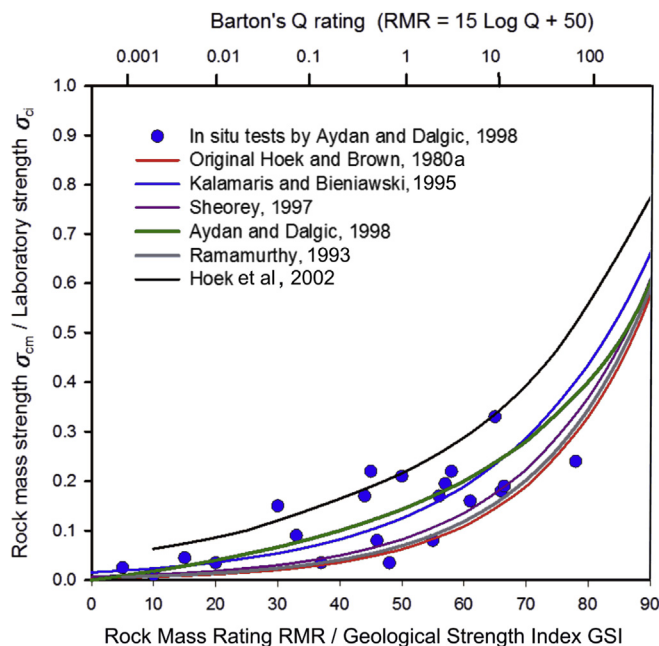


Fig. 22. Approximate relationship between the ratios of rock mass to laboratory unconfined compressive strength for a range of RMR or GSI values. (Von Kármán, 1911, Ros et al., 1928, Rosengren and Jaeger, 1968, Franklin and Hoek, 1970, Kovari and Tisa, 1974, Gerogiannopoulos and Brown, 1978, Ramamurthy, 1993, Kalamaris and Bieniawski, 1995, Sheorey, 1997, Aydan and Dalgic, 1998).

in Fig. 21, which shows that strains of the order of 10% were anticipated for the lowest GSI values, for a section of the Driskos tunnel between approximate chainages of 8300–9000. During the tunnel construction, significant strains occurred in the tunnel in this zone and the installed steel sets, rockbolts and shotcrete proved to be inadequate to prevent the deformation from encroaching on the space required to accommodate the final lining. Additional tensioned cables had to be installed to provide the support required to stabilize the tunnel.

The relationship, proposed by Hoek et al. (2002), is used to calculate the strain for different ratios of rock mass strength to in situ stress as shown in Fig. 23. A comprehensive retrospective analysis of the Driskos tunnel design and construction issues is given by Vlachopoulos et al. (2012).

13. The Ingula underground powerhouse project

The Ingula Pumped Storage Project in South Africa comprises two reservoirs interconnected by a tunnel system, with reversible pump/turbine units with a total rated generation capacity of 1332 MW located in an underground powerhouse complex. This complex consists of a 26 m span machine hall, a transformer hall with a 19 m span, 11 m diameter busbar tunnels, 5 m diameter high pressure penstocks, a 9 m diameter main access tunnel and a series of smaller adits and shafts. It is located at a depth of almost 400 m below ground level. The 184 m long machine hall has a double curvature profile roof with a relatively low span to height ratio of 2.5 and is up to 50 m deep in the turbine pits. A photograph of the partially completed underground powerhouse cavern is reproduced in Fig. 24.

The Ingula power caverns were constructed under a prominent mountain ridge off the Drakensberg escarpment between the Free State and KwaZulu Natal provinces, South Africa, in the Volksrust Formation of the Ecca Group, Karoo Supergroup which comprises horizontally bedded siltstones, mudstones, and carbonaceous mudstones. The intact rock UCS properties derived from field and laboratory testing are presented as normal distributions in Fig. 2.

In situ stresses were measured in hydro-fracture tests in boreholes and in a small number of overcoring tests. The major horizontal stress is greater, and the minor horizontal stress is slightly lower, than the estimated vertical overburden stress. Hydro-fracture tests at cavern level gave a horizontal/vertical stress ratio of 0.5–0.9, while overcoring tests indicated a ratio of approximately 1.0 in the powerhouse area.

In the design of the Ingula underground powerhouse complex, the conventional deterministic method of combining the Hoek–Brown σ_{ci} and m_i parameters was used, with GSI values

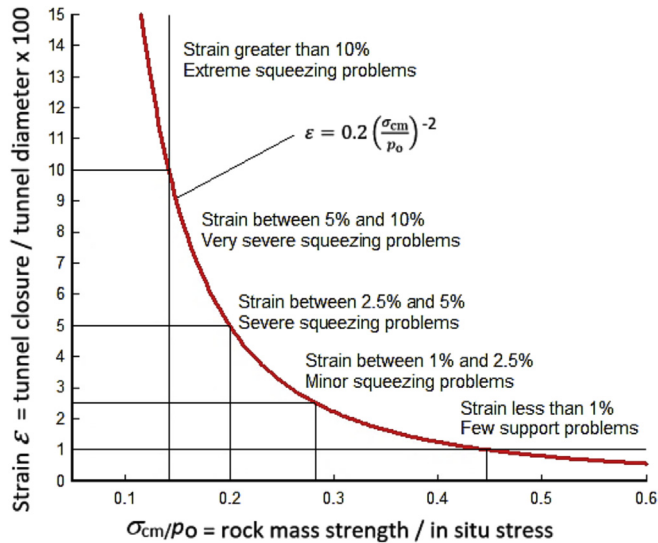


Fig. 23. Percentage strain as a function of the ratio of rock mass strength to in situ stress (Hoek and Marinos, 2000).



Fig. 24. The 26 m span, 50 m high Ingula underground powerhouse cavern after excavation of bench 3. Photograph provided by G. Keyter and reproduced with permission of ESKOM South Africa.



Fig. 25. The east slope of the Chuquicamata mine in 2013.

determined in the field to estimate rock mass strengths for different rock units. The final successful design and construction of the excavations were well documented by Keyter et al. (2008) and Kellaway et al. (2010), which provided an excellent record of this case history.

Initial geological and geotechnical investigations for the Ingula Pumped Storage Project commenced with borehole drilling in 1999. The main phases of the surface geotechnical investigation, the drilling of additional boreholes, and an exploration tunnel were completed in 2005.

The preliminary design of the Ingula underground powerhouse complex was based on the experience gained during the design and construction of the Drakensberg Pumped Storage Project, a sister scheme commissioned in 1981 (Bowcock et al., 1976). At the time of the design of this project, worldwide experience in the construction of underground powerhouse complexes was very limited. After a careful review of three published case histories, the trapezoidal roof arch in the Poatina Project in Tasmania, commissioned in 1964 (Endersbee and Hofto, 1963), was adopted for the Drakensberg

project. Since the Drakensberg powerhouse cavern was the first major underground civil engineering cavern to be constructed in South Africa, full-scale tests of the cavern arch and the concrete lined pressure tunnel were carried out to confirm the support design assumptions. These tests were very successful and provided the information required to complete the design which was successfully implemented in the construction of the underground complex.

Determinations of the deformation moduli of the in situ rock masses in the Drakensberg project were carried out by means of plate bearing tests and by back analysis of the deformations measured in the full-scale tests described above. A surprising result was that the in situ deformation moduli were close to the values determined from laboratory tests on intact samples. This suggested that under the confined stress conditions around the excavations, the rock masses were behaving as very tightly interlocked blocky structures which, in today's terms, would have to be assigned a very high GSI value. Note that the tendency of the mudstones and siltstones, as illustrated in Fig. 20, to disintegrate upon prolonged exposure to air was remedied by the immediate application of shotcrete to all excavated faces. This sealed the rock masses from exposure and preserved the intact properties very effectively.

In designing the underground caverns for the Ingula Pumped Storage Project, the rock mass behaviour in the Drakensberg project was considered, and the interbedded mudstones and siltstones were treated as intact rock with weak horizontal bedding planes. Since this was an unusual design assumption, the designers were reluctant

to assign a GSI value of 100 to the siltstone and mudstone units. Therefore, it was decided to use $GSI = 70$ in the design process.

Two-dimensional finite element models, set up during the detailed design of the cavern excavation and support, were revised towards the end of the main power cavern excavation to account for the actual geology encountered, excavation sequence, support installation, and convergence information collected during construction. The results of these analyses confirmed that, in fact, the in situ mudstones and siltstones should have been assigned a GSI value of 100. A detailed description of the comparison between the original design assumptions and the values obtained from the post-construction back analysis is presented in a comprehensive paper by Kellaway et al. (2010).

This example illustrates the fact that, in many cases, engineers tend to underestimate the capacity of rock masses when tightly confined by the stress field surrounding underground excavations. Kaiser et al. (2015) examined this issue in detail for highly stressed brittle rocks. They conclude that:

“Common use of currently available rock mass characterization systems tends to underestimate the strength of highly stressed brittle and often defected rock. It is demonstrated that this is primarily related to flawed interpretation of rock mass characteristics derived from boreholes and laboratory tests without proper consideration of, for example, GSI applicability, laboratory test results failure mode sorting, and failure modes of rock in underground settings.”

Similar comments can be made for weaker rocks, such as the mudstones and siltstones discussed in the example of the Ingula Pumped Storage Project. In particular, the tendency for these rocks to slake when removed from the in situ environments, can lead to significant underestimation of the rock mass properties.

In the case of the Ingula Pumped Storage Project, the back analysis of a carefully investigated and well-designed project provides a valuable example of the additional information that can be gained on completion of the project. Sakurai (2017) emphasized: *“Field measurement data are only numbers unless they are properly interpreted. Therefore, the most important aspect of field measurements is the quantitative interpretation of measurement results”*.

14. Chuquicamata mine slope stability analysis and conveyor transfer chamber design

The Chuquicamata mine in northern Chile has one of the largest open pits in the world, measuring approximately 4 km long, 3 km

wide, and 1 km deep. Removing ore and waste from the mine on conveyors or by truck, using the haul roads such as that illustrated in Fig. 25, is a complex and expensive process. Hence, planning started more than 10 years ago for a transition from open pit to block caving underground as the mining method (Olavarría et al., 2006). The transition is currently scheduled to occur in 2019 (see Flores and Catalan, 2019).

For many years, the ore has been transported to the surface by means of a conveyor installed in a tunnel behind the East Wall slope. The conveyor has been extended downwards as the depth of the pit increased and, due to limits in conveyor belt lengths, a transfer station was installed in the conveyor tunnel in 2005.

Progressive deepening of the open pit has resulted in ongoing displacements in the East Wall and in the rock mass surrounding the conveyor transfer chamber. This resulted in the need for detailed monitoring of the cavern deformations and periodic adjustment of reinforcement cable tensions and, in some cases, installation of replacement cables. It is important that this chamber remains stable until it is decommissioned when the open pit mining is completed.

In 2012, a review of the conveyor transfer chamber was set up by the mine management. This review was monitored by Dr. E. Hoek, a member of the mine's Technical Advisory Board. The detailed analysis was carried out by P. Varona of Itasca and Dr. F. Duran of the Chuquicamata Geotechnical Department.

An important component of this analysis was the establishment of the rock mass model to be used in numerical models of the slope and chamber. This was based on the results of a geotechnical characterization program initiated by Dr. E. Hoek and Dr. J. Read, members of the first Technical Advisory Board established in 1992. This program involved laboratory testing of intact samples and joints in the seven major rock types surrounding the open pit, as well as 185 km of borehole core logging and 195 km of bench mapping. The results of this geotechnical characterization program, agreed upon by the mine's geotechnical department and approved by the Technical Advisory Board, are summarized in Table 3.

The second important component of the analysis was the existence of a very sophisticated slope displacement monitoring program based on more than 1000 prisms located in sensitive areas of the pit, measured automatically at frequent intervals by electro-optical measuring devices. Information is telemetered to a central monitoring station for interpretation. The locations of the most important prisms around the entrance of the access tunnel to the conveyor transfer station are shown in Fig. 26.

In addition, several radar displacement monitoring units, such as that illustrated in Fig. 27, are available on the mine. One of these was deployed to monitor the displacements of the slope in which

Table 3
Rock mass and discontinuity properties.

Rock mass properties	UCS (MPa)	γ (t/m ³)	Distribution of GSI			m_i
			Minimum	Mean	Maximum	
Fortuna granodiorite (GDF)	110	2.59	29	46	63	20
Moderate shear zones (ZCM)	50	2.47	30	40	56	22
Intense shear zones (ZCI)	7.5	2.31	13	25	51	22
Brecciated shear/faults (BEF)	25	2.51	15	25	35	20
Sericite with high quartz ($Q > s$)	60	2.67	46	60	70	25
Sericite with similar quartz ($Q = s$)	40	2.63	37	47	55	14
Sericite with low quartz ($Q < s$)	20	2.59	27	34	49	15.5
Discontinuity properties	Friction angle (°)			Cohesion (kPa)		
	Minimum	Mean	Maximum	Minimum	Mean	Maximum
Structure	16	18	20	10	20	30
West fault	22	25	28	30	40	50

the transfer chamber is located. A radar image of displacements in the east face of the mine is reproduced in Fig. 28.

Analysis of the slope displacements, measured by both the electro-optical system and the radar unit, demonstrated that the displacements in a zone in the rock mass surrounding the transfer chamber were significantly larger than those in the remainder of the East Wall. This suggested that a wedge, bounded by major structural features shown by blue lines in Fig. 26, had formed in the rock mass and was moving more than the surrounding rock mass in both the face of the east slope and that surrounding the transfer chamber. This model incorporated the joint-defined rock blocks with rock mass strength and deformation properties defined by the Hoek–Brown criterion and GSI parameters given in Table 3. The major structural features were assigned strength properties defined by the discontinuity property values listed in Table 3. The cable reinforcement installed from the transfer chamber, as shown in Fig. 29, was included in the model illustrated in Fig. 30.

During the 2012 review, a 3D discrete element model, using the Itasca 3DEC program, was created to study the displacements and

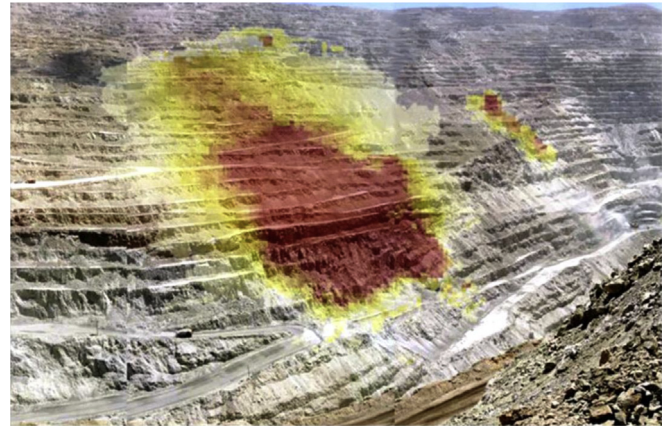


Fig. 28. Radar image showing displacements in the east face. The transition from yellow to red colors indicate increasing displacements in the rock mass.

rock mass behaviours in both the face of the east slope and that surrounding the transfer chamber. This model incorporated the joint-defined rock blocks with rock mass strength and deformation properties defined by the Hoek–Brown criterion and GSI parameters given in Table 3. The major structural features were assigned strength properties defined by the discontinuity property values listed in Table 3. The cable reinforcement installed from the transfer chamber, as shown in Fig. 29, was included in the model illustrated in Fig. 30.

The outcome of this analysis, shown in Fig. 31, was that the deformation results, for both the slope face and the transfer chamber, were in acceptable agreement with the monitored values. This provided the Geotechnical Department with a sound basis on which to plan cable reinforcement tension adjustments and cable replacement installations to ensure that the chamber remained stable for the remainder of the open pit operation.

15. Conclusions

In the almost 40 years since its introduction, the Hoek–Brown criterion for intact rock and rock masses has gained wide-spread international use for a wide range of engineering applications. The criterion for intact rock was based on brittle fracture concepts

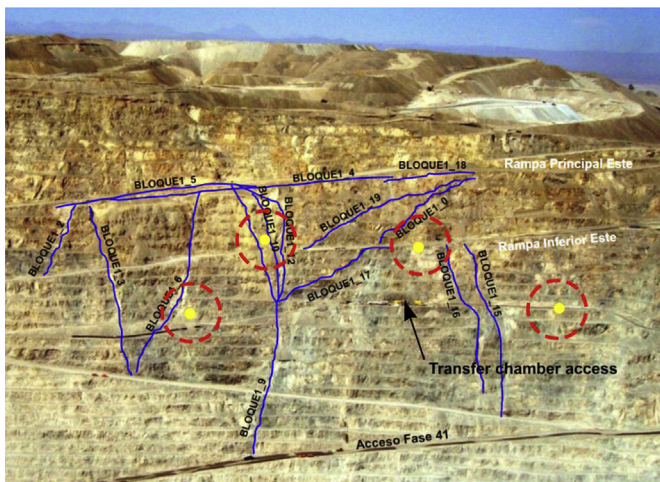


Fig. 26. View of the east face of the Chuquicamata mine showing the location of the conveyor transfer chamber, major structural features and the location of critical optical distance measurement targets (yellow spots circled in red).



Fig. 27. Radar equipment for monitoring slope displacements.

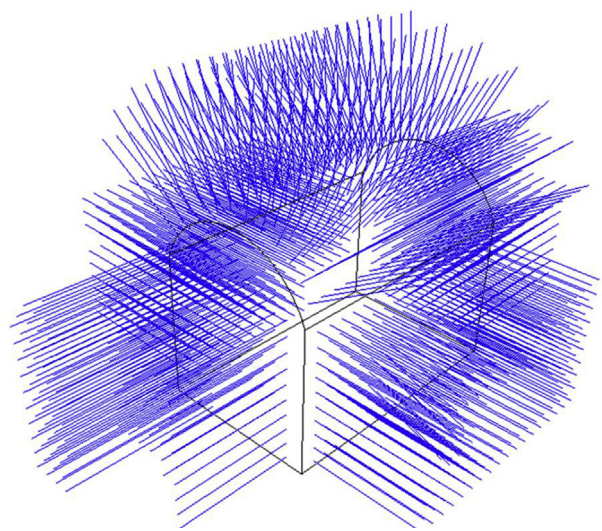


Fig. 29. Cable reinforcement installed from the conveyor transfer chamber. The cavern has a span of 20 m, a height of 25 m and a length of 60 m. Support consists of 15 and 20 m long stressed cables.

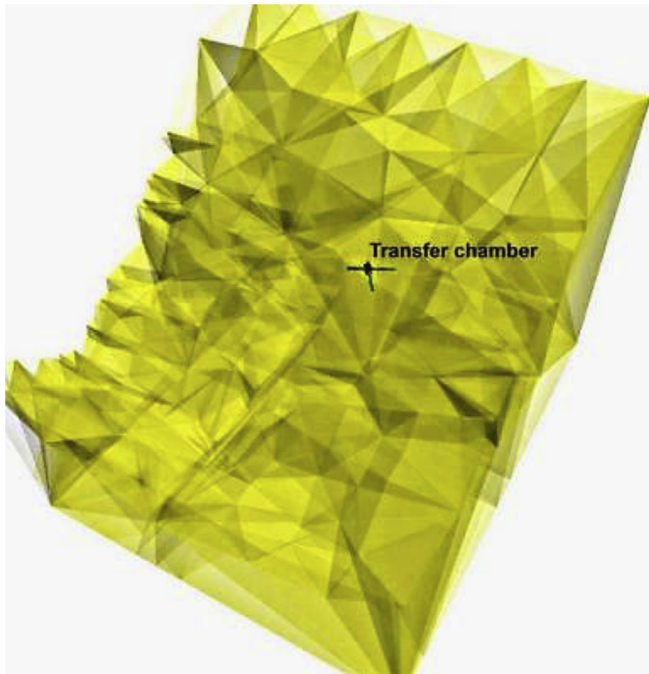


Fig. 30. 3DEC model of the East Wall including the transfer chamber.

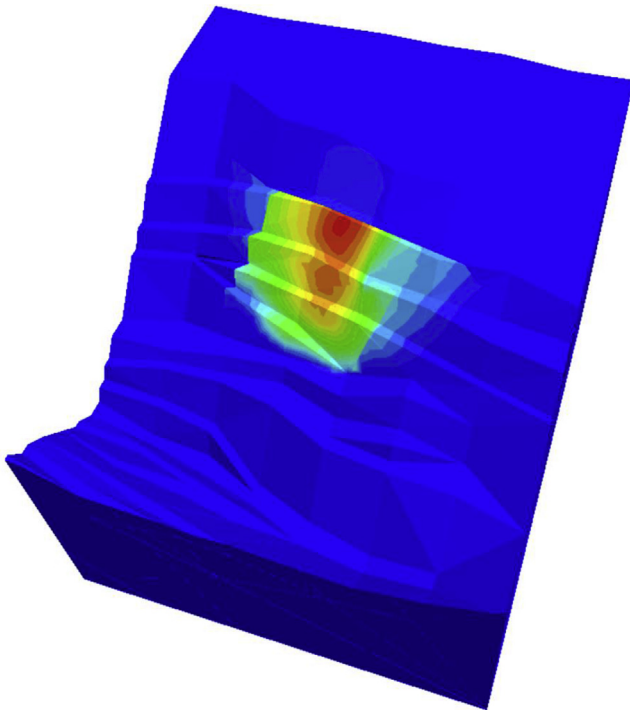


Fig. 31. Displacement contours in the East Wall, generated in a progressively mined 3DEC model. The transition of colours, from blue to red, represent increasing displacements in the rock mass.

and so it should only be used in the brittle behaviour range. Since its introduction, several revisions and updates have been made to the criterion, but its basic form has remained unchanged. A major revision made in the early 1990s accompanied the development of the GSI to quantify engineering geological observations of the structure and condition of rock masses.

The present update emphasizes the intended application of the criterion to the brittle fracture of intact rock; expands on the previously existing methods of evaluating test results for the mechanical properties of intact rock by applying the Bayesian approach to assess uncertainty; discusses the use of the GSI to describe the structure and condition of a wide range of types of rock masses; expands on the previously published guidelines for the selection of the important disturbance factor, D ; sets out a recommended sequence of calculations for use in applying the criterion; and illustrates its application to practical rock engineering through three different examples.

Despite the revisions that have been made to the criterion and the experience gained in its use over almost 40 years, care must be exercised in seeking to apply the criterion to some rock masses, particularly those at the higher and lower ranges of GSI. It is essential that the geology of the site be well understood, and that the mechanics of the engineering problems involved be evaluated critically. When this has been done, the methods discussed in this paper may be used to evaluate the parameters in the criterion for the intact rock and the rock mass.

Conflicts of interest

The authors wish to confirm that there are no known conflicts of interest associated with this publication and there has been no financial support for this work, from any source, that could have influenced its outcome.

Acknowledgements

The authors wish to express their acknowledgements to organizations and individuals who have provided permission to publish materials in case histories and who have contributed to discussions on the development of the Hoek–Brown creation and the Geological Strength Index. It is impossible to name everyone, but a partial list of organizations includes Egnatia Odos S.A. Greece, the South African Electricity Supply Commission (ESKOM), Braamhoek Consultants Joint Venture (BCJV), the Chuquicamata Division of Codelco, Chile. Individuals who have contributed are Rob Bewick, Ming Cai, Trevor Carter, Carlos Carranza-Torres, Joe Carvalho, Luis-Fernando Contreras, Brent Corkum, Mark Diederichs, Felipe Duran, Davide Elmo, Esteban Hormazabal, Jean Hutchinson, Peter Kaiser, Gerhard Keyter, Tom Lam, Loren Lorig, Derek Martin, Paul Marinos, Vassilis Marinos, Dougal McCreath, Bruno Marrai, Terry Medhurst, Bonnie Newland, Luis Olivares, Stephen Priest, John Read, Laurie Richards, Nick Rose, Peter Stacey, Pedro Varona, Nicholas Vlachopoulos, and David Wood.

Appendix. Triaxial and tensile testing.

Tensile testing can be introduced into a triaxial test program by means of a modification used by Ramsey and Chester (2004). Instead of inserting a cylindrical specimen into a triaxial cell, they substituted a dogbone specimen as illustrated in Fig. A1. The reduced section of the specimen was wrapped in Plasticine modelling clay. When subjected to triaxial confinement, this modelling clay yields plastically and transmits a uniform pressure onto the curved section of the dogbone specimen. Since the ends of the specimen are larger in diameter than the central test section, a tensile stress is induced in the test section.

If d_1 is the diameter of the core and d_2 the diameter of the reduced test section, the tensile stress σ_3 induced along the axis of the specimen, for a confining pressure of P , is

$$\sigma_3 = P(d_1^2 - d_2^2)/d_2^2 \quad (A1)$$

By adjusting the ratio of the diameters D and d , the confining pressure P and the axial load applied to the specimen, a range of σ_3 and σ_1 stresses can be generated in the tensile zone, as shown in Fig. A2. The preparation of a dogbone specimen on a lathe is illustrated in Fig. A3.

There is strong justification for using the dogbone specimen, illustrated in Fig. A2, for triaxial testing. This is because the smooth transition of the stresses from the enlarged specimen ends to the central test section reduced the potential for axial splitting, particularly at low confinement, which is common when testing cylindrical specimens loaded by steel plates.

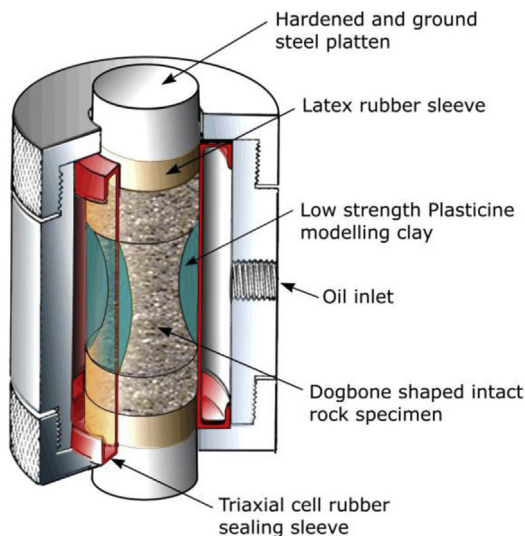


Fig. A1. Triaxial cell with a dogbone specimen for triaxial tensile testing.

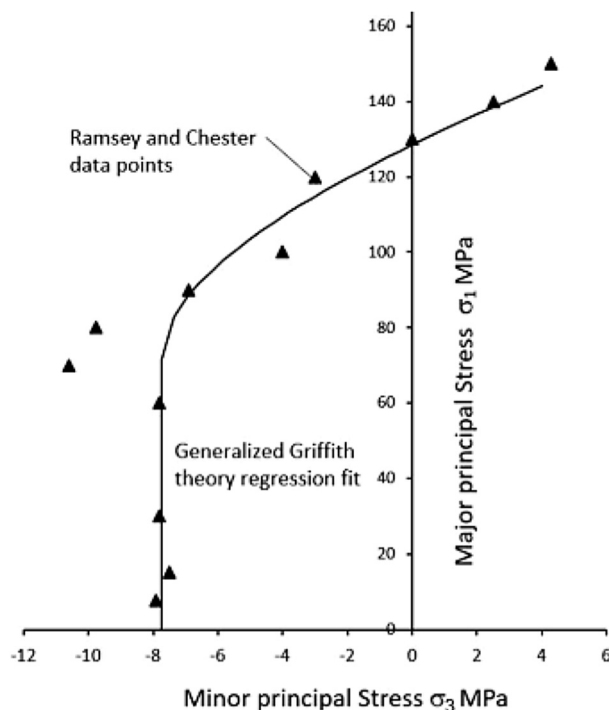


Fig. A2. Plot of triaxial tension data points obtained by Ramsey and Chester (2004).

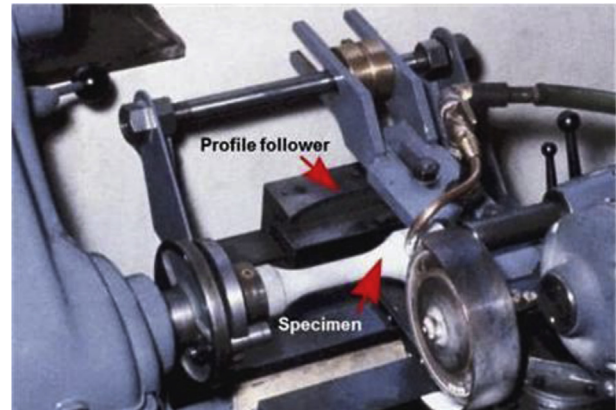


Fig. A3. Preparation of a dogbone specimen using a tool-post grinder attached to a profile follower on a lathe.

References

- Aydan O, Dalgic S. Prediction of deformation behaviour of 3-lane Bolu tunnels through squeezing rocks of North Anatolian fault zone (NAFZ). In: Proceedings of the regional symposium on sedimentary rock engineering. Taipei, China; 1998. p. 228–33.
- Andrieu GE. Brittle failure of rock materials. Rotterdam: A.A. Balkema; 1995.
- Barton N. Some new Q value correlations to assist in site characterization and tunnel design. International Journal of Rock Mechanics and Mining Sciences 2002;39(2):185–216.
- Bewick RP, Amann F, Kaiser PK, Martin CD. Interpretation of UCS test results for engineering design. In: Proceedings of the 13th international congress on rock mechanics: ISRM congress 2015 – advances in applied & theoretical rock mechanics. Montréal, Canada: International Society for Rock Mechanics; 2015. paper 521.
- Bewick RP, Kaiser PK, Amann F. Strength of massive to moderately jointed hard rock masses. Journal of Rock Mechanics and Geotechnical Engineering 2019;11(3) (in this issue).
- Bieniawski ZT. Determining rock mass deformability – experience from case histories. International Journal of Rock Mechanics and Mining Sciences and Geomechanics Abstracts 1978;15(5):237–47.
- Bobich JK. Experimental analysis of the extension to shear fracture transition in Berea sandstone. MS Thesis. Texas A & M University; 2005.
- Bowcock JB, Boyd LM, Hoek E, Sharp JC. Drakensberg pumped storage scheme: rock engineering aspects. In: Bieniawski ZT, editor. Exploration in rock engineering. Proceedings of the symposium on exploration for rock engineering. Rotterdam: A.A. Balkema; 1976. p. 121–39.
- Bozorgzadeh N, Escobar MD, Harrison JP. Comprehensive statistical analysis of intact rock strength for reliability-based design. International Journal of Rock Mechanics and Mining Sciences 2018;106:374–87.
- Brace WF. Brittle fracture of rocks. In: Judd WR, editor. State of stress in the Earth's crust. New York: Elsevier; 1964. p. 111–74.
- Brown ET. Strength of models of rock with intermittent joints. Journal of the Soil Mechanics and Foundations Division 1970;96(SM6):1935–49.
- Brown ET, Hoek E. Discussion on paper 20431 by R. Ucar entitled "Determination of shear failure envelope in rock masses". Journal of Geotechnical Engineering 1988;114(3):371–73.
- Cai M, Kaiser PK, Uno H, Tasaka Y, Minami M. Estimation of rock mass deformation modulus and strength of jointed hard rock masses using the GSI system. International Journal of Rock Mechanics and Mining Sciences 2004;41(1):3–19.
- Contreras LF, Brown ET. Bayesian inference of geotechnical parameters for slope reliability analysis. In: Slope stability 2018 – XIV international congress on energy and mineral resources. Seville, Spain: Asociación Nacional de Ingenieros de Minas; 2018. p. 1998–2026.
- Contreras LF, Brown ET, Ruest M. Bayesian data analysis to quantify the uncertainty of intact rock strength. Journal of Rock Mechanics and Geotechnical Engineering 2018;10(1):11–31.
- Cook NGW. The failure of rock. International Journal of Rock Mechanics and Mining Sciences 1965;2(4):389–403.
- Day JJ, Hutchinson DJ, Diederichs MS. A critical look at geotechnical classification for rock strength estimation. In: Proceedings of the 46th US rock mechanics/geomechanics symposium. Chicago, USA: American Rock Mechanics Association (ARMA); 2012. paper 12-563.
- Deere DU. Geological considerations. In: Stagg KG, Zienkiewicz OC, editors. Rock mechanics in engineering practice. London: Wiley; 1968. p. 1–20.
- Endersbee LA, Hofto EO. Civil engineering design and studies in rock mechanics for Poatina underground power, Tasmania. Journal of the Institution of Engineers 1963;35:187–206.
- Fairhurst C. On the validity of the "Brazilian" test for brittle materials. International Journal of Rock Mechanics and Mining Sciences 1964;1(4):535–46.
- Flores G, Catalan A. A transition from a large open pit to a novel "macroblock variant" block caving geometry at Chuquimata Mine, Codelco Chile. Journal of Rock Mechanics and Geotechnical Engineering 2019;11(3) (in this issue).

- Franklin JA, Hoek E. Developments in triaxial testing technique. *Rock Mechanics* 1970;2(2):223–8.
- Gerogiannopoulos NG, Brown ET. The critical state concept applied to rock. *International Journal of Rock Mechanics and Mining Sciences and Geomechanics Abstracts* 1978;15(1):1–10.
- Griffith AA. The phenomena of rupture and flow in solids. *Philosophical Transactions of the Royal Society of London (Series A)* 1921;221(2):163–98.
- Griffith AA. Theory of rupture. In: *Proceedings of the 1st international congress on applied mechanics*. Delft, The Netherlands; 1924. p. 55–63.
- Hoek E. Fracture of anisotropic rock. *Journal of the South African Institute of Mining and Metallurgy* 1964;64(10):501–18.
- Hoek E. Rock fracture under static stress conditions. CSIR report MEG. 1965. p. 383. Pretoria, South Africa.
- Hoek E, Brown ET. Underground excavations in rock. London: Institution of Mining and Metallurgy; 1980a.
- Hoek E, Brown ET. Empirical strength criterion for rock masses. *Journal of the Geotechnical Engineering Division* 1980b;106(GT9):1013–35.
- Hoek E. Strength of jointed rock masses. *Géotechnique* 1983;33(3):187–223.
- Hoek E. Strength of rock and rock masses. *ISRM News Journal* 1994;2(2):4–16.
- Hoek E, Kaiser PK, Bawden WF. Support of underground excavations in hard rock. Rotterdam: A.A. Balkema; 1995.
- Hoek E, Brown ET. Practical estimates of rock mass strength. *International Journal of Rock Mechanics and Mining Sciences and Geomechanics Abstracts* 1997;34(8):1165–86.
- Hoek E, Marinos P, Benissi M. Applicability of the Geological Strength Index (GSI) classification for very weak and sheared rock masses. The case of the Athens schist formation. *Bulletin of Engineering Geology and the Environment* 1998;57(2):151–60.
- Hoek E, Marinos PG. Predicting tunnel squeezing problems in weak heterogeneous rock masses. *Tunnels and Tunneling International* 2000;132(11):45–51.
- Hoek E, Carranza-Torres C, Corkum B. Hoek-Brown criterion – 2002 edition. In: Hammah R, Bawden W, Curran J, Telesnicki M, editors. *Mining and tunnelling innovation and opportunity, proceedings of the 5th North American rock mechanics symposium and 17th tunnelling association of Canada conference*. Toronto, Canada. Toronto: University of Toronto; 2002. p. 267–73.
- Hoek E, Marinos P, Marinos V. Characterization and engineering properties of tectonically undisturbed but lithologically varied sedimentary rock masses. *International Journal of Rock Mechanics and Mining Sciences* 2005;42(2):277–85.
- Hoek E, Diederichs MS. Empirical estimation of rock mass modulus. *International Journal of Rock Mechanics and Mining Sciences* 2006;43(2):203–15.
- Hoek E, Martin CD. Fracture initiation and propagation in intact rock – a review. *Journal of Rock Mechanics and Geotechnical Engineering* 2014;6(4):278–300.
- Jaeger JC, Cook NGW. *Fundamentals of rock mechanics*. 3rd ed. London: Chapman and Hall; 1969.
- Kaiser PK, Amann F, Bewick RP. Overcoming challenges of rock mass characterisation for underground construction in deep mines. In: *Proceedings of the 13th international congress on rock mechanics: ISRM congress 2015 – advances in applied & theoretical rock mechanics*. Montréal, Canada: International Society for Rock Mechanics; 2015. Paper 241.
- Kaiser PK, Kim B, Bewick RP, Valley B. Rock mass strength at depth and implications for pillar design. In: Van Sint Jan M, Potvin Y, editors. *Deep mining 2010, proceedings of the fifth international seminar on deep and high stress mining*, Santiago, Chile. Perth, Australia: Australian Centre for Geomechanics; 2010. p. 463–76.
- Kalamaris GS, Bieniawski ZT. A rock mass strength concept for coal incorporating the effect of time. In: Fuji T, editor. *Proceedings of the 8th congress on rock mechanics, ISRM*. Tokyo, Japan. Rotterdam: A.A. Balkema; 1995. p. 295–302.
- Kellaway M, Taylor D, Keyter GJ. The use of geotechnical instrumentation to monitor ground displacement during excavation of the Ingula power cavern, for model verification and design verification purposes. In: *Proceedings of South African tunnelling 2012 – lessons learned on major projects*, Ladysmith, South Africa. Johannesburg: Southern African Institute of Mining and Metallurgy; 2010. p. 1–23.
- Keyter GJ, Ridgeway M, Varley PM. Rock engineering aspects of the Ingula powerhouse caverns. In: *Proceedings of the 6th international symposium on ground support in mining and civil engineering construction*, Cape Town, South Africa. Johannesburg: Southern African Institute of Mining and Metallurgy; 2008. p. 409–45.
- Kovari K, Tisa A. Multiple failure state and strain controlled triaxial tests. *Rock Mechanics* 1974;7(1):17–33.
- Kruschke JK. *Doing Bayesian data analysis: a tutorial with R, JAGS and Stan*. 2nd ed. Amsterdam, New York: Academic Press; 2015.
- Langford JC, Diederichs MS. Quantifying uncertainty in Hoek-Brown intact strength envelopes. *International Journal of Rock Mechanics and Mining Sciences* 2015;74:91–104.
- Lau JSO, Gorski B. Uniaxial and triaxial compression tests on URL rock samples from boreholes 207-045-GC3 and 209-069-PH3. Divisional Report (Mining Research Laboratories (Canada)), MRL 92-025(TR). Ottawa: Mining Research Laboratories; 1992.
- Marinos P, Hoek E. GSI – a geologically friendly tool for rock mass strength. In: *Proceedings GeoEng 2000, International conference on geotechnical and geological engineering*. Melbourne, Australia, Lancaster, PA: Technomic Publishing Co.; 2000. p. 1422–40.
- Marinos P, Hoek E. Estimating the geotechnical properties of heterogeneous rock masses such as flysch. *Bulletin of Engineering Geology and the Environment* 2001;60(2):85–92.
- Marinos V, Marinos P, Hoek E. The geological strength index: applications and limitations. *Bulletin of Engineering Geology and the Environment* 2005;64(1):55–65.
- Marinos V. A revised geotechnical classification GSI system for tectonically disturbed rock masses, such as flysch. *Bulletin of Engineering Geology and the Environment* 2017;19:1–14. <https://doi.org/10.1007/s10064-017-1151-z>.
- Marinos V, Carter TG. Maintaining geological reality in application of GSI for design of engineering structures in rock. *Journal of Engineering Geology* 2018;239:282–97.
- McClintock FA, Walsh JB. Friction on Griffith cracks in rocks under pressure. In: *Proceedings of the 4th US National congress of applied mechanics*. Berkeley, USA. New York: American Society of Mechanical Engineers; 1962. p. 1015–21.
- Mogi K. Pressure dependence of rock strength and transition from brittle fracture to ductile flow. *Bulletin Earthquake Research Institute* 1966;44:215–32.
- Murrell SAF. The strength of coal under triaxial compression. In: Walton WH, editor. *Mechanical properties of non-metallic brittle materials*. London: Butterworths Scientific Publications; 1958. p. 123–45.
- Olavarria S, Adriasola P, Karzulovic A. Transition from open pit to underground mining at Chuquicamata, Antofagasta, Chile. In: *Proceedings of the international symposium on stability of rock slopes in open pit mining and civil engineering*. Cape Town: South Africa. Johannesburg: Institute of Mining and Metallurgy; 2006. p. 421–34.
- Perras MA, Diederichs MS. A review of the tensile strength of rock: concepts and testing. *Geotechnical and Geological Engineering* 2014;32(2):525–46.
- Ramamurthy T. Strength, modulus responses of anisotropic rocks. In: Hudson JA, editor. *Compressive rock engineering*, vol. 1. Oxford: Pergamon; 1993. p. 313–29.
- Ramsey JM, Chester FM. Hybrid fracture and the transition from extension fracture to shear fracture. *Nature* 2004;428:63–6.
- Read SAL, Richards LR, Perrin ND. Applicability of the Hoek-Brown failure criterion to New Zealand greywacke rocks. In: Vouille G, Berest P, editors. *Proceedings of the 9th international congress on rock mechanics*. Paris, France. Lisse: A.A. Balkema; 1999. p. 655–60.
- Ros M, Eichinger A. Experimental study of theories of rupture. *Non-metallic materials*, No. 28. Eidgenöss. Materialprüfungsanstalt, E.T.H. Zurich; 1928 (in German).
- Rosengren KJ, Jaeger JC. The mechanical properties of an interlocked low-porosity aggregate. *Géotechnique* 1968;18(3):317–26.
- Rose ND, Scholz M, Burden J, King M, Maggs C, Havaei M. Quantifying transitional rock mass disturbance in open pit slopes related to mining excavation. In: *Slope stability 2018 – XIV International congress on energy and mineral Resources*. Seville, Spain: Asociación Nacional de Ingenieros de Minas; 2018. p. 1273–88.
- Sakurai S. *Back analysis in rock engineering*. ISRM Book Series, London: Taylor & Francis Group; 2017.
- Schwartz AE. Failure of rock in the triaxial shear test. In: *Proceedings of the 6th rock mechanics symposium*. Rolla, USA: University of Missouri; 1964. p. 109–51.
- Serafim JL, Pereira JP. Consideration of the geomechanical classification of Bieniawski. In: *Proceedings of the international symposium on engineering geology and underground construction*. Lisbon, Portugal. Lisbon: SPG/LNEC; 1983. p. 33–44.
- Sheorey PR. Empirical rock failure criteria. Rotterdam: A.A. Balkema; 1997.
- Stephens RE, Banks DC. Moduli for deformation studies of the foundation and abutments of the Portuguese Dam - Puerto Rico. In: Khair AW, editor. *Rock mechanics as a guide for efficient utilization of Natural resources*, proceedings of the 30th US symposium on rock mechanics. Morgantown, USA. Rotterdam: A.A. Balkema; 1989. p. 31–8.
- Ulusay R, Hudson JA, editors. *The complete ISRM suggested methods for rock characterization, testing and monitoring: 1974–2006*. Ankara: ISRM Turkish National Group; 2007.
- Vlachopoulos N, Diederichs MS, Marinos V, Marinos P. Tunnel behaviour associated with the weak Alpine rock masses of the Driskos Twin Tunnel system, Egnatia Odos Highway. *Canadian Geotechnical Journal* 2012;50(1):91–120.
- Von Kármán T. Festigkeitsversuche unter allseitigem Druck. *Zeitschrift Verein Deutscher Ingenieure* 1911;55:1749–57 (in German).
- Walton S, Hasan O, Morgan K, Brown MR. Modified cuckoo search: a new gradient free optimization algorithm. *Chaos, Solutions and Fractals* 2011;44(9):710–8.
- Zuo JP, Li HT, Xie HP, Ju Y, Peng SP. A nonlinear strength criterion for rocklike materials based on fracture mechanics. *International Journal of Rock Mechanics and Mining Sciences* 2008;45(4):594–9.
- Zuo JP, Liu H, Li H. A theoretical derivation of the Hoek-Brown failure criterion for rock materials. *Journal of Rock Mechanics and Geotechnical Engineering* 2015;7(4):361–6.



Dr. Evert Hoek was born in Zimbabwe, graduated in mechanical engineering from the University of Cape Town and became involved in the young science of rock mechanics in 1958 when he started working in research on the problems of brittle fracture of rock, associated with rockbursts in very deep mines in South Africa. His degrees include a PhD from the University of Cape Town, and a DSc (Engineering) from the University of London. He spent 9 years as a Reader and then Professor of Rock Mechanics at the Imperial College of Science and Technology in London, 12 years as a Principal of Golder Associates in Vancouver, Canada, 6 years as an Industrial Research Professor of Rock Engineering at the University of Toronto, Canada, and 25 years as an independent consulting engineer, living in Vancouver. His consulting work involved

major mining and civil engineering projects including rock slopes, dam and bridge foundations and underground caverns and tunnels. He retired from active consulting in 2013 to the age of 80, but he maintains an interest in education in rock engineering.